July 2020

The Use of Refined Analysis in the Evaluation and Determination of Load Capacity of Existing Steel Plate Girder Swing Span Bridges

Patrick Duffy

THE USE OF REFINED ANALYSIS IN THE EVALUATION AND DETERMINATION OF LOAD CAPACITY OF EXISTING STEEL PLATE GIRDER SWING SPAN BRIDGES

A Thesis

Submitted to the Graduate Faculty of the
Louisiana State University and
Agricultural and Mechanical College
in partial fulfillment of the
requirements for the degree of
Master of Science

in

The Department of Civil and Environmental Engineering

by
Patrick Gabriel Duffy
B.S. Louisiana State University, 2016
August 2020

TABLE OF CONTENTS

LIST OF TABLES

LIST OF FIGURES

ABSTRACT

Steel Plate Girder Swing Span Bridges are a common and traditional movable bridge type typically used in rural areas of Louisiana but can also be found all over the world. As a result of structural analysis code updates that reflect the increase in highway traffic loads and changes in analysis provisions, many of these bridges have become load posted due to deficient ratings using current traditional AASHTO bridge rating methods. This thesis will explore a more accurate load capacity of these bridges using two identical load posted bridges in Louisiana. Refined analysis methods such as finite element (FE) methods are known to capture the structural performance of complex structural systems in a way that simplified, e.g. two-dimensional (2D) models, cannot. The goal of this study is to demonstrate the feasibility of using calibrated refined analysis methods to remove load postings established using traditional load rating methods. Load testing and finite element analysis will be used to provide a comparison of actual bridge performance versus suggested traditional analysis. The results of this study show that the load carrying capacity is higher than what is calculated using traditional rating methods. Consequently, load posting could be removed for the analyzed bridge. This conclusion may be applicable to similar movable bridges but will have to be confirmed with a procedure similar to the one presented in this research.

1. INTRODUCTION

1.1. Introduction

The natural landscape of Louisiana consists of many bayous and canals leading to many natural bridge crossings. While ranking only 25th nationally in population, Louisiana ranks 4th in bridge surface area; 12,915 bridges and 16,387,706 square feet of bridge deck (FHWA, 2016). Louisiana ranks 1st in number of movable bridges, 145, and 2nd in number of structurally deficient bridges based on square footage of bridge deck, amounting to 1,739 bridges (FHWA, 2016). As of 2016, Louisiana had 1,900 load posted bridges, which translates to about 15% of all bridges in Louisiana (FHWA, 2016). The majority of load posted bridges in Louisiana are on state routes and local roads (ASCE, 2017).

As a result of Louisiana's important role in oil, gas, and shipping industries, many of these rural bridges experience heavy truck loads and are sometimes the only route in the area. These industries are especially dependent on movable bridges because they not only facilitate vehicular traffic to traverse water features, they also allow for the passage of marine traffic by opening to vessels. This creates a bridge maintenance challenge because these bridges are seemingly always in use to either facilitate vehicular or marine traffic. In other words, movable bridges are of paramount importance for the operation of the transportation network, while at the same time facing more strenuous conditions than fixed bridges.

1.2. Scope of Work

In this case study, the focus will be on applying refined analysis techniques for bridge load rating of steel plate girder swing span bridges through the use of finite element analysis and diagnostic load testing. Specific focus will be put on refined analysis and model calibration.

1.3. Research Approach

The goal of this research is to demonstrate the feasibility of using calibrated refined analysis methods in the evaluation and load rating of existing bridges for the purpose of removing load posting. Specifically, this research is aimed at displaying the superiority of refined analysis and load testing to traditional evaluation methods in capturing a more accurate load capacity of steel plate girder swing span bridges.

1.4. Objective

Diagnostic load testing captures the actual performance of a structure and accounts for load carrying capacity factors that are not included in the approximate methods used for design and load rating of bridges. The hypothesis of this study is that the load carrying capacity of bridges is larger than what is typically assumed in design, which can have a positive impact on load rating. This hypothesis will be tested using diagnostic load testing along with detailed three-dimensional finite element analysis to reveal whether the chosen bridges can carry higher loads than those estimated using traditional simplified design code methods.

1.5. Thesis Organization

This thesis is organized into five chapters. Chapter 1 introduces the current state of bridges in Louisiana and the importance of movable bridges. Chapter 2 conducts a review of relevant literature on the topics discussed in this research. Chapter 3 provides a description of the two tested structures as well as describes the procedures and techniques used in this study. Chapter 4 presents the detailed results obtained from field testing and refined analyses. Chapter 5 summarizes the research effort and lists conclusions drawn from this study.

2. LITERATURE REVIEW

In this chapter, a review of relevant literature on the topics of load rating, nondestructive load testing, unrealized load carrying capacity factors, and refined analysis is presented.

2.1. Load Rating

Load rating is a structural analysis process used to compute the maximum allowable live loads that can be carried by a bridge. The guidelines for load rating are described in the AASHTO Manual for Bridge Evaluation (MBE). Load rating of bridges is performed using the Load and Resistance Factor Rating (LRFR) method (AASHTO, 2011), which is based on the same probabilistic concepts adopted for the development of AASHTO Load and Resistance Factor Design (LRFD) Bridge Design Specifications (AASHTO, 2017). LRFR was introduced by AASHTO in 1989 in the Guide Specifications for Strength Evaluation of Existing Steel and Concrete Bridges and added to the MBE in 2008 (AASHTO, 2011). LRFR incorporates the bridge structural conditions, traffic conditions, material properties, ductility and redundancy, and loads into the overall bridge load rating factor which was not recognized in previous rating methods. LRFR uses a probabilistic approach to properly address bridge preservation concerns, properly addressing both public safety and economics.

The rating factor equation shown in Equation (1) in its most basic form is effectively live load capacity divided by live load demand. In load rating, a rating factor value equal to 1.0 implies that the bridge design is capable of resisting the design live load exactly. A rating factor greater than 1.0 for design inventory means that the live load capacity is greater than the design live load demand. Thus, a rating factor greater than 1.0 for design inventory is accepted as safe for unrestricted traffic. The AASHTO LRFD HL-93 design vehicle is used for this purpose. If

the HL-93 inventory rating is greater than 1.0, then all legal loads that fall within the LRFD exclusion limits will also have satisfactory load ratings (AASHTO, 2011).

The general equation for load rating of each component and connection subjected to single force effect (i.e., axial force, flexure, or shear) is as follows (AASHTO, 2011):

$$RF = \frac{C - (\gamma_{DC})(DC) - (\gamma_{DW})(DW) \pm (\gamma_P)(P)}{(\gamma_{LL})(LL + IM)} \quad (1)$$

For the Strength Limit States: $$C = \phi_c \phi_s \phi R_n \quad (2)$$

Where the following lower limit shall apply: $$\phi_c \phi_s \geq 0.85 \quad (3)$$

For the Service Limit States : $$C = f_R \quad (4)$$

where,

RF	=	Rating Factor
C	=	Capacity
f_R	=	Allowable stress specified in LRFD code
R_n	=	Nominal member resistance
DC	=	Dead load effect due to structural components and attachments
DW	=	Dead load effect due to wearing surface and utilities
P	=	Permanent loads other than dead loads
LL	=	Live load effect
IM	=	Dynamic load allowance
γ_{DC}	=	LRFD load factor for structural components and attachments
γ_{DW}	=	LRFD load factor for wearing surfaces and utilities
γ_p	=	LRFD load factor for permanent loads other than dead loads = 1.0
γ_{LL}	=	Evaluation live load factor
ϕ_c	=	Condition factor
ϕ_s	=	System factor
ϕ	=	LRFD resistance factor

Legal load models are representative of actual vehicular loads seen on bridges. The loads described in the Manual for Bridge Evaluation, AASHTO Type 3, Type 3S2, and Type 3-3 are load models derived to recreate the effects of 3-axle single trucks, 5-axle tractor semi-trailers, and 6-axle tractor-trailers on bridges respectively. Specialized Hauling Vehicles (SHV) have also been added to the list of analyzed loads for bridge load rating due to changes in vehicles introduced by the trucking industry. A Notional Rating Load (NRL), and four single unit load

models are included in the AASHTO SHV load models. The four single unit loads are SU4, SU5, SU6, and SU7. The NRL serves as a screening process for the additional SHV loads, if the NRL rating is greater than 1.0 the unit load models of SU4 through SU7 will be greater than 1.0 (FHWA, 2014).

Load posting is the process of restricting the vehicular loads that can safely travel across a bridge because of load ratings that indicate certain vehicle loads exceed the bridge's live load capacity. The bridge need not be posted when each legal vehicle rating factor is greater than 1.0. When the rating factor for any legal vehicle is between 0.3 and 1.0, Equation (5) is used (AASHTO, 2011). Equation (5) establishes the safe posting load for that specific vehicle type. This weight restriction ensures the structural integrity of the bridge, extending its service life rather than closing the bridge entirely.

$$Safe\ Posting\ Load = \frac{W}{0.7}[(RF) - 0.3] \tag{5}$$

where,
RF = Legal load rating factor
W = Weight of rating vehicle

Load rating has several applications in bridge maintenance and preservation. Load rating can be used to determine scope and type of rehabilitation for a structure to comply with new bridge standards. As stated earlier, it can be used for posting weight limits on existing bridges. Load rating can also be used for permit applications for overweight vehicles that exceed the legal weight limit. It should be noted that less frequent bridge loads such as wind, earthquake, and collision loads are not considered during load rating analysis as bridges are rated for only normal loading conditions.

The standards for design and load rating differ in many ways, including the approach to reliability index. A reliability index represents the probability that the capacity of the bridge will be exceeded. In AASHTO, this reliability index (β) is equal to 3.5 for design. This value represents a probability that the bridge capacity will be exceeded of 0.000233, or 1/4292. This probability is reflected in the design live loads, and load and resistance factors used in AASHTO. It is economically infeasible for all existing bridges to maintain new design standards whose target risk level corresponds to a reliability index equal to 3.5. This is because many existing bridges were designed for lighter loads than currently employed, and some have experienced deterioration or fatigue cracks reducing their capacity. It is important to note, however, that many of these bridges are still servicing normal daily traffic without noticeable structural issues. To address this issue, AASHTO introduced a second level of reliability index of 2.5 (0.00621 probability that a bridge member's nominal resistance will be exceeded) thus lowering the safety expectation allowing for most existing bridges to meet rating requirements; i.e., not requiring load posting or rehabilitation (Zhao & Tonias, 2012). Load rating consists of two levels of bridge performance as outlined by AASHTO, inventory rating and operating rating. Inventory rating represents a comparison of the capacity of the structure to be utilized for an indefinite period of time. Essentially the inventory rating provides a direct comparison to current design standards using the higher reliability index of β=3.5. Operating rating is a description of the maximum live load that the bridge is expected to safely endure (AASHTO, 2011).

The variable used for dynamic load allowance, IM, in the rating factor equation described in Equation (1) stands for impact. This factor is used to increase the live load effect to account for the dynamic response of the bridge to vehicular loading. The most significant contributor is a result of irregular deck surfaces and changes in elevation and surface from approach spans to the

bridge structure. For design, since the condition of the deck is unknown, a conservative factor of 0.33 (or 33%) is used to simplify the process and to increase the overall bridge margin of safety (NCHRP, 2001). For movable bridges, this factor is increased further. The end floorbeams shall be proportioned for full factor live load plus a 0.66 impact factor; twice the normal dynamic allowance specified in the AASHTO LRFD Bridge Design Specifications (AASHTO, 2007).

2.2. Nondestructive Load Testing

Nondestructive load testing is the process of deliberately loading a bridge with a predetermined load and measuring the bridge's response. The test load shall be large enough to invoke a response without creating structural damage to the bridge. The general goal of load testing is to determine the actual performance of a bridge. This practice is most useful when either the original plans of the structure are no longer available, or it is believed that the bridge contains a higher load carrying capacity than is being calculated by traditional analysis.

There are several types of nondestructive load testing, including dynamic load testing and static load testing. In dynamic load testing, the bridge is loaded with either time-varying or moving loads to create vibration excitations in the structure. In static loading, the load remains stationary and all measurements and observations are taken in a static state.

Load testing can be further subdivided as proof load testing and diagnostic load testing. Proof load testing is the process of incrementally increasing the load applied to the bridge until the maximum load capacity of the structure can be determined. This consists of reaching the linear limit of the stress-strain curve cautiously as to not harm or reduce the structural integrity of the bridge. This test is simple in nature but complicated in practice. It is paramount to properly calculate the goal load as to not cause irreversible distress onto the bridge.

Diagnostic testing is the process of loading the bridge to observe under normal, or slightly larger than normal, loading conditions how the different elements of the bridge perform and interact with one another. Proof load testing is generally only used in static load testing, while diagnostic load testing is commonly used in both static and dynamic load test scenarios.

Nondestructive load testing provides many benefits to understanding the actual performance of a bridge. It may be used to analyze deteriorated or damaged members, evaluate the remaining fatigue life of steel bridges, obtain the dynamic load allowance unique to the bridge, determine load distribution, and assess the live load capacity of unknown or low-rated bridge components (AASHTO, 2011).

Often older bridges see lower load ratings over time as design loads become larger than what the existing bridge was initially designed for, which is typically compounded with component deterioration due to aging and deterioration due to environmental effects. This can lead to posted or even closed bridges that have no visible structural deficiencies upon inspection and at the time of posting or closure were successfully carrying normal loading conditions from daily traffic. Load testing in many instances can be used to provide the necessary data to establish a more accurate load capacity of the structure which is not realized in theoretical rating calculations.

2.2.1. Load Rating Using Load Test Results

Load rating values can also be obtained using load testing. Nondestructive load testing can be used to compare the differences in the predicted bridge response using AASHTO approximate methods to the measured response from load testing. After obtaining results from load testing, Equation (6) can then be used to modify the calculated load rating considering the load testing results (AASHTO, 2011).

$$RF_T = RF_C K \tag{6}$$

where,

RF_T = Load-rating factor for the live-load capacity based on the load test result

RF_C = Rating factor based on calculations prior to incorporating test results (Equation (5) should be used)

K = Adjustment factor resulting from the comparison of measured test behavior with the analytical model (represents the benefits of the field load test, if any)

To determine the Adjustment Factor K, Equation (7) is used (AASHTO, 2011):

$$K = 1 + K_a K_b \tag{7}$$

where,

K_a = Account for both the benefit derived from the load test, if any, and consideration of the section factor (area, section modulus, etc.) resisting the applied lest load

K_b = Accounts for the understanding of the load test results when compared with those predicted by theory

Without conducting a load test, the Adjustment Factor is therefore K=1. If the response of the bridge is more favorable than the predicted results using AASHTO approximate methods, then K will be greater than 1.0. If the response of the bridge is more severe than the predicted results, ie. higher strain values recorded from testing than expected indicating lower capacity, then K will be less than 1.0. In general, after the completion of load testing K is not equal to 1.0.

To determine K_a, Equation (8) is used (AASHTO, 2011):

$$K_a = \frac{\varepsilon_C}{\varepsilon_T} - 1 \tag{8}$$

where,

ε_T = Maximum member strain measured during load test

ε_C = Corresponding calculated strain due to the test vehicle, at its position on the bridge which produced ε_T

To determine ε_C, Equation (9) is used (AASHTO, 2011):

$$\varepsilon_C = \frac{L_T}{(SF)E} \tag{9}$$

where,

L_T = Calculated theoretical load effect in member corresponding to the measured strain ε_T

SF = Member appropriate section factor (area, section modulus, etc.)

E = Member modulus of elasticity

The value of K_b is determined by the test team and is applied based on their understanding of the load test results. Specifically, K_b is a numerical representation of the test team's confidence as to why the results are different than those predicted using traditional methods and if the factors that created these different results can be depended upon at higher loading levels. The factor K_b is a value between 0 and 1.0 and is an indication of the reliability that the test team sees in the test benefit at the rating load level. If $K_b = 0$, then the test team is unable to explain or rely on the benefits of the load test. If $K_b = 1.0$, then the test team believes that the testing results can be extrapolated to performance at higher loads than the current rating level. To assist in deriving this factor, the MBE has included Table 1; T is the unfactored test vehicle effect and W is the unfactored gross rating load effect.

Table 1. Values of K_b

Can member behavior be extrapolated to 1.33W?		Magnitude of Test Load			
Yes	No	$\frac{T}{W} < 0.4$	$0.4 < \frac{T}{W} < 0.7$	$\frac{T}{W} > 0.7$	K_b
✓		✓			0
✓			✓		0.8
✓				✓	1.0
	✓	✓			0
	✓		✓		0
	✓			✓	0.5

Source: (AASHTO, 2011)

It is important for even experienced engineers to use appropriate caution when determining and applying the K adjustment factor to determine load ratings. Stress and strain are localized in nature, with the potential to vary greatly in short distances. Therefore, it is possible for large non conservative K factors to be yielded at critical locations and all other locations yield a small

conservative K factor. This is a product of two issues, only one ratio is used to determine the K factor, test result strain vs analytical strain values from the structures critical location, and that the obtained test result strain values are dependent on the strain gage locations which are placed on preliminary analysis and understanding of the structure. This understanding of the bridge performance can change after performing load testing due to unexpected bridge behaviors. Therefore a more accurate load rating may result from using the load testing data to calibrate a finite element model, and then use the model to calculate the overall bridge load rating (Catbas, et al., 2010).

2.2.2. Testing Instrumentation

The type of sensors used in load testing is dependent on the type of response intended to be captured. This is determined after performing a preliminary assessment of the structure and determining the required measurements for the load testing goal as well as instrumentation limitations and testing feasibility. As outlined in the Manual for Bridge Evaluation, load testing can be utilized to measure strains (stresses) in bridge components, relative or absolute displacement of bridge components, relative or absolute rotation of bridge components, and dynamic characteristics of the bridge (AASHTO, 2011).

2.2.3. Instrumentation of Moveable Bridges and Floorbeam Stringer Systems

Catbas et al. (2010) instrumented a bascule bridge for a long-term bridge maintenance monitoring demonstration on a movable bridge. The goal of this research was to properly model, instrument, and monitor movable bridges to therefore increase the effectiveness of damage detection and bridge maintenance of these structures. Movable bridges are difficult to maintain as well as rehabilitate. Rehabilitation and repairs to movable bridges can cost approximately 100 times more than a fixed bridge per square foot (Catbas, et al., 2010).

This study included the instrumentation of mechanical and electrical components as well as structural components. The mechanical and electrical elements that were instrumented consisted of the electrical motors, gear boxes, shafts, rack and pinion, open gears, trunnions, live load shoe, and span lock area. The structural components instrumented consisted of the main girders, floorbeams, and stringers. In this study, many different sensors were deployed to capture the performance of the main girders. Dynamic strain gages were installed to measure the traffic induced strain in the top and bottom flanges. Vibrating wire strain gages were installed to collect slow speed temperature and strain data; this data was collected continuously and in the top and bottom flanges of the main girder but at separate locations from the dynamic strain gages. Strain rosettes were installed to record critical shear values at the center of the web. Accelerometers were installed to measure acceleration in both the vertical and horizontal directions. Tilt meters were installed to measure the angle of inclination at the tip of each main girder as the bridge transitions from its open and closed positions. The floorbeams and stringers were instrumented in a similar manner. Dynamic strain gages were installed to measure the traffic induced strain in the top and bottom flanges. Vibrating wire strain gages were installed to collect slow speed temperature and strain data; this data was collected continuously and in the top and bottom flanges of the floorbeams and stringers but at separate critical locations from the dynamic strain gages (Catbas, et al., 2010).

Laurendeau et al. (2014) instrumented a 65-year-old Pratt Truss bridge to quantify the live load performance of the bridge superstructure. In this study, the bridge was instrumented with 151 strain gages and 8 displacement gages to monitor the bridge response during live load testing. The results were recorded through the use of a wireless data acquisition system. The strain gages were used to record axle and bending effects from the test trucks. The displacement

transducers were used to record changes in deflection from the application of the test trucks (Laurendeau, et al., 2014).

Shahsavari et al. (2019) performed a diagnostic load test on a vertical lift truss bridge in the interest of developing long term structural health monitoring programs for moveable bridges. In this study, both long term and short term monitoring strategies were deployed to capture the bridge response at critical locations. These locations are prone to fatigue, impact damage based on bridge operation, and significant dynamic movements. The short term monitoring system goals consisted of providing information about the bridge's immediate environmental conditions, such as the wind speed, and how this affected the bridge while it was moving between open and closed positions. This monitoring effort was achieved through the usage of accelerometers and strain transducers. The long term monitoring goals consisted of monitoring the dynamic response of the structure, the strain distribution through the gusset-less connection featured in this bridge's design, and the impact of corrosion on load carrying capacity over time. This monitoring effort was achieved through the usage of accelerometers, uniaxial strain gages, strain rosettes, and tiltmeters. To verify the effectiveness of these systems a diagnostic load test was performed on the bridge and model calibration was completed. The model was calibrated using strain time history response (Shahsavari, Mashayekhi, Mehrkash, & Santini-Bell, 2019).

2.3. Unrealized Load Carrying Capacity Factors

Approximate methods are used for design and load rating in AASHTO. These methods were derived to be applicable to a wide range of bridge types. As a result, many factors that may be beneficial to a bridge's load carrying capacity, and therefore load rating, are not accounted for in approximate methods.

The AASHTO LRFD approximate methods can in some scenarios oversimplify the load distribution model in a manner that may not reflect the actual performance of a specific structure. In Figure 1, Figure 2, and Figure 3 a bridge configuration of two exterior steel plate girders, two interior stringers, and two floorbeams is shown to create a single stringer unit of a bridge. A point load P is then placed between the two interior stringers and three load distribution models are described to demonstrate the different resulting forces applied to the floorbeams and how this may affect the bridge load carrying capacity.

The direct load model, as shown in Figure 1, consists of distributing a point load longitudinally to adjacent floor beams on the span while neglecting lateral distribution through the slab to the stringers. This method is very simple to use and very conservative, as an applied point load would then cause the maximum moment in the floorbeams when compared to other load models. The lever rule may also be used in the load distribution on floorbeams, as seen in Figure 2. This model is a better representation of the load path observed from bridge load testing in this type of bridge when compared to the direct load model. This system distributes the load to each stringer and then to the floorbeam at the floorbeam stringer connection. While simple to use and fairly accurate this method of analysis may still be too conservative when evaluating the real loading conditions on a floorbeam in certain scenarios, specifically when the floorbeam is in contact with the deck.

In scenarios where contact between the floorbeam and deck exists, the slab lateral load distribution model, shown in Figure 3, may be the most accurate in portraying the load distribution of a stringer floorbeam system. Rather than the load moving directly to the floorbeam as a point load, some of the load first passes to the stringers and then to the floorbeams, while some of the load passes from the deck to the floorbeams as a distributed load.

The transverse load distribution is dependent on the spacing of the system and the stiffness of the members (Pennings, Frank, Wood, Yura, & Jirsa, 2000). In Pennings et al. (2000) it was determined through finite element analysis that the current analysis methods are over-conservative. In this study, the finite element modeled floorbeams experience moments 10% less than those estimated by current rating procedures. This reduction can be attributed to lateral load distribution and moment carried by the slab (Pennings, Frank, Wood, Yura, & Jirsa, 2000).

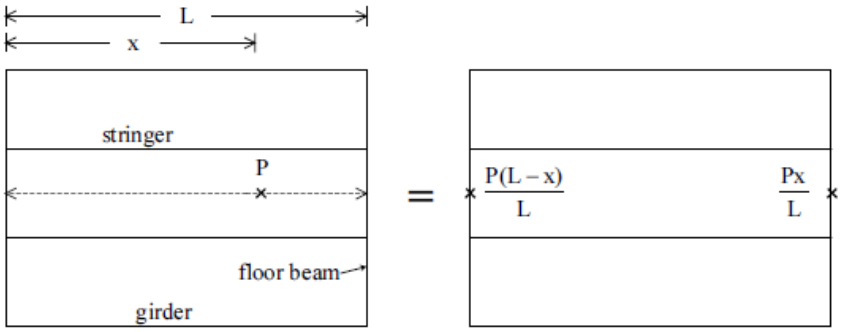

Figure 1. Direct Load Model for Load Distribution
Source: (Pennings, Frank, Wood, Yura, & Jirsa, 2000)

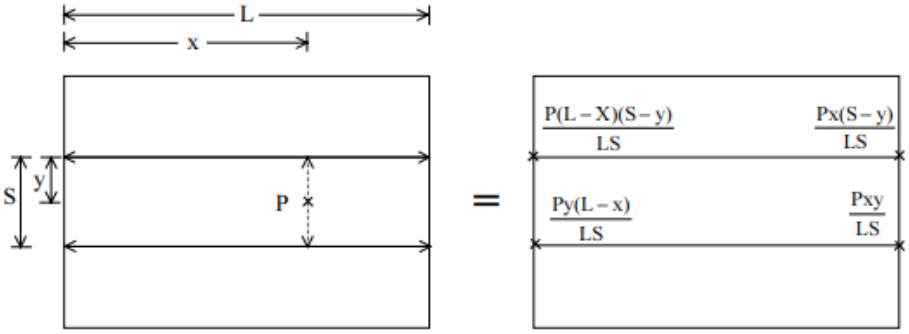

Figure 2. Lever Rule Model for Load Distribution
Source: (Pennings, Frank, Wood, Yura, & Jirsa, 2000)

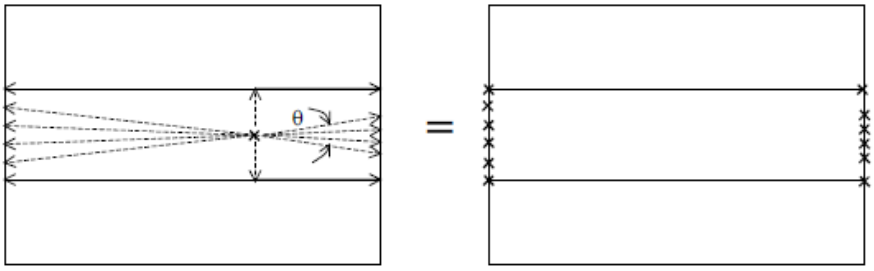

Figure 3. Slab Lateral Load Distribution Model
Source: (Pennings, Frank, Wood, Yura, & Jirsa, 2000)

The distribution of loads also affects the capacity of the stringers. AASHTO specifications have long preferred the usage of Live Load Distribution Factors (LLDFs) to other means of structural analysis. These factors were initially developed for narrow-spaced straight girders with no skew, representative of the bridge inventory of the time in the 1930s and 1940s. They also were developed assuming non-composite girders with nominal cross frames. As a result of their simplicity, the accuracy of these factors varied from bridge to bridge. In the 1980s and 1990s, LLDFs were improved to include more complex parameters than simply girder spacing. Key updates consisted of the recognition that in modern bridges the critical girder is often the exterior girder, the separation of shear and moment into their own sets of factors, and approximate correction factors developed to account for the effects of skew. The LLDFs that are currently in the AASHTO LRFD Specification were derived from a study of a randomly selected bridge inventory of 800 bridges from random states across the country. This inventory was subdivided into separate beam-slab bridge categories based on bridge type, of which average bridges were obtained and refined analysis was performed. In the development of these factors, cross-frames/diaphragms were ignored. This effectively decreases the moment in exterior girders and increases the moment in interior girders. The width of concrete parapets was also ignored, thus increasing the load of the exterior girders. The effects of bottom lateral bracing in steel I-girder bridges are ignored. The LLDF results from the derived equations were then compared to those of the refined analysis. The equation results were then adjusted further, such that the ratio of equation LLDF to the refined analysis LLDF was greater than 1.0 in most cases (FHWA, 2015).

In AASHTO LRFD Section 4.6.2.2 for Beam Slab Bridges, the suggested Load Distribution Factors for beams are provided (AASHTO, 2017). For steel grid deck bridges, the

suggested method is the lever rule for exterior beams regardless of whether the bridge is loaded with only one design lane or loaded with two or more design lanes. Steel grid decks are often used in movable bridges and bridge rehabilitations where weight reduction or speed of construction are important. The lever rule consists of first assuming that the deck is hinged at the interior girder locations. Moments as a result of applied live loads and support reaction are then summed about one girder to find the LLDF of the other, Figure 4. This method is known to be even more conservative because it does not consider the characteristics of the analyzed beam or adjacent beams. In other words, it limits the load path to the structural elements in the immediate vicinity of the applied load. Furthermore, the equation of Live Load Distribution for interior beams does not account for the relative stiffness of the beams as well. These factors can be seen in Table 2.

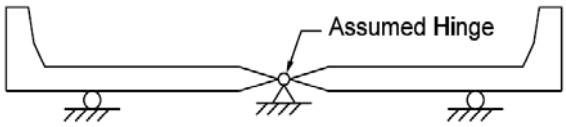

Figure 4. Notional Model for Applying Lever Rule to Three-girder Bridges
Source: (AASHTO, 2017)

Table 2. Distribution Factors

AASHTO LRFD Table	Type of Superstructure	Distribution Factors
4.6.2.2.2b-1 Live Load Distribution Factor For Moment in Interior Beams	Concrete Deck or Filled Grid, Partially Filled Grid on Steel Beams	One Design Lane Loaded: $0.06 + \left(\frac{S}{14}\right)^{0.4}\left(\frac{S}{L}\right)^{0.3}\left(\frac{K_g}{12.0Lt_s{}^3}\right)^{0.1}$ Two Design Lanes Loaded: $0.075 + \left(\frac{S}{9.5}\right)^{0.6}\left(\frac{S}{L}\right)^{0.2}\left(\frac{K_g}{12.0Lt_s{}^3}\right)^{0.1}$
	Open Steel Grid Deck on Steel Beams	One Design Lane Loaded: S/7.5 If $t_g < 4.0$ S/10.0 If $t_g \geq 4.0$ Two or More Design Lanes Loaded: S/8.0 If $t_g < 4.0$ S/10.0 If $t_g \geq 4.0$
4.6.2.2.2d-1 Live Load Distribution Factor For Moment in Exterior Longitudinal Beams	Concrete Deck or Filled Grid, Partially Filled Grid on Steel Beams	One Design Lane Loaded: Lever Rule Two or more Design Lanes Loaded: $g = e\, g_{interior}$ $e = 0.77 + \frac{d_e}{9.1}$
	Open Steel Grid Deck on Steel Beams	One Design Lane Loaded: Lever Rule Two or more Design Lanes Loaded: Lever Rule
4.6.2.2.3a-1 Live Load Distribution Factor For Shear in Interior Beams	Concrete Deck or Filled Grid, Partially Filled Grid on Steel Beams	One Design Lane Loaded: $0.36 + \frac{S}{25}$ Two or more Design Lanes Loaded: $0.2 + \frac{S}{12} - \left(\frac{S}{35}\right)^{2.0}$
	Open Steel Grid Deck on Steel Beams	One Design Lane Loaded: Lever Rule Two or more Design Lanes Loaded: Lever Rule
4.6.2.2.3a-1 Live Load Distribution Factor For Shear in Exterior Beams	Concrete Deck or Filled Grid, Partially Filled Grid on Steel Beams	One Design Lane Loaded: Lever Rule Two or more Design Lanes Loaded: $g = e\, g_{interior}$ $e = 0.6 + \frac{d_e}{10}$
	Open Steel Grid Deck on Steel Beams	One Design Lane Loaded: Lever Rule Two or more Design Lanes Loaded: Lever Rule

In Yousif and Hindi (2007) several finite element modeling techniques were investigated in a study of the limitations and applicability of AASHTO LRFD live load distribution for simple span beam-slab concrete bridges. For a significant number of cases, the AASHTO LRFD live load distribution factors were greater than those generated from finite element. Most of such cases occurred when the lever rule was used (Yousif & Hindi, 2007).

In all cases investigated by Laurendeau et al. (2014), the live load distribution factors were found to be conservative when calculated using AASHTO LRFD specifications compared to those derived from finite element models. The single-lane load case controlled for the exterior girders, where the distribution factor was 17% conservative on average. The multilane load case controlled for the interior girders, where the distribution factor was 44% conservative (Laurendeau, et al., 2014).

The following factors have been attributed to the higher capacity in bridges by the MBE: unintended composite action, unintended continuity/fixity, participation of secondary members, participation of non-structural members, and portion of load carried by deck (AASHTO, 2011). Unintended composite action is the functioning of a beam as a composite member without the presence of a composite connection between beam and deck elements. This phenomenon is seen under normal live loading. It is important to note that as loads increase on the structure the horizontal shear force between the member and the deck can exceed the limiting bond strength. Under these circumstances slippage occurs, the composite action is lost, and there is a sudden increase in member stresses. For this reason, non-composite members which are acting compositely cannot have their stress values extrapolated to higher load cases. Therefore, the composite action of non-composite designed members cannot be expected to significantly increase the load capacity of a bridge if that capacity is defined as the load producing first yield

of tensile steel. However, the capacity can be seen to significantly increase for such members in loading from zero to yield (Suetoh, Burdette, Goodpasture, & Deatherage, 1990).

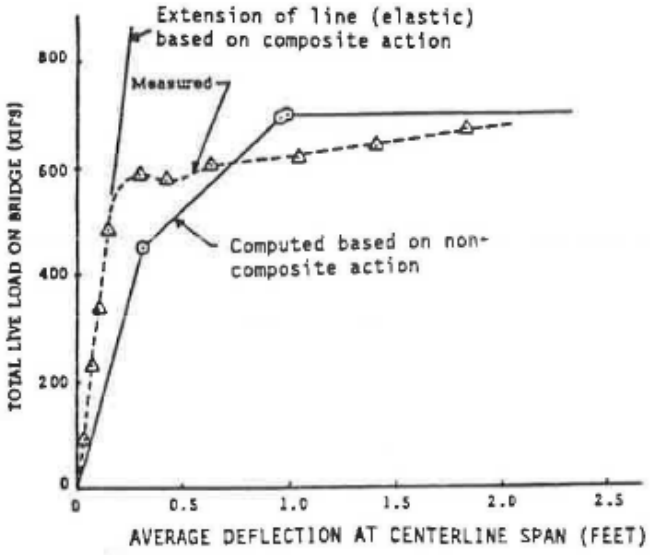

Figure 5. Comparison of measured and computed load-deflection curves for Bridge 4
Source: (Suetoh, Burdette, Goodpasture, & Deatherage, 1990)

Unintended continuity/fixity occurs when a bridge which was designed to act as simply supported acts in reality as though it were continuous. This can be attributed to continuity provided by the deck slab at stringer-to-floorbeam connections and to frozen bearings (AASHTO, 2011). Connections between different structural components that are often assumed to be simply a hinge or a roller, may provide some level of resistance to the movement that designers assume to be released. Because of the nature of unintended continuity/fixity, its influence is seen most prominently in simple span bridges, both single span and multi-span, or at the ends on continuous bridges (Burdette & Goodpasture, 1988).

Participation of secondary members is the effect seen when members not part of the direct load path of the structure assist in load carrying by increasing the overall stiffness of the bridge. A secondary member is a bracing member that does not carry calculated loads but keeps the

primary member from buckling. Participation of non-structural members consists of the influence of railings, parapets, and curbs on the stiffness of the structure. Both participation from secondary members and non-structural members cannot be depended upon at the bridge's ultimate loading conditions. In Eamon & Nowak (2002), for fifteen composite steel girder and concrete deck bridges studied, it was found that structures with barriers and diaphragms saw a reduced girder distribution factor of 11-25%. Structures with barriers, sidewalks, and diaphragms saw a reduced girder distribution factor of 17-42% (Eamon & Nowak, 2002).

Portion of load carried by the deck occurs when the deck slab spanning between the end supports of the bridge carries some fraction of the applied load on its own without the assistance of other bridge elements. This depends on the length of the span and the thickness of the deck.

Burdette & Goodpasture (1988) performed a study to both identify and evaluate aspects of bridge behavior that may be important in estimating the actual load capacity of a bridge but are not normally considered during bridge evaluation and rating (Burdette & Goodpasture, 1988). This research was conducted under NCHRP Project 12-28(8). The projects consisted of assembling, reviewing, and evaluating all available test data relating to the load capacity of highway bridges. The results of this study are recorded in Table 3.

Table 3. Summary of factors influencing bridge strength estimates.

Variable	Bridge Type			
	Beam and Slab	Concrete Slab	Truss	Box Girder
Unintended Composite Action	P, I/T	N/A	S[1], I/T	P, I/T
Participation of Parapets and Railings	P, A	P, A	N/A	P, A
Differences Between Actual & Assumed Material Properties	S, I/T	S, I/T	S, I/T	S, I/T
Participation of Bracing and Secondary Members	S	N/A	S	S
Two-Way Slab Action	N/A	S	N/A	S
Confinement	S[2]	N/A	S[2]	S[2]
Differing Support Characteristics and Unintended Continuity	S, I/T	S, I/T	S, I/T	S, I/T
Participation of Floor System with Chords of Trusses	N/A	N/A	S, I/T	N/A
Analysis/Load Distribution Effects	P, A	P, A	P, A	P, A
Effects of Skew	S, A	P[3]	N/A	S, A

Source: (Burdette & Goodpasture, 1988)

KEY
- P - Primary Factor
- S - Secondary Factor
- A - Include in Conventional Analysis
- I/T - Inspection and or Testing Needed to Verify
- N/A - Not Applicable
- 1 Composite Action Between Floorbeams and Concrete Deck
- 2 Influences Local Deck Strength Only
- 3 Short Span Bridges Only (S for Longer Span Bridges)

2.4. Refined Analysis

Refined analysis is a generic term used in AASHTO and FHWA specifications to express a need for a more detailed or sophisticated structural modeling analysis than the simple application of established structural design or evaluation codes. In May 2019, the U.S. Department of Transportation (US-DOT) Federal Highway Administration (FHWA) published the Manual for Refined Analysis in Bridge Design and Evaluation (FHWA, 2019). This publication serves as a repository for simple refined analysis guidelines and techniques while

still leaving the ultimate application of refinement to the judgment of engineering professionals. Often references suggest the use of Finite Element Analysis (FEA) when referring to refined analysis. This is mainly due to the fact that FEA provides a wealth of element types with an abundance of features that allow for the modeling of complex structures that may not be possible with simpler analysis methods.

In a report titled Assuring Bridge Safety and Serviceability in Europe (2010), an 11-member team was assembled to investigate practices of U.S. bridge engineers and compare them to European host countries (International Technology Scanning Program, 2010). The team was comprised of three FHWA members, four state transportation department representatives, one representative from academia, and three structural engineering design consultants. In the United States, refined analysis is often reserved for unique or complex bridges. For all other purposes, the AASHTO approximate analysis methods as defined in LRFD 4.6.2 Approximate Methods of Analysis are typically utilized. In LRFD 4.6.2.2 Beam-Slab Bridges the live load distribution factors of different bridge types and elements are presented. These factors are then applied to a one-dimensional model. However, in the European host countries bridges are typically analyzed using refined analysis methods of either 2-D or 3-D models while approximate methods are used mainly to provide quick calculation checks. In these countries, grillage or beam-shell analysis is the common analysis procedure. The process of refined analysis is particularly beneficial in rating, even more so than design, as the conservatism of rating through approximate analysis can result in costly reconstruction or rehabilitation of bridges with already safe load carrying capacities. This is because when compared to the results from refined analysis, approximate analysis yields more conservative and less certain force effects. The concluding opinion of this

committee is that the United States needs to develop a plan to increase the usage of refined analysis in bridge engineering (International Technology Scanning Program, 2010).

In the linear elastic finite element method, the bridge is divided into a finite set of elements representative of the structure. A mathematical model of the bridge is arranged in a matrix formulation which is then solved by a computer. The stiffness of each element must be computed in all directions, rotational or translational, that the element resists displacement. The mass and other material properties are also included in the matrix. The point at which each element connects to another is known as a node. The bridge supports are known as boundaries, and their restrictions to displacement are therefore boundary conditions. The node connections are critical in assembling the global matrix of the structure. These create the relationship between the elements which must match in all six translational and rotational displacement directions with their connected element (FHWA, 2015).

Three-dimensional finite element modeling allows for the most realistic representation of a structure and requires few simplifying assumptions (FHWA, 2015). Three-dimensional finite element models can be constructed using bar elements, beam elements, surface elements, volume elements, constraints and rigid links, and spring and point elements (FHWA, 2019). These models can contain one element type or a combination of several element types. The construction of the model and the element type is left to the discretion of the engineer.

2.4.1. Modeling Bridge Members

Bar (truss) elements are two force elements and the simplest members available to model in FEA. These members are only capable of resisting deformation in the longitudinal member

direction; therefore, this member is used in modeling bridge elements such as trusses or cross-frames. Elements such as these are subjected to primarily axial forces (FHWA, 2019).

Beam elements are capable of resisting axial fore, biaxial shear, biaxial moment, and torsion. These elements have stiffness and transmit loads to all six degrees of freedom at each node. For steel bridges, beam elements are typically used to model steel cross-frame top and bottom chords, girder flanges, diaphragm flanges, diaphragms, longitudinal stiffeners, transverse stiffeners, and shear connectors (FHWA, 2019).

When modeling elements where the thickness of the element is in general much less than the other two orthogonal directions a surface element is often used. Surface elements include both shell elements and plate elements. Surface elements are particularly useful in modeling situations where a stress output is desired. At each node of a surface element, nodal solutions such as moments and shear forces can be accessed. In contrast, solid elements, which only have three degrees of freedom, result in stresses that will have to be post processed to obtain these same nodal forces (Okeil, Ulger, & Elshoura, 2018). For steel bridges, surface elements are typically used to model concrete deck slabs, girder flanges and webs, and plate diaphragms. If surface elements are used to create the flanges of an I-shaped girder, two elements are needed to define the flange width: one on each side of the web centerline. If surface elements are used to create the web of an I-shaped girder, a minimum of four elements are recommended to be used in the vertical direction of the member to properly capture the parabolic shear (FHWA, 2019).

Volume elements, also known as solid or brick elements, are useful when thickness normal stresses along the X, Y, and Z plane are of importance. Modeling girders or bridge deck slabs with volume elements can potentially result in long solution times. This is a result of the

fine mesh size and therefore high number of degrees of freedom used when modeling with volume elements (FHWA, 2019).

2.4.2. Refined Analysis of Moveable Bridges and Floorbeam Stringer Systems

Susoy et al. (2007) modeled a bascule bridge for system reliability evaluation using a field calibrated model. The main girders were modeled using shell elements. The transverse beams and floorbeams were modeled using frame elements. The steel grid deck was originally modeled using a grid of frame elements. It was then replaced with shell elements with constant thickness chosen to exhibit the same behavior as the steel grid deck with less computation time. Rigid links were used to connect the web and flange shell elements of the main girder, to connect the frame element transverse beams to the main girder, and to connect the deck elements to the girders (Susoy, Zaurin, & Catbas, 2007).

Catbas et al. (2010) modeled a bascule bridge for a long-term bridge maintenance monitoring demonstration on a movable bridge. The main girders were modeled using 4-node quadrilateral elements. The secondary beams, sidewalk and roadway brackets, and diagonal bracing were modeled using frame elements. Frame elements were used to reduce complexity and computation time. The steel grid deck was modeled using 4-node quadrilateral elements representing a single homogenous steel plate as an equivalent deck. The first consideration for modeling the deck was to model it using frame elements. This would have taken a long time to construct and would also increase model processing time. In the interest of simplicity, an equivalent deck using shell elements was employed. The creation of this equivalent deck consisted of an iterative process that resulted in a best match of a 1.45-inch thickness of the element. This deck behaved similarly to the real deck with only minimum error when comparing the model deflection and rotations to field results (Catbas, Zaurin, Susoy, & Gul, 2007). The

deck was connected to the main girders and secondary beams by rigid links. The concrete counterweight was modeled using 8-node brick solid elements (Catbas, et al., 2010).

Liu et al. (2013) modeled a bascule bridge for rehabilitation analysis. The truss members were modeled using 3D beam elements. The segmental girders and track girders were modeled using shell elements. The counterweights were modeled using solid elements (Liu, Macdonald, & Chen, 2013).

Laurendeau et al. (2014) modeled a 65-year-old Pratt Truss bridge to quantify live-load performance of the bridge superstructure. The concrete deck, sidewalk, and parapets were modeled using solid elements. No solid element aspect ratio exceeded 10 to avoid distortion of the results. The steel beams, stringers, cross bracing, and truss systems were modeled using frame elements. The floorbeams and stringers were connected to the deck using body constraints to replicate the composite action field measurements. The truck loads were applied as point loads to the bridge deck elements (Laurendeau, et al., 2014).

Shahsavari et al. (2019) modeled a vertical lift truss bridge for model verification using a multi-scale modeling approach. A global model of the bridge was created in which all members were modeled with shell elements. The second model was developed to simulate the lifting action of the bridge and consisted of both beam and shell elements. The deck and both east and west trusses were modeled with shell elements. The braces in the tower, the floorbeams, and the skewed floorbeams were modeled with beam elements. The third model was developed to assess the gusset-less connections of the bridge. The floorbeams and braces were modeled by beam elements. The gusset-less connections and chord members were modeled by shell elements. The replacement of shell elements with beam elements was made to increase the efficiency of the model by reducing computation time. The modeled shell elements would be replaced by a single

beam element and appropriate constraint equations (Shahsavari, Mashayekhi, Mehrkash, & Santini-Bell, 2019).

3. METHODOLOGY

This chapter presents the application of the topics presented in Chapter 2 to two movable bridges in Louisiana. Detailed descriptions of the tested bridges, finite element model, diagnostic load test, and model calibration used in this research are provided.

3.1. Bridge Description

The bridges tested in this thesis are two nearly identical steel plate girder swing span bridges. The first bridge covered in this study was built in 1964 and is currently posted for a weight limit of 15-25 tons. For the remainder of this thesis, this structure will be referred to as Bridge1. The second bridge covered in this study was built in 1971 and is currently posted for a weight limit of 25-40 tons. For the remainder of this thesis, this structure will be referred to as Bridge2.

The steel plate girder swing span is comprised of two unequal arms of 45 ft. and 90 ft. The two arms are made up of seven floorbeams, Floorbeams A through G, and six stringer units, Units 1 through 6. The 45-foot arm consists of two stringer units, Units 1 and 2, each containing four stingers. The exterior stringers are 18WF64 members and the interior stringers are 18WF50 members. The deck for stringer Units 1 and 2 is a 7-inch concrete deck. The 90-foot arm consists of four stinger units, Units 3 through 6, each containing seven stingers. All seven stringers are 16WF40 members. The deck for stringer Unit 3 is a partially filled steel grid deck. The deck for Units 4, 5, and 6 is a 5-inch open grid floor. The framing plan of the steel plate girder swing span is shown in Figure 6. The material properties as determined from the as-built plans are given in Table 4.

Table 4. As-Built Material Properties

Material	Designation	f_c' (ksi)	f_y (ksi)	f_u (ksi)
Concrete (Bridge1)	Class A	3.0	-	-
Concrete (Bridge2)	Class AA	3.2	-	-
Reinforcing Steel	Grade 40	-	40	70
Structural Steel	Carbon Steel ASTM A-7	-	33	60
Structural Steel	ASTM A94 ≤ 1 1/8”	-	50	75
Structural Steel	ASTM A441 ≤ ¾”	-	50	70
Structural Steel	ASTM A441 > ¾” to 1 ½”	-	46	67

An initial load rating report of both bridge superstructures was recovered from the bridge owner before load testing. Rating analysis was performed prior to this study using AASHTOWare Bridge Rating (BrR). The design live load for both bridges was H15-44 or one H20-S16-44 truck placed to cause maximum stress in the member under consideration. The most recent load ratings of these two bridges show deficiencies in Floorbeam B, Floorbeam E, and Unit 2 Interior Stringers resulting in rating factors less than 1.0. The controlling condition is related to the allowable stress limit in the flanges as specified in AASHTO Provision 6.10.8.1. The deficient member ratings have resulted in the load postings of both structures. The rating report of Bridge1 resulted in a recommended load posting of 15-25 tons. The rating report of Bridge2 resulted in a recommended load posting of 25-40 tons. Details of the deficient members for both spans are given in Table 5.

Table 5. Details of Deficient Members

Member	Section	Material
Floorbeam B	33WF130	ASTM A94
Floorbeam E	30WF108	ASTM A94
Unit 2 Interior Stringer	18WF50	ASTM A94

The main difference between these two existing bridges is the condition factor provided from the most recent bridge inspection. The superstructure condition ratings of Bridge1 and Bridge2 are 4 and 6, respectively. These values can be seen in Table 6 and Table 7 which contain bridge data from both structures. Using Table 8 and Table 9, the resulting superstructure condition factors, ϕ_c, for Bridge1 and Bridge2 were determined to be 0.85 and 1.00, respectively (AASHTO, 2011). The superstructure condition factor for Bridge1 is 0.85 as a result of its "poor" inspection rating, 4. The superstructure condition factor for Bridge2 is 1.0 as a result of its "good" inspection rating, 6. Because of this discrepancy, the load posting for Bridge1 is lower than that of Bridge2.

Table 6. Bridge Data Bridge1

Bridge Posting	15-25	Year Built	1964	Bridge Type	PGSWNG
Design Load	H15-44 & H20-S16-44	Bridge Length	202 ft.	Roadway Width	24 ft.
Deck Condition	7	Super Condition	4	Sub Condition	4

Table 7. Bridge Data Bridge2

Bridge Posting	25-40	Year Built	1971	Bridge Type	PGSWNG
Design Load	H15-44 & H20-S16-44	Bridge Length	462 ft.	Roadway Width	24 ft.
Deck Condition	6	Super Condition	6	Sub Condition	5

The outcome of these low load rating factors and necessity to load post the bridges prompted the effort to explore whether refined analysis methods can alleviate some of these concerns by revealing more accurate behavior and load carrying capacity. The refined analysis adopted for this study is based on the finite element method and will be presented in Section 3.2.

Table 8. Approximate Conversion in Selecting ϕ_c

Superstructure Condition Rating (SI & A Item 59)	Equivalent Member Structural Condition
6 or higher	Good or Satisfactory
5	Fair
4 or lower	Poor

Source: (AASHTO, 2011)

Table 9. Condition Factor, ϕ_c

Structural Condition of Member	ϕ_c
Good or Satisfactory	1.00
Fair	0.95
Poor	0.85

Source: (AASHTO, 2011)

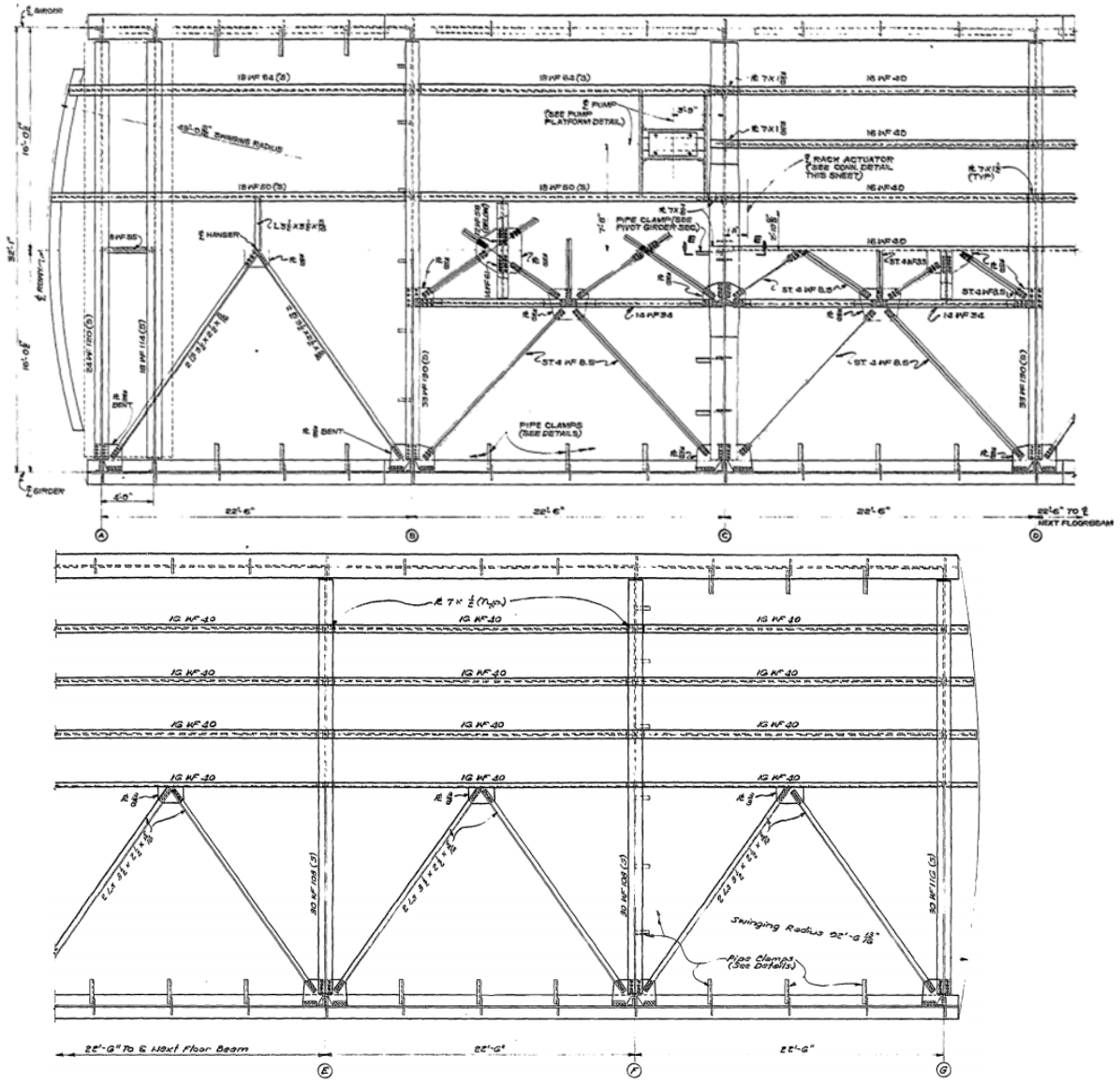

Figure 6. Framing Plan of Steel Plate Girder Swing Span

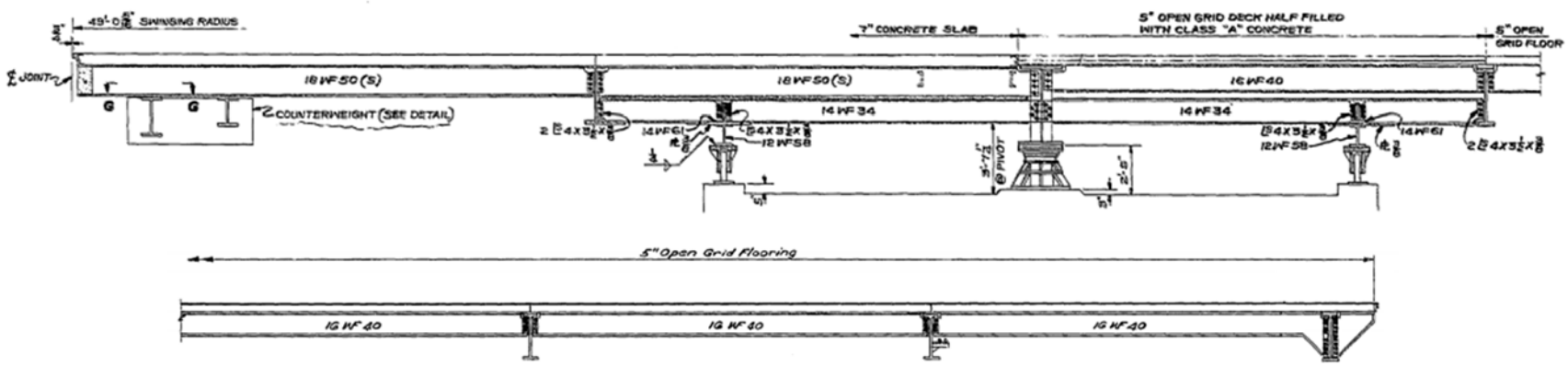

Figure 7. Section Thru Centerline of Roadway

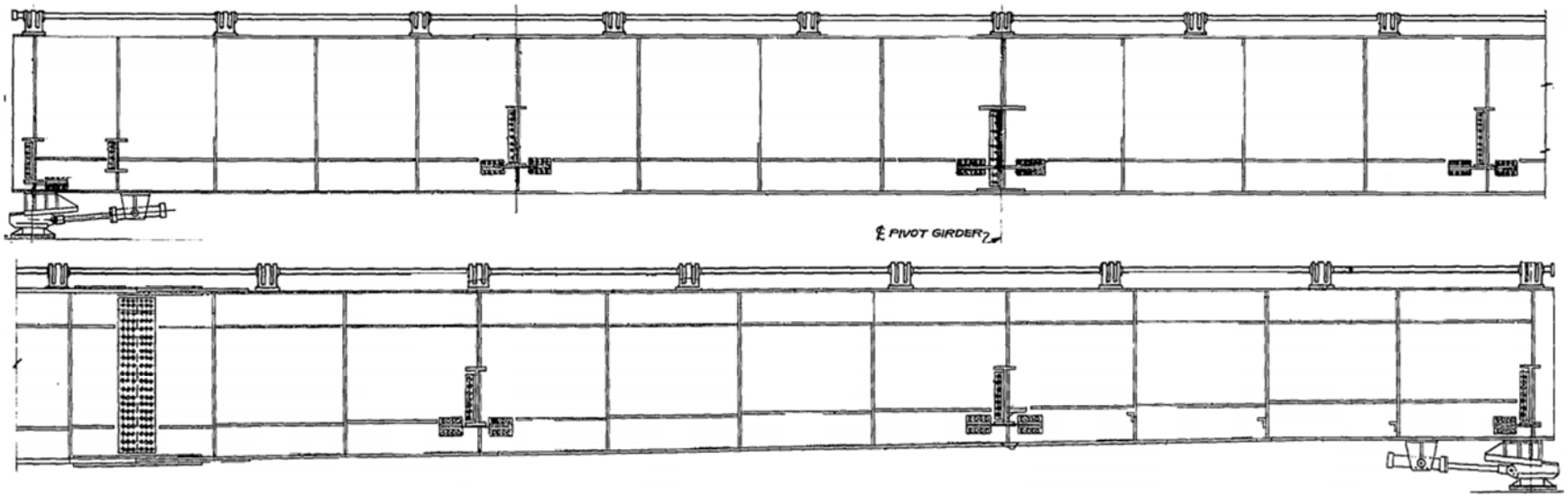

Figure 8. Plate Girder Elevation

3.2. Finite Element Model

Prior to load testing the bridges, an initial Finite Element (FE) model of the bridge was created based on as-built plans and realistic parameters of the structure. The FE analysis was carried out using the commercially available software package MIDAS Civil. The initial finite element model was used to predict strains due to expected testing loads. These strains were then compared to strain values recorded during bridge loading to ensure that the bridge was not loaded past its safe capacity limits. The FE model was created using plate elements for all components. Plate elements are more ideal for this model than solid elements. For engineering purposes plate elements produce adequate results while also taking less time to construct and receive results from than solid elements. Plate elements also are particularly useful in modeling situations where a stress output is desired. In this study, access to stress outputs allows for direct comparison of the FE results to the testing data. Furthermore, solid elements are known to be stiffer and require much finer meshes to produce acceptable results.

The initial FE model used varying boundary conditions to model the floorbeam supports. Floorbeams A, C (pivot), and G were restrained at their ends in the Z direction representing the bridge supports during the bridge's "closed" position allowing for the crossing of vehicular live load. Floorbeam C was also restrained in the X, Y, and Z directions on its bottom flange at its midpoint to account for the connection to the bridge pivot, as can be seen in Figure 9. In lieu of modeling the plate girders, equivalent springs representing the restraint provided by the plate girders were applied to the components to which they are connected. For intermediate Floorbeams B, D, E, and F, vertical and horizontal equivalent springs were used to represent the stiffness of the supporting plate girders, Figure 10.

To create the equivalent springs the steel plate girders were modeled independently using beam elements. Boundary conditions were set to restrict displacement in the Y and Z directions at both ends of the bridge and X, Y, and Z directions at the pivot point. A unit load was then applied on the plate girder at Floorbeams B, D, E, and F locations. This unit load was applied at each location once in the Z direction and once in the Y direction. Displacement results were recorded, and springs of equivalent stiffness were then applied to the ends of the floorbeams divided by the number of nodal points.

The deck was modeled as two separate sections. The concrete deck from Floorbeam A to the pivot point at Floorbeam C was modeled as a 7-inch thick concrete plate with an eccentricity of 3.5”-inch from the stringer top flanges. The filled grid deck was ignored between Floorbeam C and D and replaced with an equivalent steel grid deck from Floorbeam C to Floorbeam G. This equivalent steel grid deck was modeled as a homogenous steel plate of thickness 2/3-inch and eccentricity from stringer top flanges of 1/3-inch.

Two variations of the initial FE model were created: assuming composite and non-composite deck connection interactions. Composite action was modeled between the concrete deck and stringers by use of rigid links, linking the deck to the top flange of all eight stringers in stringer Units 1 and 2 in the X, Y, and Z directions throughout their entire length (see Figure 12). This was made even though no composite connection was considered in the design because the stringer flanges were constructed embedded into the concrete deck and therefore see unintended composite action. Composite action was modeled between the equivalent steel grid deck and stringers by use of rigid links, linking the deck to the top flange of all remaining stringers in the X, Y, and Z directions throughout their entire length (see Figure 12). The design of these components also did not consider composite connection, however, during the construction of the

bridge, the steel grid deck was welded to the top flanges of the stringers providing unintended composite action to these elements. This was performed in accordance with AASHTO LRFD Article 9.8.2.2, which states that open grid steel decks must be welded or mechanically fastened to its supporting component for each main element. For the non-composite model, all rigid link connections were changed to be only linked in the Z direction. Figure 12 shows the location of the rigid links as they appear in both the composite and non-composite model. It is the manipulation of the restraint definition of these rigid links in the two models that then yields different results.

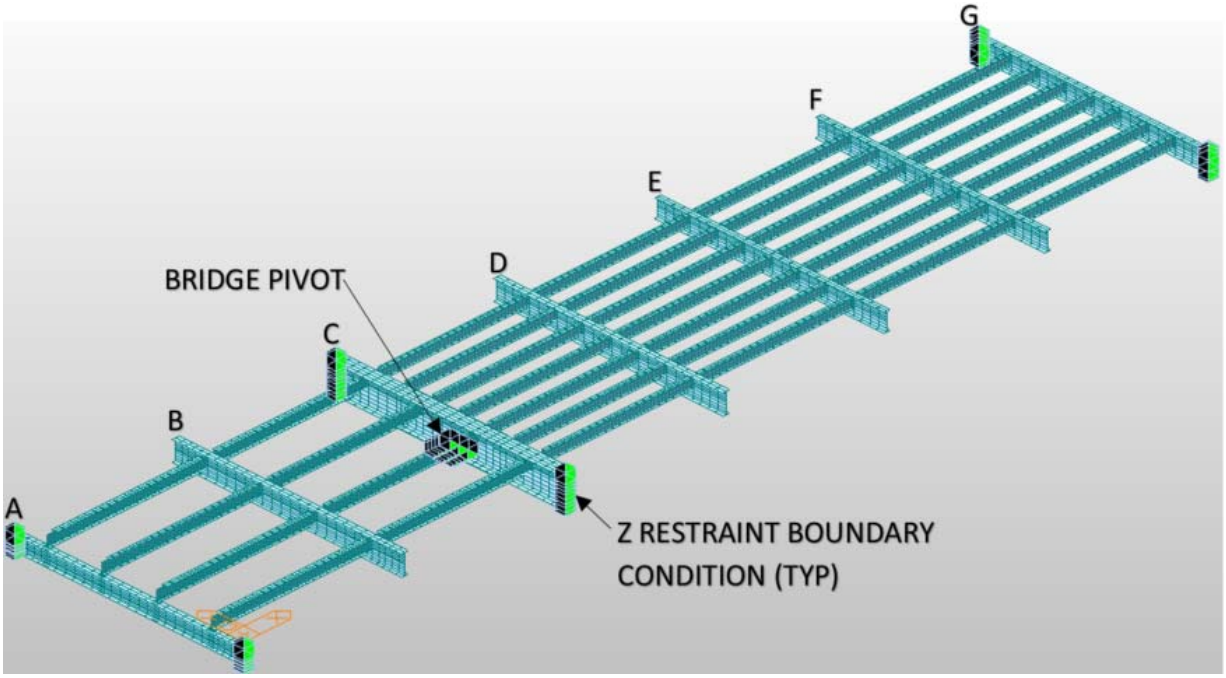

Figure 9. Initial FE Model Supports

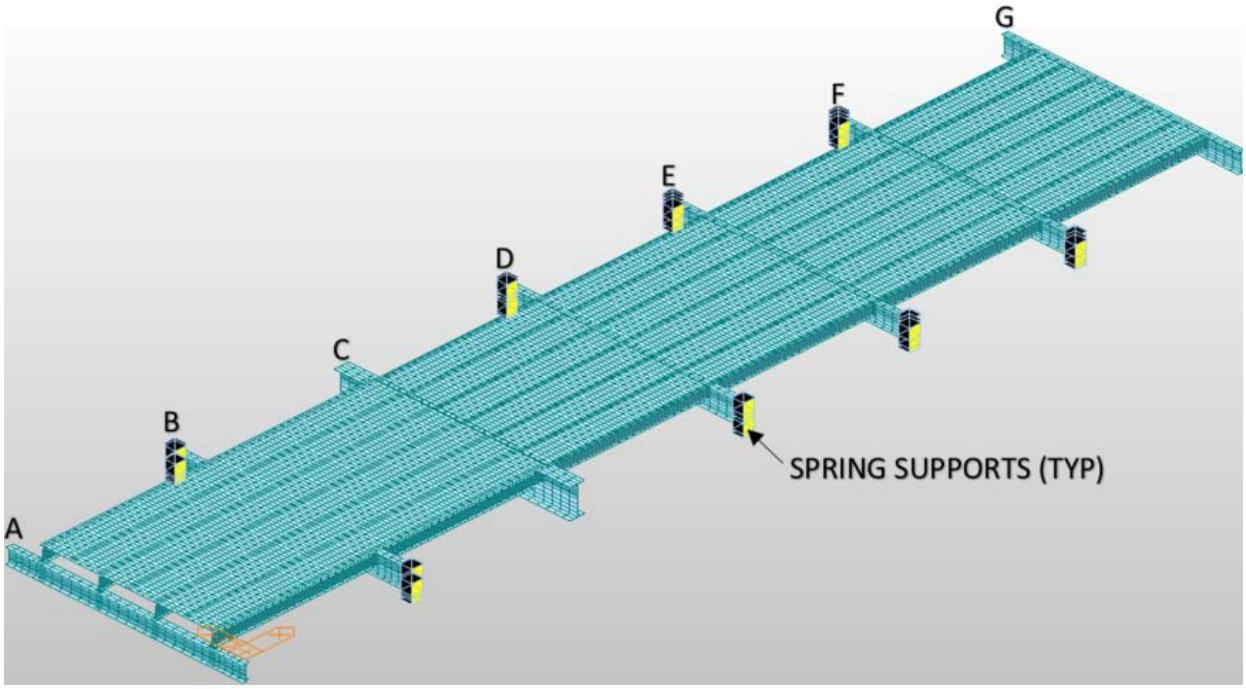

Figure 10. Initial FE Model Equivalent Spring Connections Floorbeams B, D, E, & F

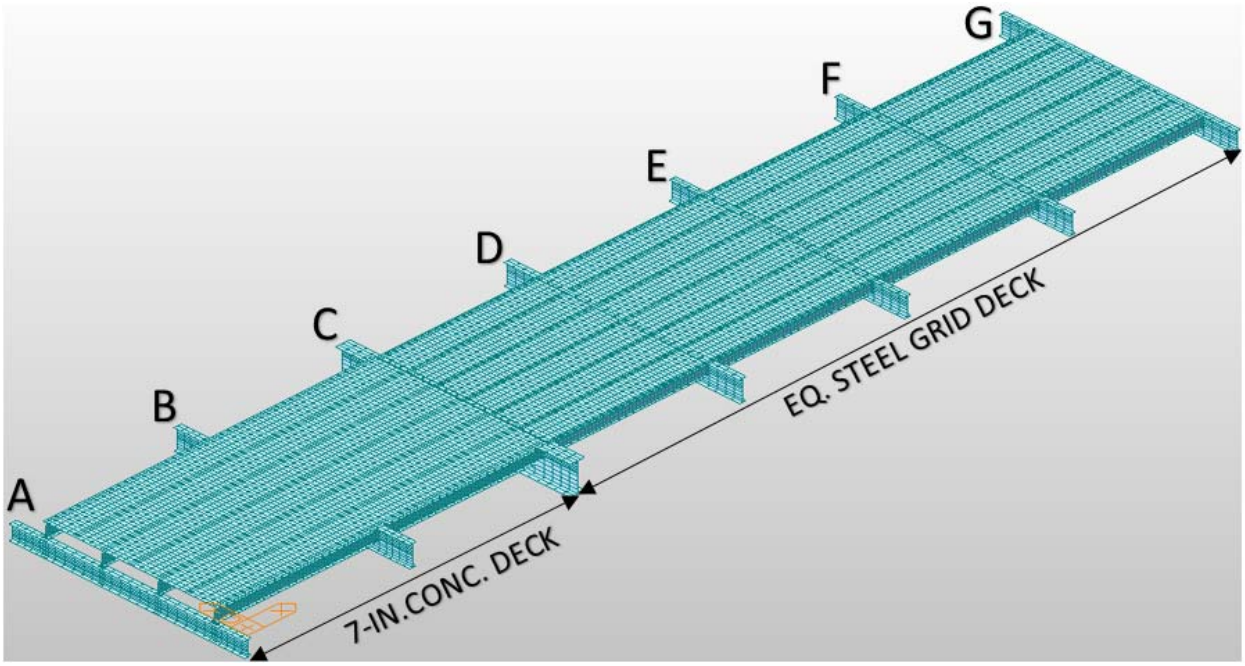

Figure 11. Initial FE Model Decks

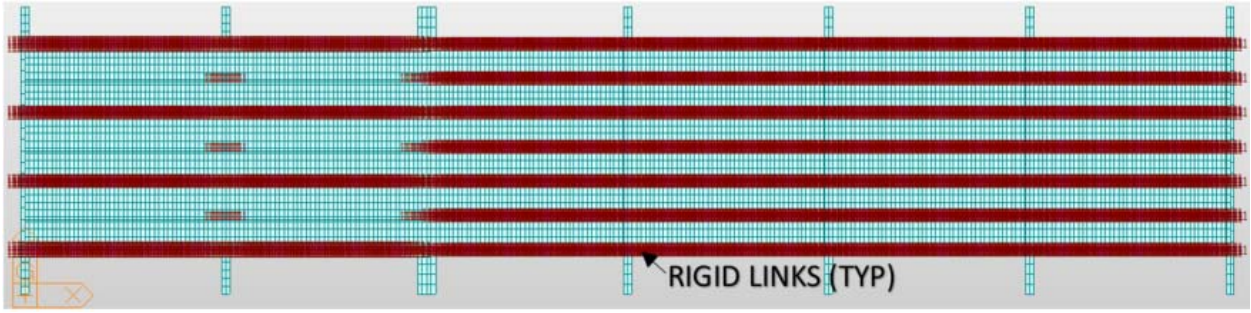

Figure 12. Initial FE Model Rigid Links

3.3. Diagnostic Load Test

The diagnostic test was carried out by attaching 22 strain gages to the stringers of Unit 2 and transverse Floorbeams B and E of the steel plate girder swing span bridge. The sensor locations can be seen in the instrumentation plans in Figure 13. For deficient Floorbeams B and E, strain gages were placed at five locations along its length (L): 0.0L, 0.25L, 0.5L, 0.75L, and 1.0L. This same technique was repeated for one interior and one exterior stringer of deficient stringer unit 2. For the remaining two stringers, gages are only placed at midspan to confirm results from the other two stringers. Thus minimizing labor, time, and unnecessary duplicate data.

There are several challenges to instrumenting movable bridges. Most gages on movable bridges need to be applied while working from either a snooper truck or a boat. The movable bridges in this study are both two-lane bridges with traffic flowing in both directions. As a result, gages were applied from a boat, rather than a snooper truck, to minimize traffic disruption on the roadway overhead. This method is sometimes a necessity for movable bridges because in many instances they are low lying near the water surface reducing vertical clearance. This makes accessing them with a bucket difficult and in some cases impossible. It is also important to account for disruptions due to marine traffic when estimating instrumentation times. When a vessel needs to pass, all installation needs to pause to “swing” the bridge into its open position. All wiring must be secured before opening the bridge. The wires connecting the strain gages to

the nodes must be secured as to not be lower than their tested elements while the bridge is in motion. Safe care of these wires is to prevent the wire from being damaged through contact with other bridge elements and breaking as the bridge swings open.

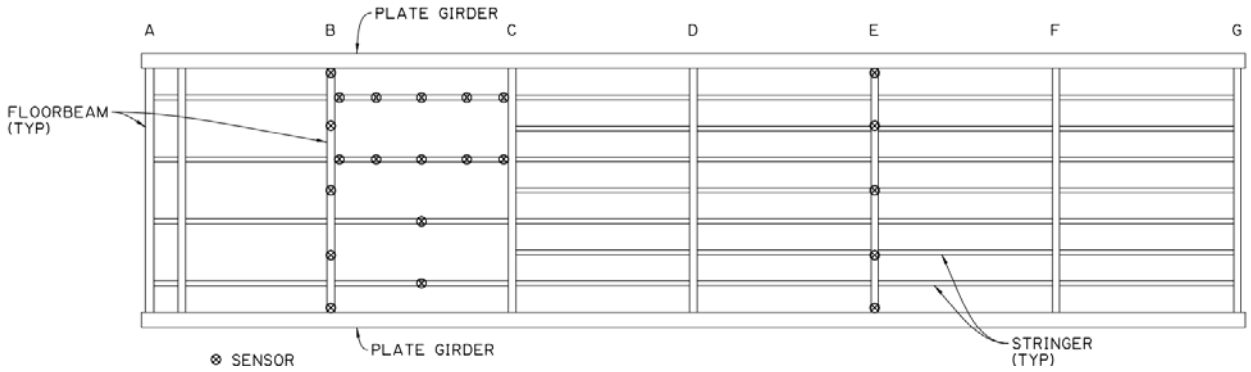

Figure 13. Location of Installed Gages for Steel Plate Girder Swing Span

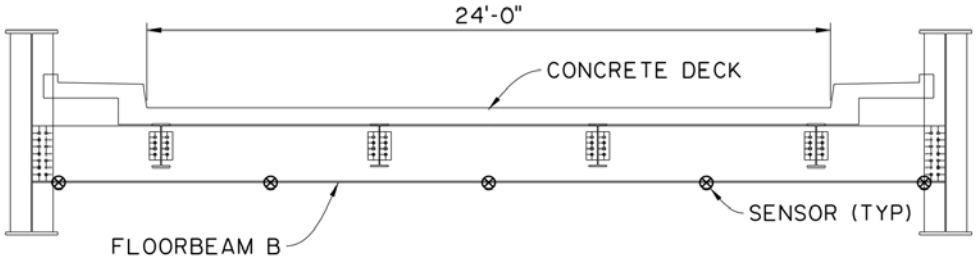

Figure 14. Typical Section at Floorbeam B

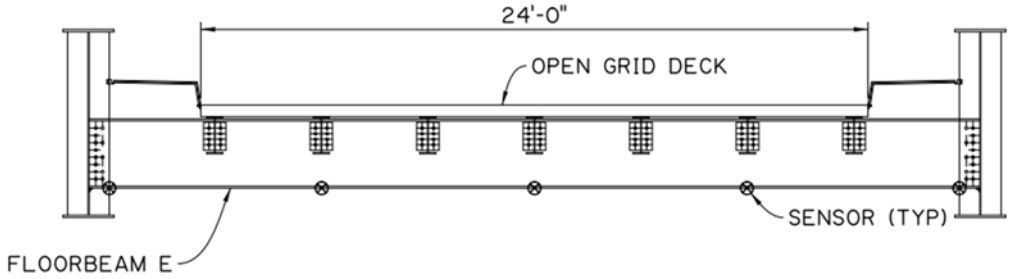

Figure 15. Typical Section at Floorbeam E

The testing instrumentation system consisted of both sensors and data acquisition hardware. After sensing the bridge response, the system translates it into a voltage signal. This signal is proportional to the measured response that the engineer is trying to retrieve. Each sensor has a calibration factor that can be used to convert the recorded voltage into the desired engineering

units. The ST350 strain gage is a Wheatstone bridge strain transducer provided by Bridge Diagnostics Inc. The schematic for the transducer can be seen in Figure 16.

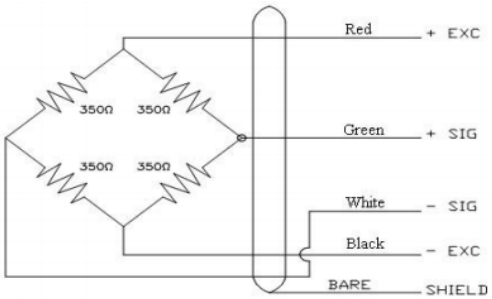

Figure 16. BDI ST350 Schematic
Source: (Campbell Scientific, Inc., 2008)

Strain gages were applied directly to the members of interest. The process of application begins with cleaning the steel element at the anticipated gage locations to remove any paint and debris. Then several measurements are taken to ensure the proper placement of the gage. First, measuring along the length of the member to locate the exact location as specified in instrumentation plans, then measuring along the width of the bottom flange to place the gage at the centerline the member, directly below the web. The reason for this is when a beam is not perfectly straight or if the end conditions are not level with one another, the beam will begin to experience some kind of torsion or lateral bending after applying loading to the element. The gage is then applied to the member longitudinally, in the direction of bending, with a fast setting adhesive.

Each gage is connected to a four channel node, such as the one shown in Figure 17-c. These nodes transmit the gage readings by way of a broadband system to the wireless data acquisition system. The strain data is then closely monitored and recorded throughout the entire diagnostic load test.

(a) Gage Installation to Unit 2 Interior Stringer

(b) Gage Installation to Floorbeam E

(c) Typical Four Channel Node

(d) Typical Installed Strain Gage

Figure 17. Installation of Gages

Figure 18. Boats used in installation.

After sensor application was completed, the bridge was prepared for loading. To ensure that the test trucks were loaded into the correct positions for testing, distance measurements were taken and marked on the bridge deck for each loading position. The bridge was then loaded with one truck at a time, each truck moving incrementally into more critical locations for both the instrumented stringers and floorbeams. Before each position change, the field results were compared to the predicted strains from the FE model. If the field strains were below the allowable strains of the bridge, ensuring the safety of the test without creating damage to the structure, the truck then proceeded to its next position. Finally, both trucks were placed on the bridge following the same procedure as the one-lane loaded scenario.

Two three-axle trucks were used to load the bridge. Table 10 and Table 11 provide the measured gross vehicle weight (GVW) of both loading trucks for bridges Bridge1 and Bridge2 respectively. The tests for each of these bridges were conducted on separate days and the trucks were reloaded each morning, resulting in slightly different testing weights. Figure 19 provides the truck configurations measured on site. The same two trucks were used for each testing day, therefore, preserving the truck configuration for both bridges. Only gross vehicle weight (GVW) was provided, i.e., individual wheel loads of each loading truck were not available. After a review of truck specifications, the front axle weight of the trucks used in this study is around 18,000 to 20,000lbs while the truck is unloaded (MACK Dump Trucks, 2020). The following assumptions are then made for the truck axle distributions: the front axle is conservatively taken as 18,000lbs, the remaining weight is distributed evenly between the two rear axles.

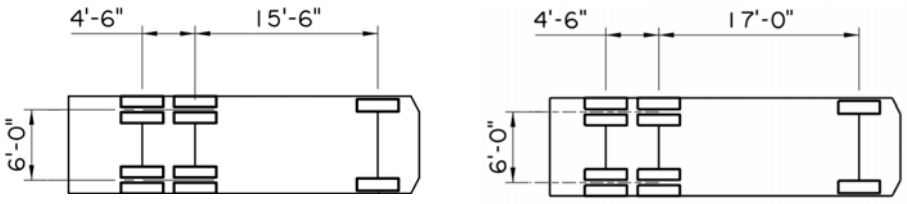

Test Truck No. 1 Test Truck No. 2

Figure 19. Loading Truck Configuration

Table 10. Loading Truck Weights (Bridge1)

Truck	Front Axle Weight (lbs.)	Rear Axle Weight (lbs.)		GVW (lbs.)
		Rear Axle 1	Rear Axle 2	
Truck No. 1	18,000	26,030	26,030	70,060
Truck No. 2	18,000	26,100	26,100	70,200

Table 11. Loading Truck Weights (Bridge2)

Truck	Front Axle Weight (lbs.)	Rear Axle Weight (lbs.)		GVW (lbs.)
		Rear Axle 1	Rear Axle 2	
Truck No. 1	18,000	26,140	26,140	70,280
Truck No. 2	18,000	26,140	26,140	70,280

The diagnostic load test consisted of seven total loading configurations, as can be seen in Table 12. Each tested floorbeam, Floorbeam B and E, was loaded in three load cases, as can be seen in Figure 21 and Figure 23. The first two cases consisted of two variations of one-lane loaded; a case in which one truck is loaded in one lane at a time. These two load cases are denoted as One-Lane Loaded (L1) and One-Lane Loaded (L2). The third case consists of both test trucks being loaded onto the test element at the same time in the Two-Lanes Loaded (L1L2) case. In all three load cases, the test truck or test trucks moved through four positions. The trucks begin in Position 1, with the centerline of the second axle of the truck six feet from the test

element location. The truck then moves in two feet increments until Position 4 is reached zero feet from the test element location. Figure 20 shows the truck positions for floorbeam cases.

Unit 2 Interior Stringer was loaded with one load case, Longitudinal Loading (One-Lane Loaded). In this loading case, the test truck is positioned directly on top of the tested element and moves longitudinally along the element. The trucks began in Position 1, with the centerline of the second axle of the truck six feet from the midpoint of the stringer. The truck was then moved in two feet increments until Position 4 was reached, zero feet from the midpoint of the stringer. To aid in clarity of the truck placement, the truck positions for the stringer are taken with respect to Floorbeam B, as can be seen in Figure 22; providing an easier reference point when measuring from on the bridge deck.

The changing of positions for all load cases from Position 1 to Position 4 increases the midspan moment in the tested element with Position 4 producing the maximum moment of the test load positions. At each load position, the measured strains were monitored and compared to both the predicted strains of the initial finite element model and the allowable strains. Once readings were verified as safe, the truck proceeded to the next position. The test concluded safely with no signs of distress observed.

Table 12. Testing Load Cases

Element	Load Case	Description
Floorbeam “B”	LC 1	One-lane loaded (L1)
	LC 2	One-lane loaded (L2)
	LC 3	Two-lane loaded (L1L2)
Floorbeam “E”	LC 4	One-lane loaded (L1)
	LC 5	One-lane loaded (L2)
	LC 6	Two-lane loaded (L1L2)
Unit 2 Interior Stringer	LC 7	Longitudinal Loading (One-Lane loaded)

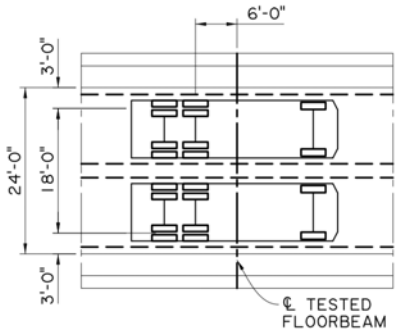

(a) Position 1

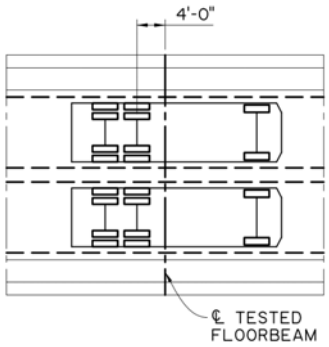

(b) Position 2

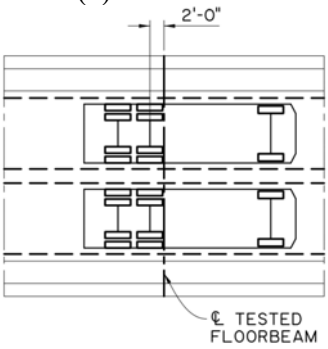

(c) Position 3

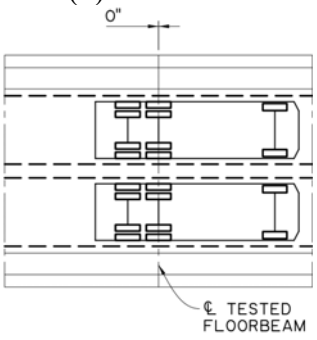

(d) Position 4

Figure 20. Plan View of Truck Positions for Floorbeam Cases

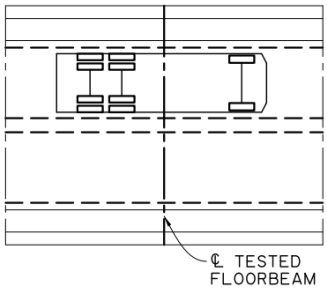

One-Lane Loaded (L1)

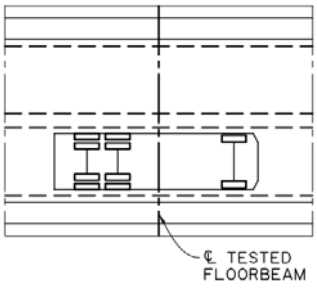

One-Lane Loaded (L2)

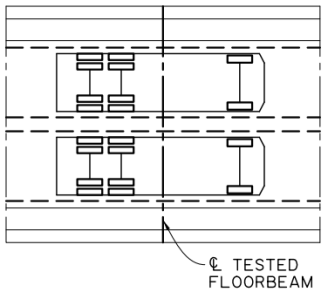

Two-Lanes Loaded (L1L2)

Figure 21. Plan View of Lane Positions with One-Lane Loaded and Two-Lanes Loaded

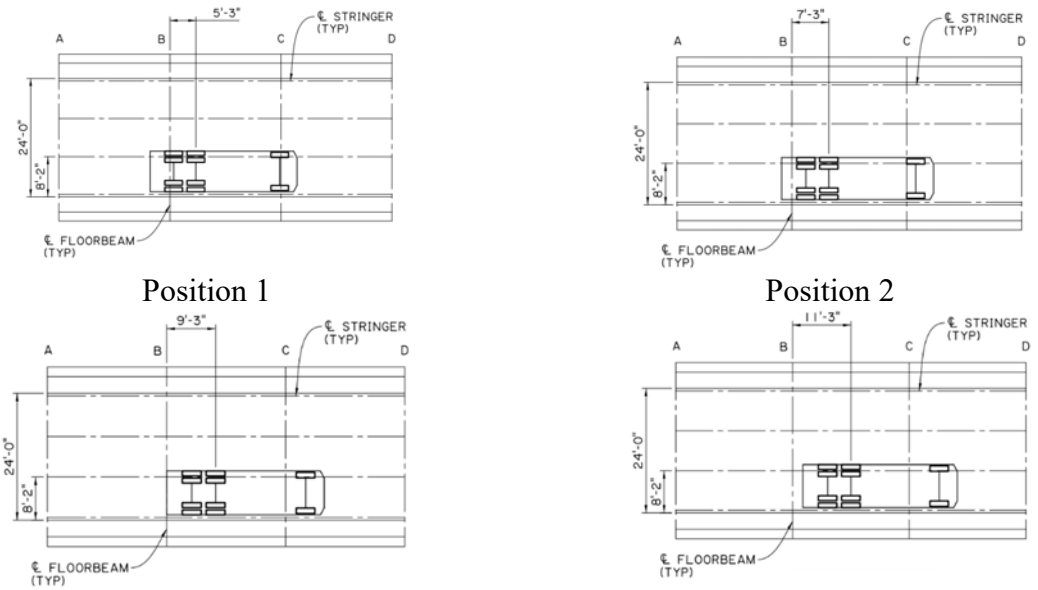

Position 1 Position 2

Position 3 Position 4

Figure 22. Plan View of Truck Positions for Stringer Longitudinal Loading

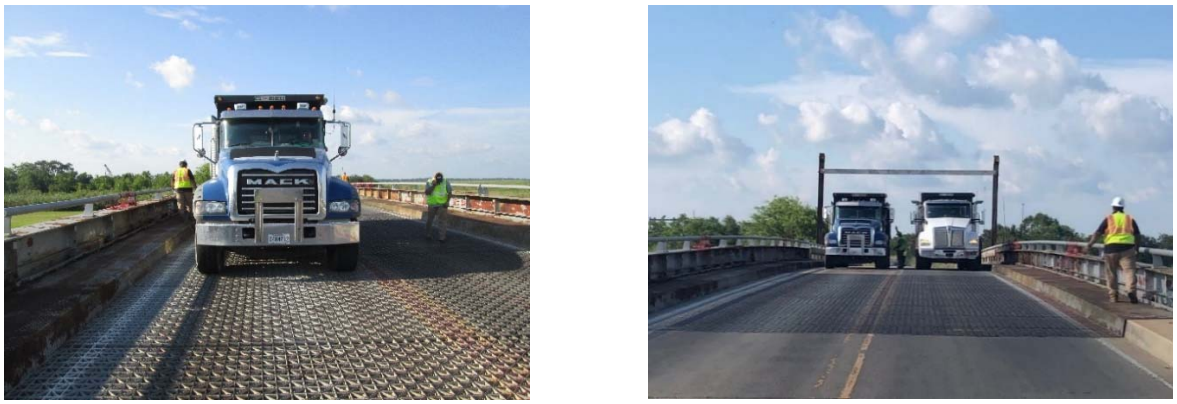

One-Lane Loaded Two-Lanes Loaded

Figure 23. Truck positions during testing for different load cases.

3.4. Finite Element Model Calibration

Once the load test was completed, the results were compared to the initial finite element model. The initial model was created based on the provided dimensions and materials from the as-built plans. Discrepancies in field results and FE model results are often a result of wrong modeling assumptions caused by insufficient knowledge of structural details and materials properties, simplifications of details, exclusion of important non-structural components, or

misinterpretation of boundary conditions (Shahsavari, Mashayekhi, Mehrkash, & Santini-Bell, 2019). A review of the diagnostic load test results clearly showed that the bridges were stiffer than what was predicted by the initial FE model. As a result, the model was calibrated to reflect the real bridge performances.

To evaluate the effectiveness of the model, an error estimator was utilized to assess the difference in load test and calibrated FE model results. In this study, Equation (10) is used to collectively estimate the error from the sensors employed in the field testing. The minimum error was obtained by properly modeling boundary conditions based on interpretations derived from testing results, including participation of secondary and non-structural elements, and incorporating unintended composite action. The model was considered acceptable when an error below 20% was achieved.

It should be noted that Equation (10) provides an overall estimate of the model error based on multiple sensors rather than relying on just one sensor, which becomes sensitive to the conditions at this one sensor location. Furthermore, sensors recording readings below a certain threshold were not considered when evaluating the error according to Equation (10). This was done to avoid overestimating the error when sensors away from the considered floorbeam or stringer record minimal readings, for which the slightest change translates into a large error.

$$Error = \sum^{n_S} \left(\sqrt{\left[\frac{\left(y_{exp} - y_{FE}\right)}{y_{exp}} \right]^2} \right) * \frac{1}{n_S} \tag{10}$$

where,
y_{exp} = Sensor data obtained from field results
y_{FE} = Sensor data obtained from FE model
n_S = Number of sensors connected to tested member

4. RESULTS

This chapter first provides the results of the diagnostic load test for both tested bridges, Bridge1 and Bridge2. The results are then compared to the predicted values from the initial finite element model. Finally, FE model calibration to minimize the differences in the finite element model and testing results is described. Finally, load rating analysis was performed on the three tested elements.

4.1. Diagnostic Load Test Results

Comparison between field measurements and finite element results will be conducted for the strain sensors at the position shown on the instrumentation plan described earlier in Section 3.3. Figure 24 to Figure 27 show the measured strain along the length of Floorbeam B for the four truck positions of one-lane loaded (Load Case 1) and two-lanes loaded (Load Case 3), respectively. The strains increase as the induced moments increase associated with the different truck positions. For the one-lane loaded case, the maximum measured strain in Bridge1 and Bridge2 is approximately 160 microstrain for both bridges as can be seen in Figure 24 and Figure 25, respectively. For the two-lanes loaded case, Figure 26 and Figure 27 show that the maximum measured strain in Bridge1 and Bridge2 is approximately 290 microstrain and 270 microstrain, respectively. For both bridges, the maximum measured strain occurred at the element midpoint as a result of Position 4 of two-lanes loaded.

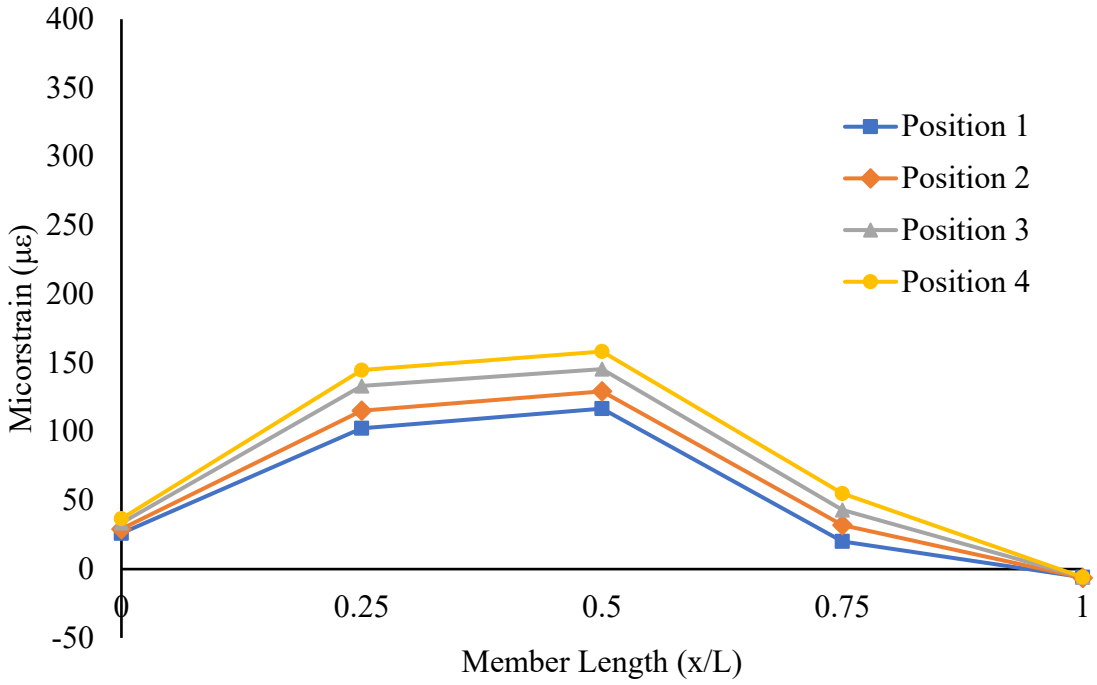

Figure 24. Measured Strain of Floorbeam B for One-Lane Loaded (Load Case 1) (Bridge1)

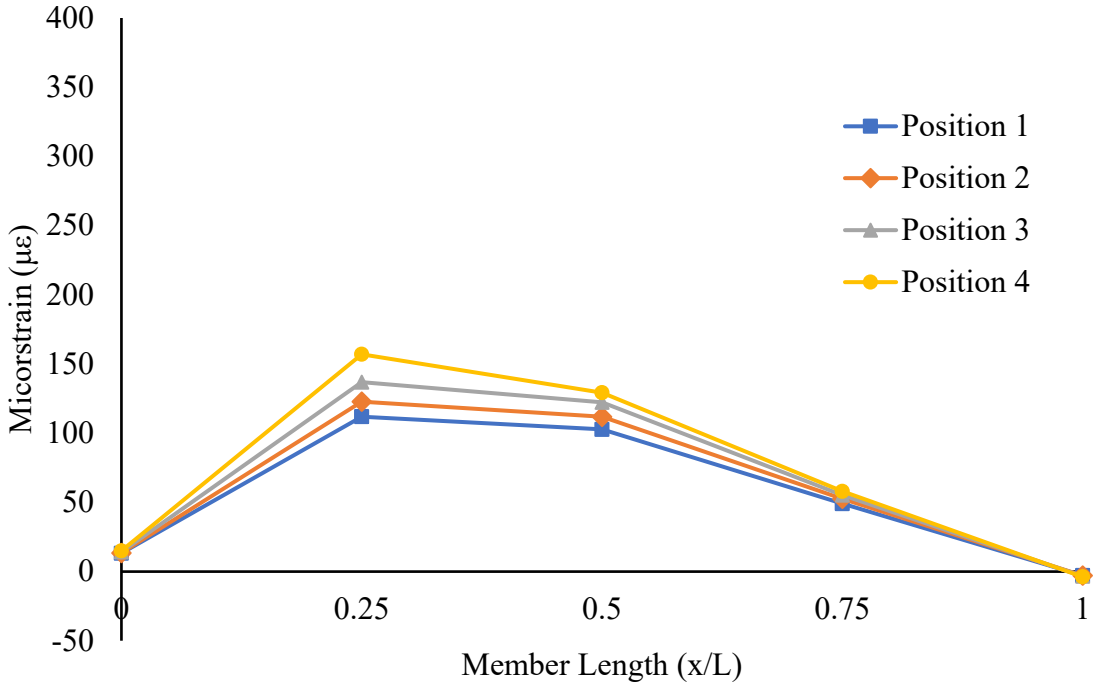

Figure 25. Measured Strain of Floorbeam B for One-Lane Loaded (Load Case 1) (Bridge2)

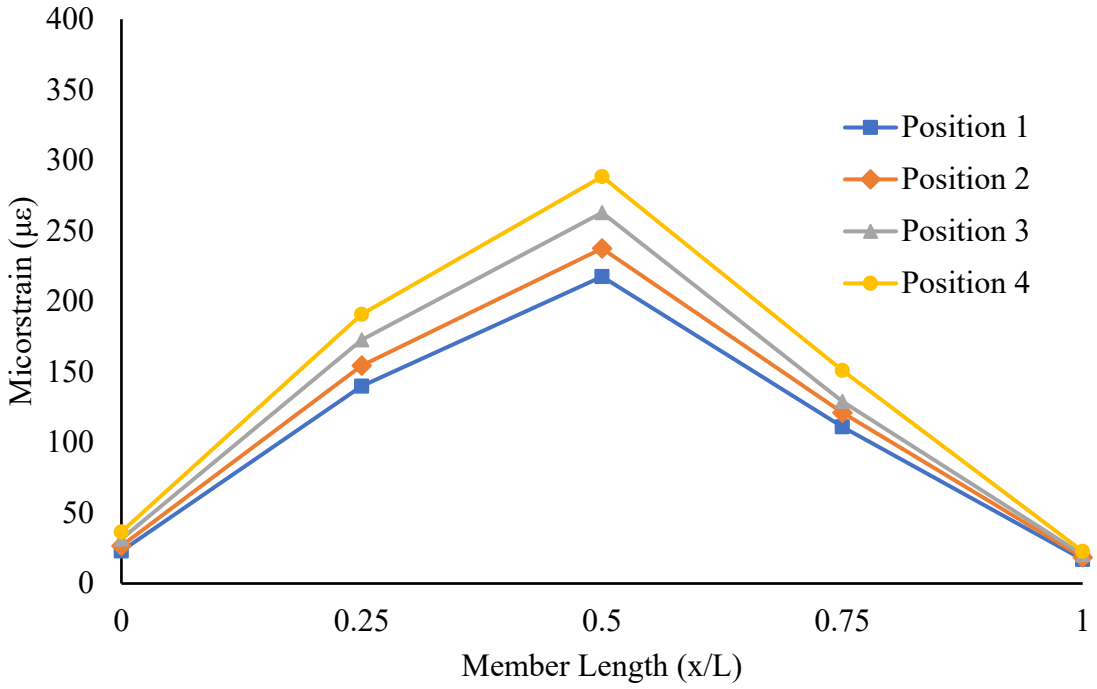

Figure 26. Measured Strain of Floorbeam B for Two-Lanes Loaded (Load Case 3) (Bridge1)

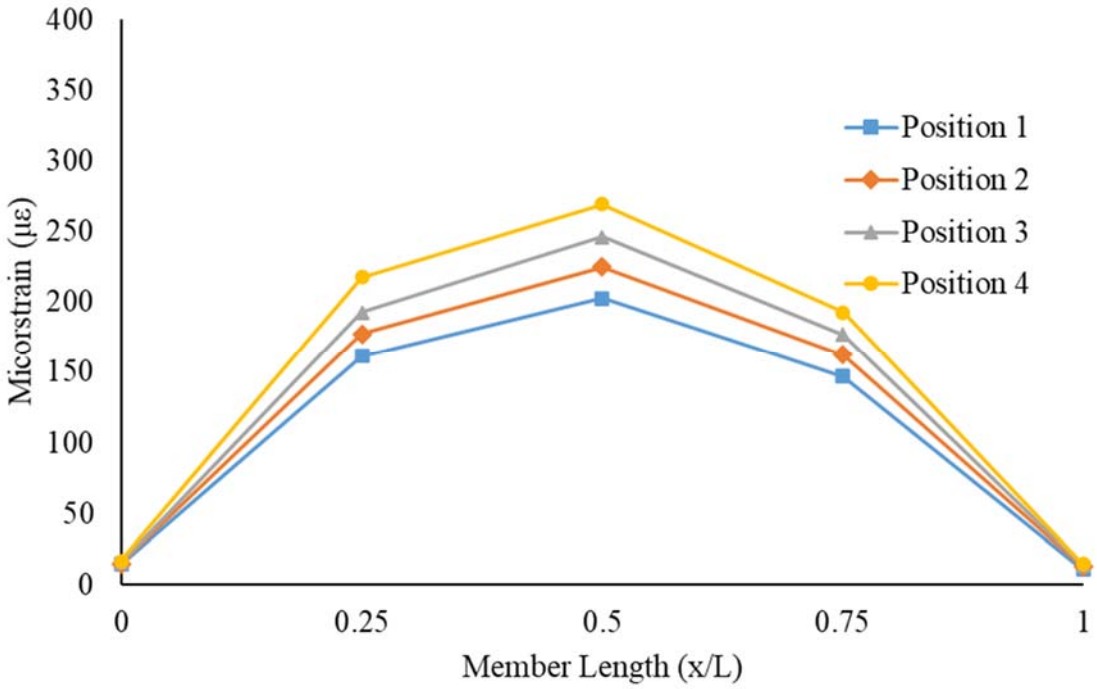

Figure 27. Measured Strain of Floorbeam B for Two-Lanes Loaded (Load Case 3) (Bridge2)

Figure 28 to Figure 31 show the measured strains along the length of Floorbeam E for the four truck positions of one-lane loaded (Load Case 5) and two-lanes loaded (Load Case 6), respectively. As with Floorbeam B, the strains increase as the induced moments increase associated with the truck positions. Figure 28 and Figure 29 show that the maximum measured strain for the one-lane loaded case in Bridge1 and Bridge2 is approximately 200 microstrain and 230 microstrain, respectively. For the two-lanes loaded case, the maximum measured strain in Bridge1 and Bridge2 is approximately 360 microstrain and 325 microstrain, respectively, as can be seen in Figure 30 and Figure 31. The maximum measured strain for Bridge1 occurred at the element midpoint as a result of Position 4 two-lanes loaded, narrowly greater than the strain value recorded at 0.25L of approximately 350 microstrain. The maximum measure strain for Bridge2 occurred at the gage location 0.75L.

It should be noted that the diagnostic load test strain values for both tested bridges are not symmetric about 0.5L for Floorbeam E, which may be a result of the beam condition and applied load placement. During testing, a steel plate was found bolted to the top and bottom flange of Floorbeam E. This is a result of a bridge rehabilitation project and was not a part of the original structure. The steel plate's thickness is ½-inch and a length of approximately 7'-8" centered at the midpoint of Floorbeam E. The presence of the plate can also exacerbate discrepancies in the off-center position loading of the two testing trucks as they are positioned on the bridge deck, leading to skewed strain curves.

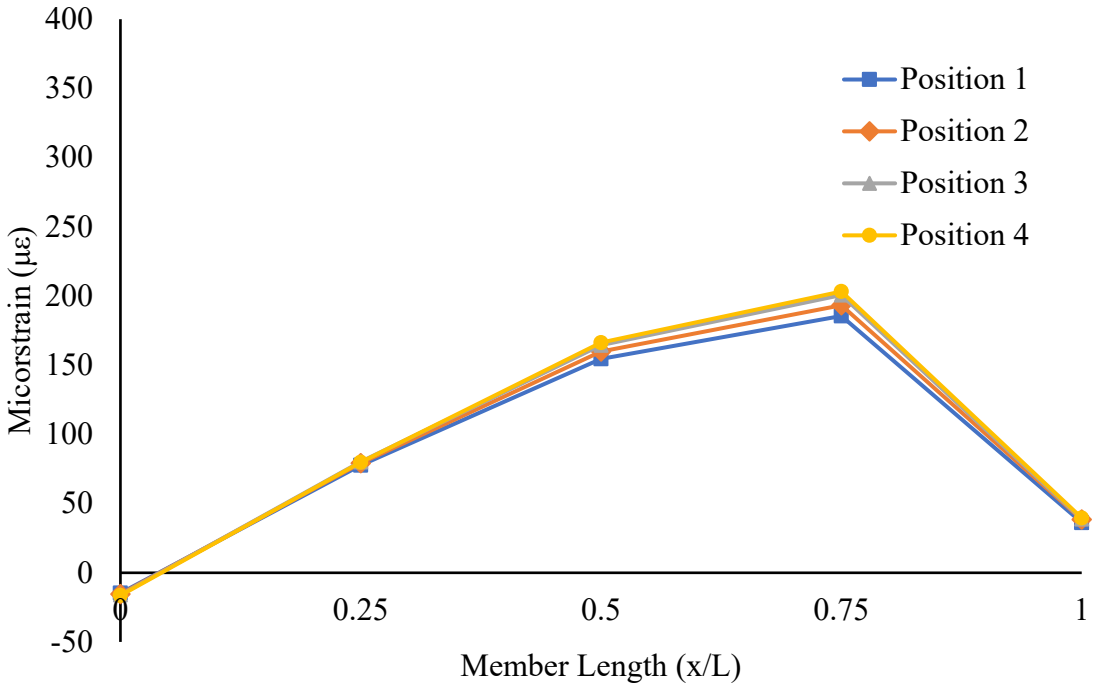

Figure 28. Measured Strain of Floorbeam E for One-Lane Loaded (Load Case 5) (Bridge1)

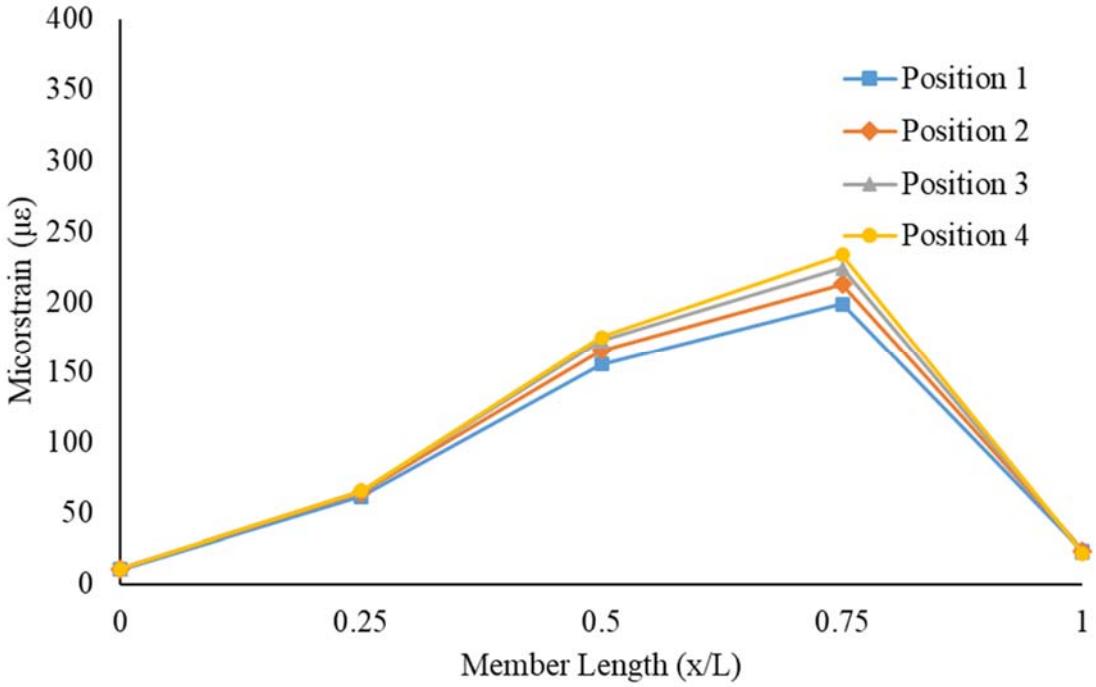

Figure 29. Measured Strain of Floorbeam E for One-Lane Loaded (Load Case 5) (Bridge2)

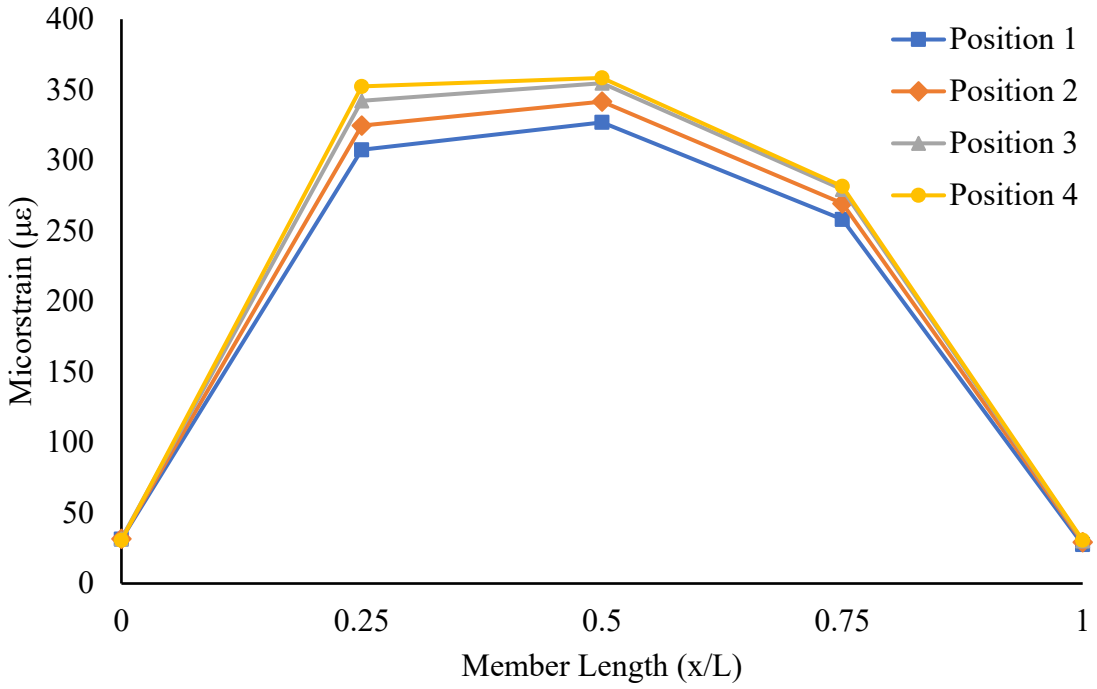

Figure 30. Measured Strain of Floorbeam E for Two-Lanes Loaded (Load Case 6) (Bridge1)

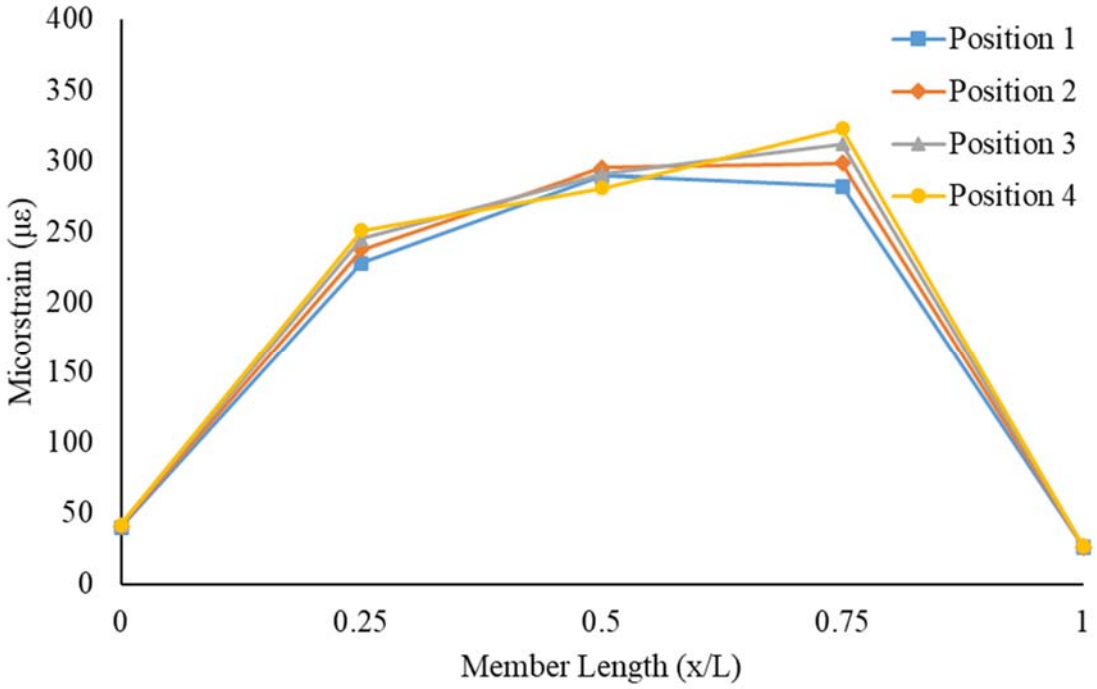

Figure 31. Measured Strain of Floorbeam E for Two-Lanes Loaded (Load Case 6) (Bridge2)

Figure 32 and Figure 33 show the measured strain along the length of Unit 2 Interior Stringer for the four truck positions of longitudinal loading case (Load Case 7). As expected, the strains increase as the induced moments increase associated with the truck positions. The maximum measured strain for the interior stringer in Bridge1 and Bridge2 is approximately 160 microstrain and 140 microstrain, respectively (see Figure 32 and Figure 33). For both bridges, the maximum measured strain occurred at the element midpoint as a result of Position 4 of the longitudinal loading case.

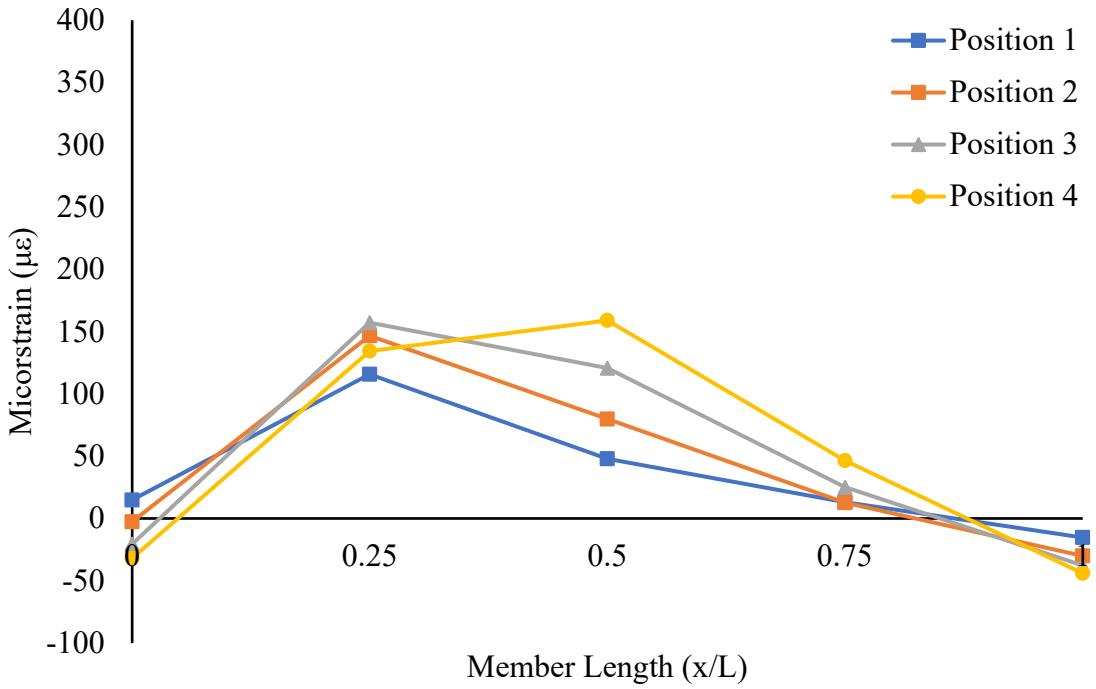

Figure 32. Measured Strain of Unit 2 Interior Stringer for Longitudinal Loading (Load Case 7) (Bridge1)

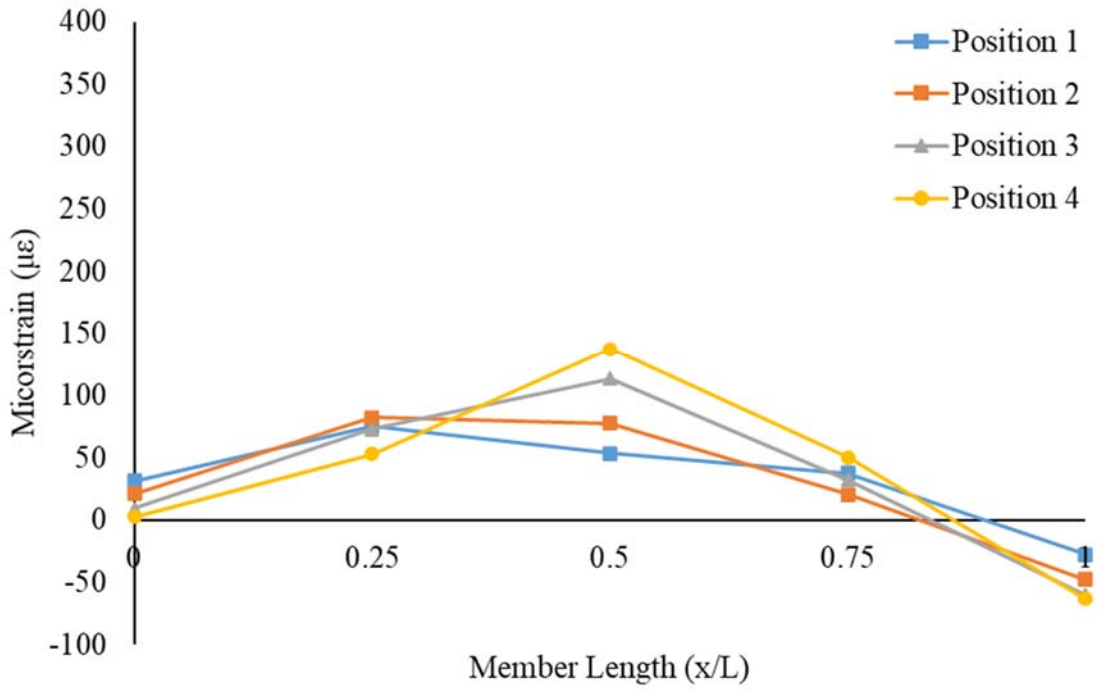

Figure 33. Measured Strain of Unit 2 Interior Stringer for Longitudinal Loading (Load Case 7) (Bridge2)

4.2. Initial Finite Element Results

Strain results were extracted from the initial finite element model for Floorbeam B for Position 4 of two-lanes loaded (Load Case 3), for Floorbeam E for Position 4 of two-lanes loaded (Load Case 6), and for Unit 2 Interior Stringer for Position 4 of Longitudinal Loading (Load Case 7). Position 4 produces the maximum mid-span moment of all tested load case positions in each element. The initial FE model strain results considering both the composite (C) and non-composite (NC) models are compared to those obtained from the diagnostic load test in Figure 34, Figure 36, and Figure 38. Figure 35, Figure 37 and Figure 39 show the deformed shapes of the bridge under the aforementioned load cases and positions causing the maximum effect. It should be noted that the deck is not shown in these figures for clarity.

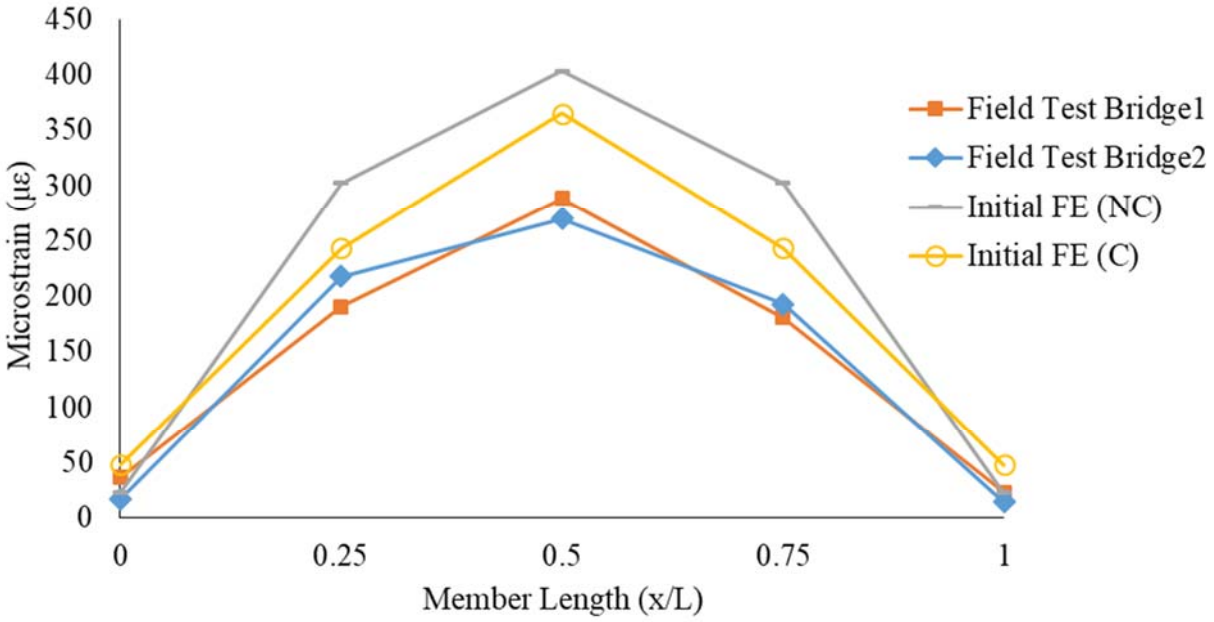

Figure 34. Measured and Computed Strain Comparison for Floorbeam B for Position 4 of Two-Lanes Loaded (Load Case 3)

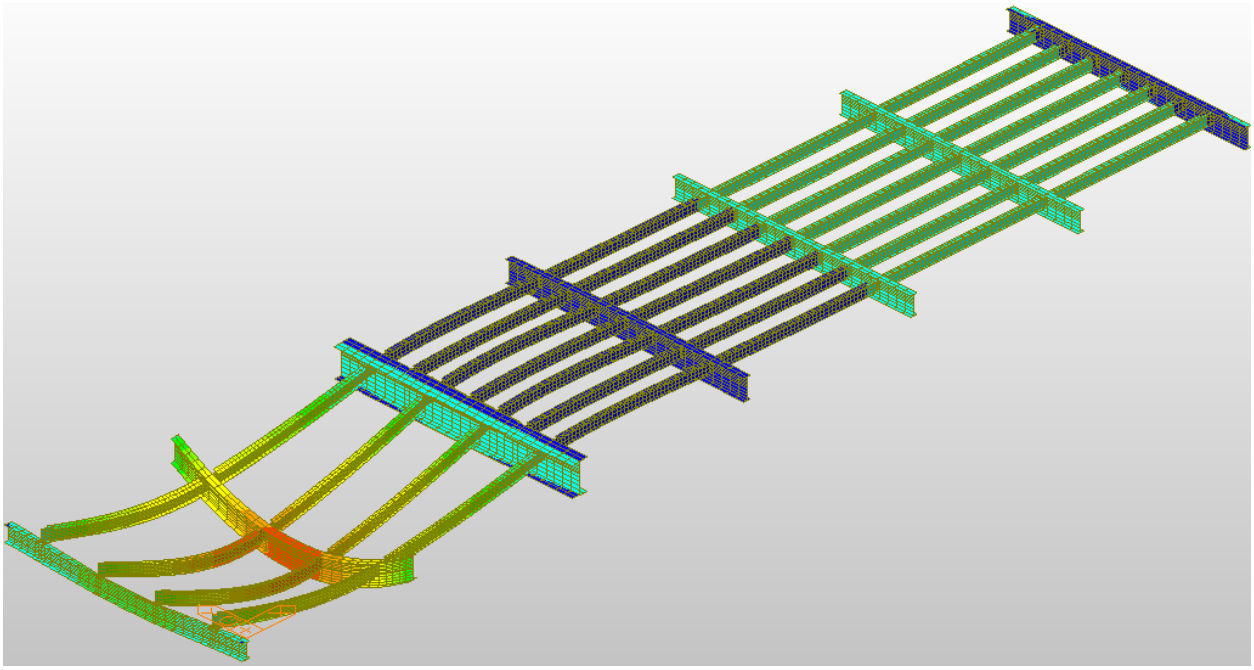

Figure 35. Deformed Shape and Displacement Contour (DZ) for Position 4 of Two-Lanes Loaded (Load Case 3) (Deck Not Shown for Clarity)

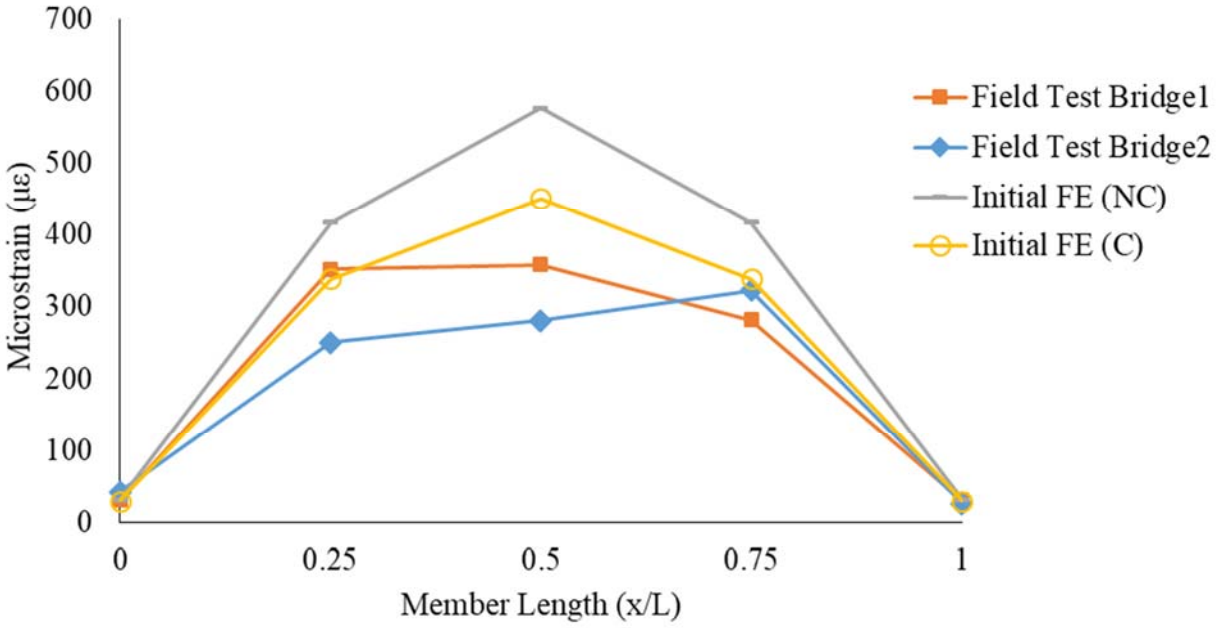

Figure 36. Measured and Computed Strain Comparison for Floorbeam E for Position 4 of Two-Lanes Loaded (Load Case 6)

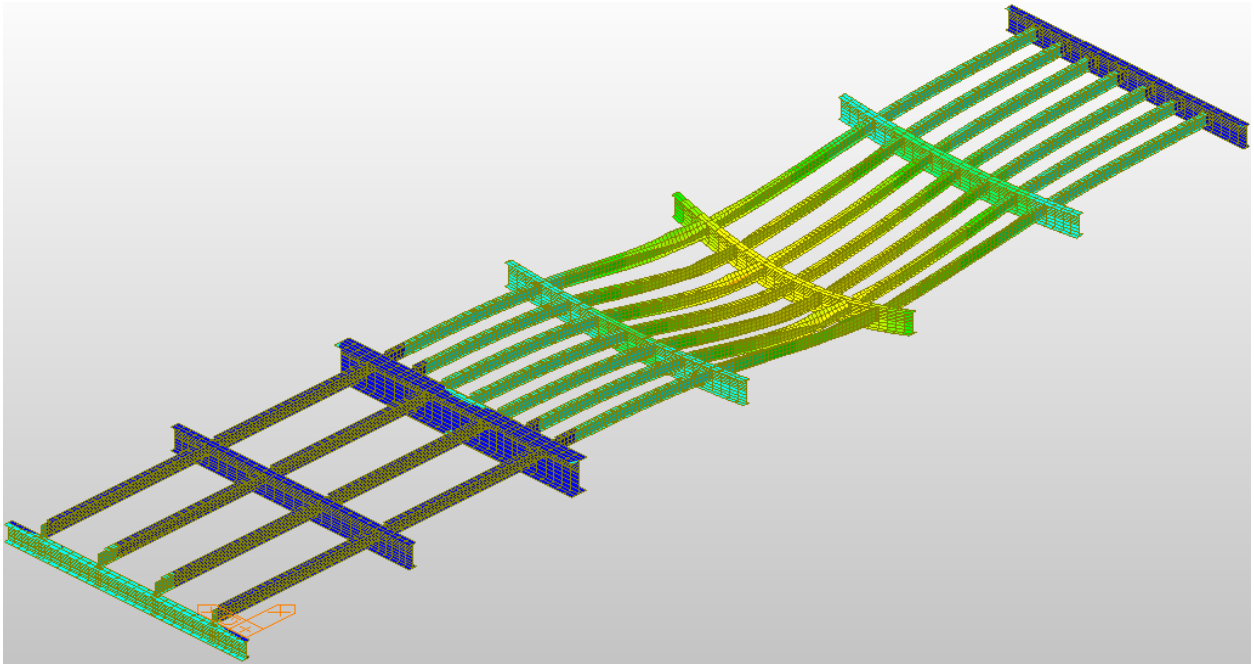

Figure 37. Deformed Shape and Displacement Contour (DZ) for Position 4 of Two-Lanes Loaded (Load Case 6) (Deck Not Shown for Clarity)

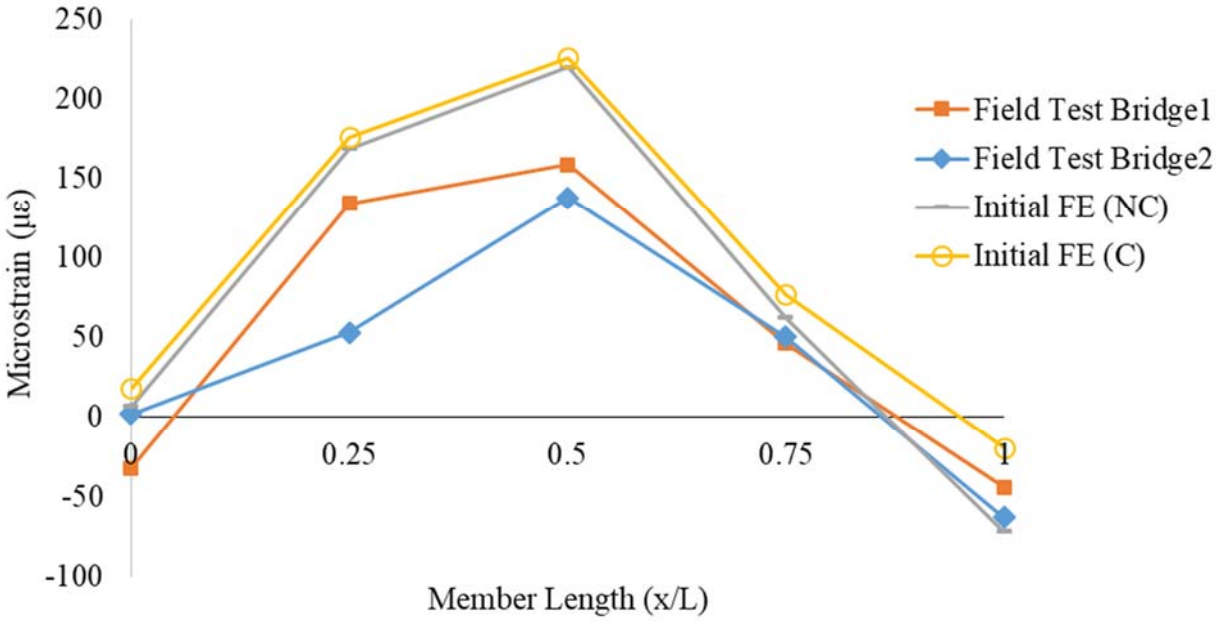

Figure 38. Measured and Computed Strain Comparison for Unit 2 Interior Stringer for Position 4 of Longitudinal Loading (Load Case 7)

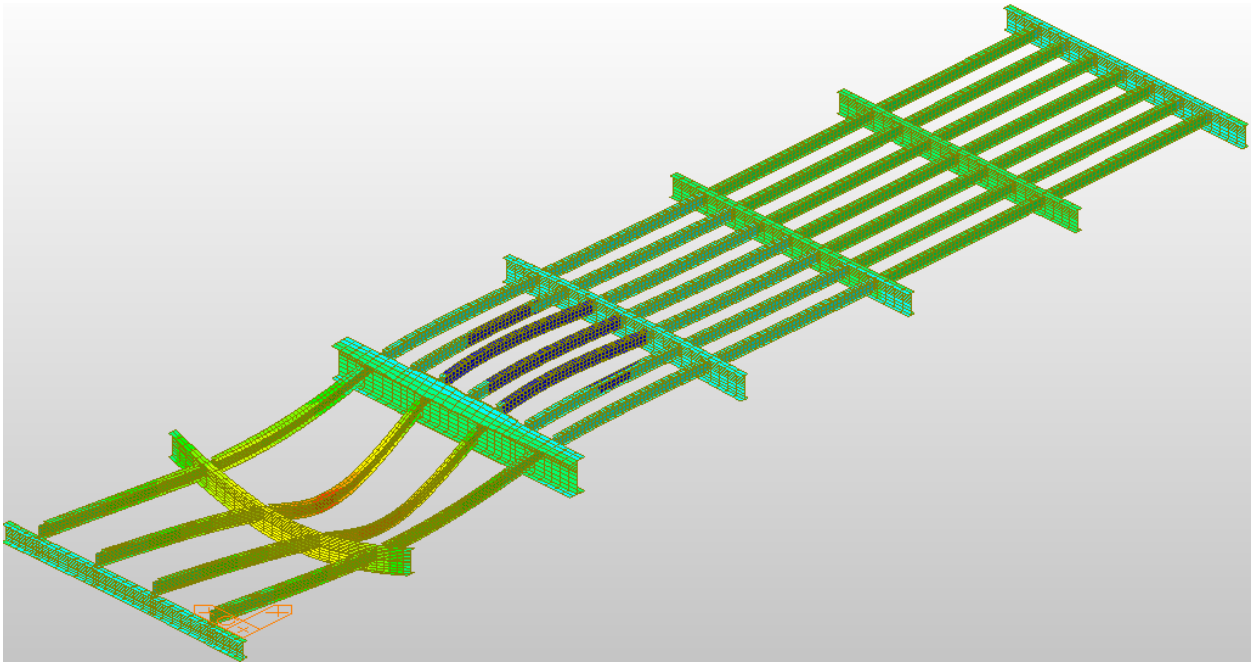

Figure 39. Deformed Shape and Displacement Contour (DZ) for Position 4 of Longitudinal Loading (Load Case 7) (Deck Not Shown for Clarity)

It can be seen from the strain plots that the non-composite and composite initial FE model curves are higher than the measured strain values in both tested bridges for all load cases.

The initial FE model values are closest to the tested values at the member ends, 0.0L and 1.0L, where a strain close to zero is to be expected. For tested Floorbeam E, at gage location 0.25L the strain value recorded from the composite FE model is approximately equal to the strain recorded from Bridge1 for Position 4 of two-lanes loaded. For all other comparisons at gage locations 0.25L, 0.5L, and 0.75L in Figure 34, Figure 36, and Figure 38 the FE model results are greater than the recorded value from both diagnostic load tests.

Utilizing the Error Estimator from Equation (10), the error values from the initial FE model compared to the field results are shown in Table 13. The error estimation in Table 13 includes all five strain gages on each tested member, however, far away sensors on other components not affected by the most critical load case were excluded as stated earlier. The data compared for each tested member consists of the most critical loading position, Position 4, for all three members. For Floorbeams B and E, the compared loading case included two lanes loaded. The largest error for Floorbeam B, Floorbeam E, and Unit 2 Interior Stringer were 98%, 49%, and 220%, respectively. These error levels are extremely high, and therefore, it can be said that the initial finite element model does not accurately represent the actual bridge behavior. Consequently, a more representative model was deemed necessary, which is described next along with its calibration.

Table 13. Error Estimation Initial FE Model vs Field Tests

Error				
	Field Test Bridge1		Field Test Bridge2	
Element	Initial FE Model (NC)	Initial FE Model (C)	Initial FE Model (NC)	Initial FE Model (C)
Floorbeam B	41%	46%	46%	98%
Floorbeam E	27%	11%	49%	28%
Unit 2 Int. Stringer	57%	71%	103%	220%

4.3. Final Finite Element Model and Calibration

After comparing the initial finite element model results to those from the diagnostic load test, the model was calibrated until the necessary error result was reached for an acceptable calibrated model. In the model calibration process, several changes were made to the initial model to replicate the field results more accurately.

4.3.1. Major Model Changes

The first change made to the finite element model was the inclusion of secondary members that exist as part of the pivoting structure of the bridge. Below Stringers 2 and 3 of stringer Unit 2 and Stingers 3 and 5 of stringer Unit 3 additional stringers are used to support the pivoting motion of the bridge. These additional stringers are 14WF34 members and are connected directly to Floorbeams B, C, and D and can be seen in Figure 40 and Figure 41. Also seen in Figure 40 is the wheel at the pivot. This is another adjustment made in the calibrated model. Included in the calibrated model was the presence of the extra wheel contact points from the pivot location in the longitudinal direction along the bridge. These two additional contact points can be seen in Figure 41 and were modeled in the finite element model as point supports restricting displacement in the Z direction, Figure 50.

Figure 40. Additional Stringers at Pivot

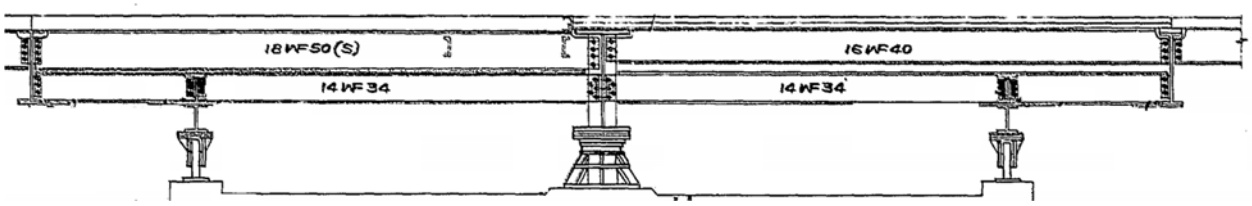

Figure 41. Additional Supports at Pivot

Next in the model calibration process was the inclusion of non-structural members. The two bridges tested were asymmetrical about the pivot point, consisting of one arm at 45-feet in length with a concrete deck and one arm at 90-feet in length with a steel grid deck. For the first stringer unit after the pivot point, Unit 3, the grid is filled with concrete. For every unit thereafter, the grid is open to ensure a balance of the weights of the asymmetric sides while the bridge is in the opened position, shown in Figure 42. To assist in the even weight balance about the pivot, a concrete counterweight is added to the shorter 45-foot arm, cast around Floorbeam A as seen in Figure 43. After diagnostic testing, it is understood that the concrete counterweight, while not its primary intention, increases the stiffness of Floorbeam A since it is fully embedded inside the counterweight. The counterweight was modeled in the calibrated FE model using eight node solid elements.

Figure 42. Bridge in Open Position

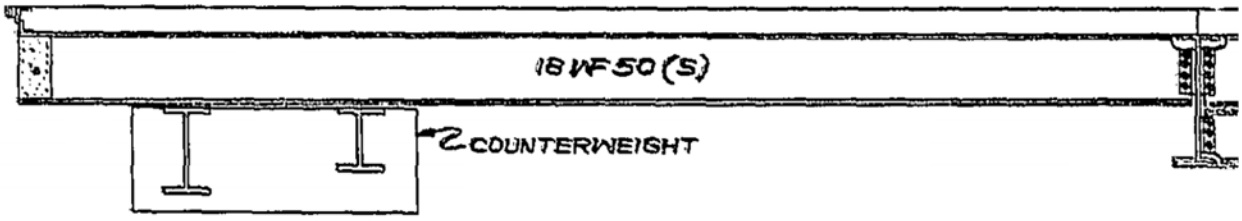

Figure 43. Elevation View of Concrete Counterweight

After a comparison of the tested and modeled results of Floorbeam E, reevaluation was needed for the equivalent steel grid deck modeled in the initial FE model. In the initial FE model, the steel grid deck was modeled using an equivalent deck at a thickness of 2/3-inch at an eccentricity from the top of the stringer flanges of 1/3-inch. For the updated model, the equivalent steel grid deck is modeled as a homogeneous steel plate equal to the height grid cross bar, 2.0625”. The new eccentricity of the deck was therefore located at the center of the cross bar, a distance of 4.15625” from the top of the stringer flanges. A detail of the steel grid deck can be seen in Figure 44.

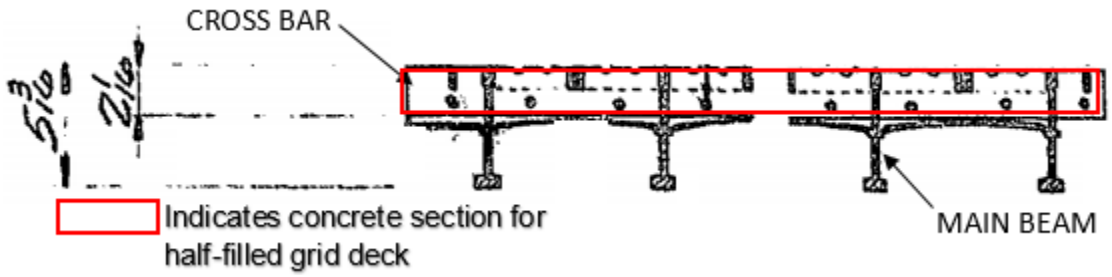

Figure 44. Steel Grid Deck

4.3.2. Modeling of Connection between Floorbeams and Plate Girders

A separate analysis was performed to determine the proper conditions for the floorbeam ends. As stated previously in Section 3.2, the plate girder was not modeled in the initial FE model. Instead, equivalent springs were modeled to simulate the floorbeam and plate girder connection. To test this modeling technique four different floorbeam end conditions were modeled and compared to the diagnostic load test results. The modeled floorbeam was Floorbeam B. The loading applied consisted of point loads from Rear Axle 1 of the two test trucks in Two-Lanes Loaded Position 4 (Load Case 3).

Four separate end conditions were analyzed, as can be seen in Figure 45. In the first two models, springs equivalent to the vertical (V) and horizontal (H) stiffness of the plate girders were used to simulate the plate girder and floorbeam connection in both vertical and horizontal directions. In the first model (VH-cent), the equivalent springs were applied directly to the center of the web of Floorbeam B. In the second model (VH-dist), the equivalent springs were distributed evenly vertically along the web to simulate the rivet connections. The third model (Comp-Restricted), a fixed boundary condition was placed on the web and flanges of Floorbeam B at both ends. For this case, the flanges were extended until the end of the floorbeam to create a connection that acted across the entire end plane. The final model (WebOnly-Restricted), a fixed boundary condition was placed on the web of Floorbeam B at both ends. The results of all four

models can be seen in Figure 46. When compared to the test results shown in Figure 26 and Figure 27 the modeling technique used in the initial FE model (VH-dist), as shown in Figure 46, appeared to be an appropriate approximation. As will be discussed later, completely restricting end movement is not realistic due to the fact that the plate girder deforms, which releases, or substantially reduces, this end constraint. Therefore, after further investigation, the plate girders were modeled to allow for the inclusion of the lateral bracing members.

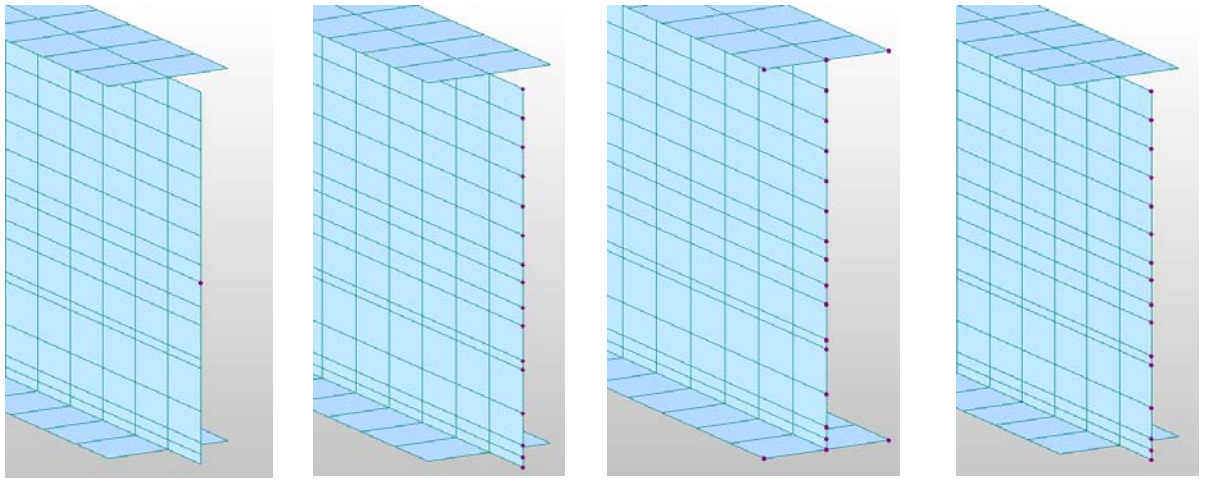

Figure 45. Floorbeam End Conditions

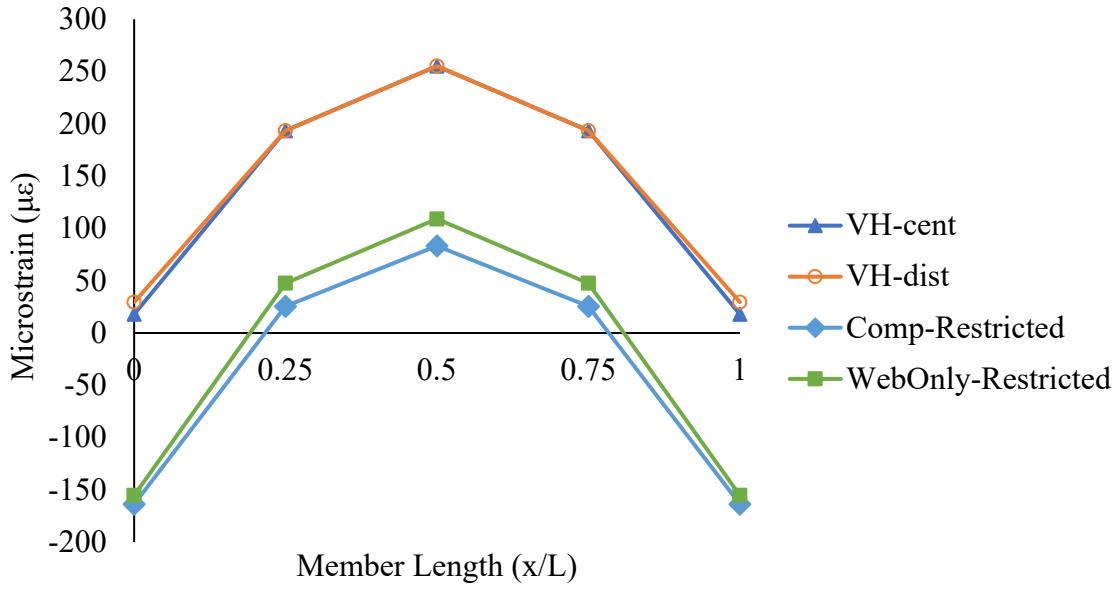

Figure 46. Floorbeam B End Condition Comparisons

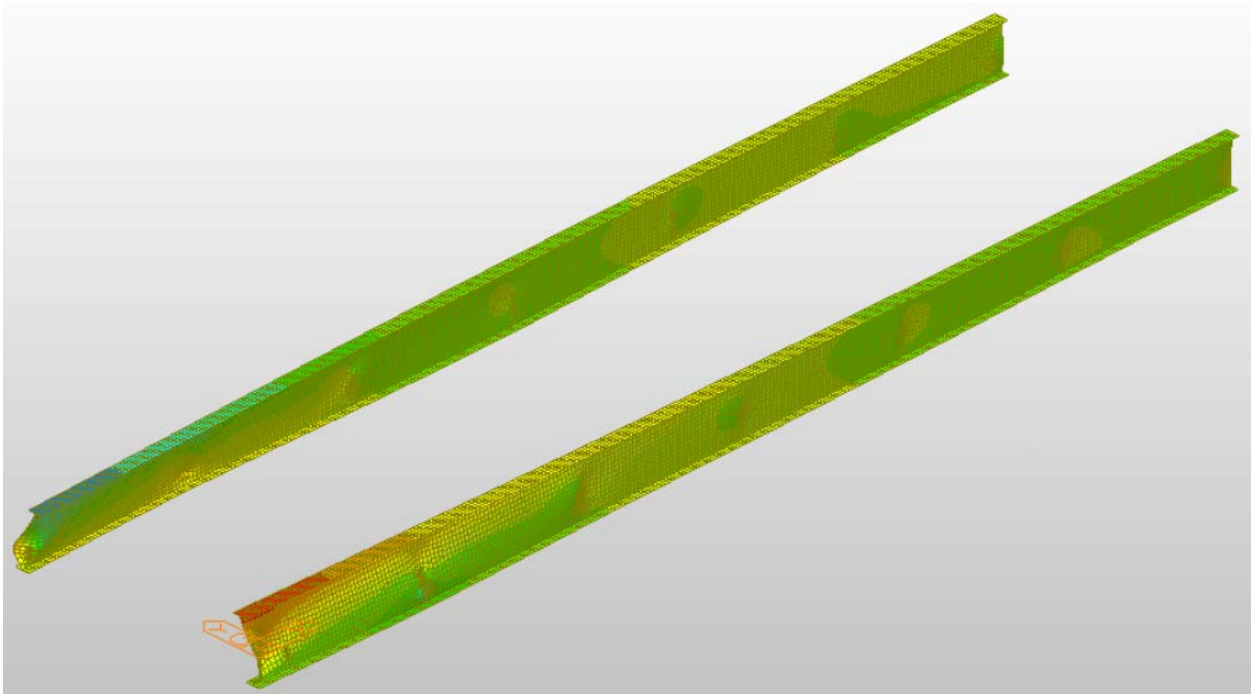

Figure 47. Plate Girder Displacement Contour (DY) for Position 4 of Two-Lanes Loaded (Load Case 3)

4.3.3. Modeling of Plate Girders and Bracing Elements

The addition of the plate girder and lateral bracing proved to be an integral part of the model calibration process. The plate girders were assembled using plate elements and can be seen in Figure 48. The lateral bracing members are assembled on the structure in a crossing pattern at each stringer unit, this pattern being doubled in Unit 2 and 3 surrounding the pivot point of the swing span, as seen in Figure 6. The lateral bracing members are connected to both plate girders at 6'- $0\frac{9}{16}$" from the top flange. This provides the second connection between the two plate girders, the first being the connection provided from the two ends of each floorbeam which starts at 3'- $3\frac{3}{4}$" from the top flange of the plate girder for Floorbeams B through G and 4'- $10\frac{3}{4}$" for Floorbeam A. When the bridge is loaded, the bottom of the plate girders begins to deflect out of plane in the positive and negative Y direction away from the centerline of the

roadway, as shown in Figure 47. This is a displacement that occurs as the bridge effectively folds inward under loading. The lateral bracing prevents this displacement and by effect improves the rotational stiffness of these plate girder members. The interaction, therefore, decreases the strain in the loaded floorbeam. The lateral bracing members were introduced to the model using truss elements, as shown in Figure 49.

As a result of the plate girders being introduced to the model, the equivalent spring supports at the floorbeam ends were removed and the floorbeams were connected directly to the plate girder webs by sharing nodes at the floorbeam ends. The addition of the plate girders also changes the support conditions for Floorbeam A, C, and G. These floorbeams were previously restricted in the Z direction at their ends and are now also connected to the plate girder webs. The supports that were previously at these floorbeam ends are now moved to the bottom flange of the plate girder at these locations, shown in Figure 50. These boundary conditions represent the wheel contact points of Floorbeam C, Figure 51, and wedges at Floorbeams A and G, Figure 52. The rigid links used in the initial FE model were also updated to include the contact between Floorbeam B and the concrete deck throughout the entire length of the member.

During inspection of the bridge prior to testing, a steel plate was found bolted to the top and bottom flange of Floorbeam E. This is a result of a bridge rehabilitation project and was not a part of the original structure. This was accounted for in the calibrated FE model by increasing the top and bottom flange thickness of Floorbeam B by ½-inch for a length of 7’-8” centered at midspan.

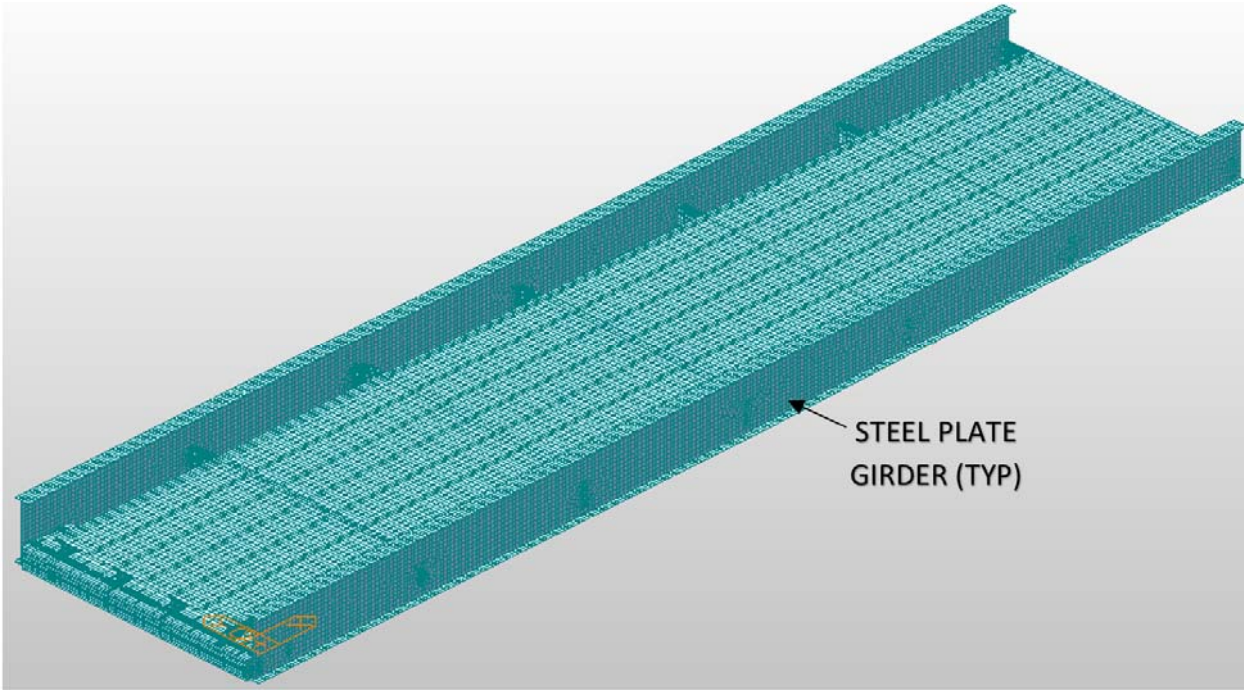

Figure 48. Calibrated FE Model

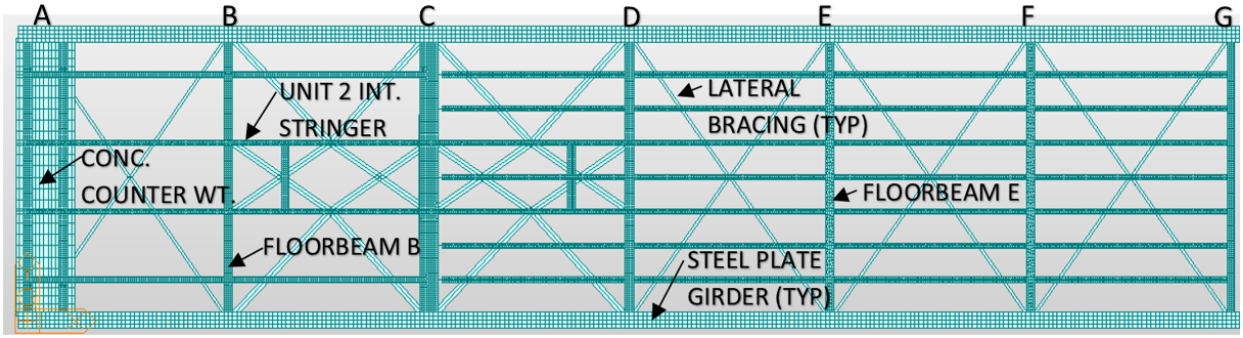

Figure 49. Calibrated FE Model Plan View (Deck Not Shown for Clarity)

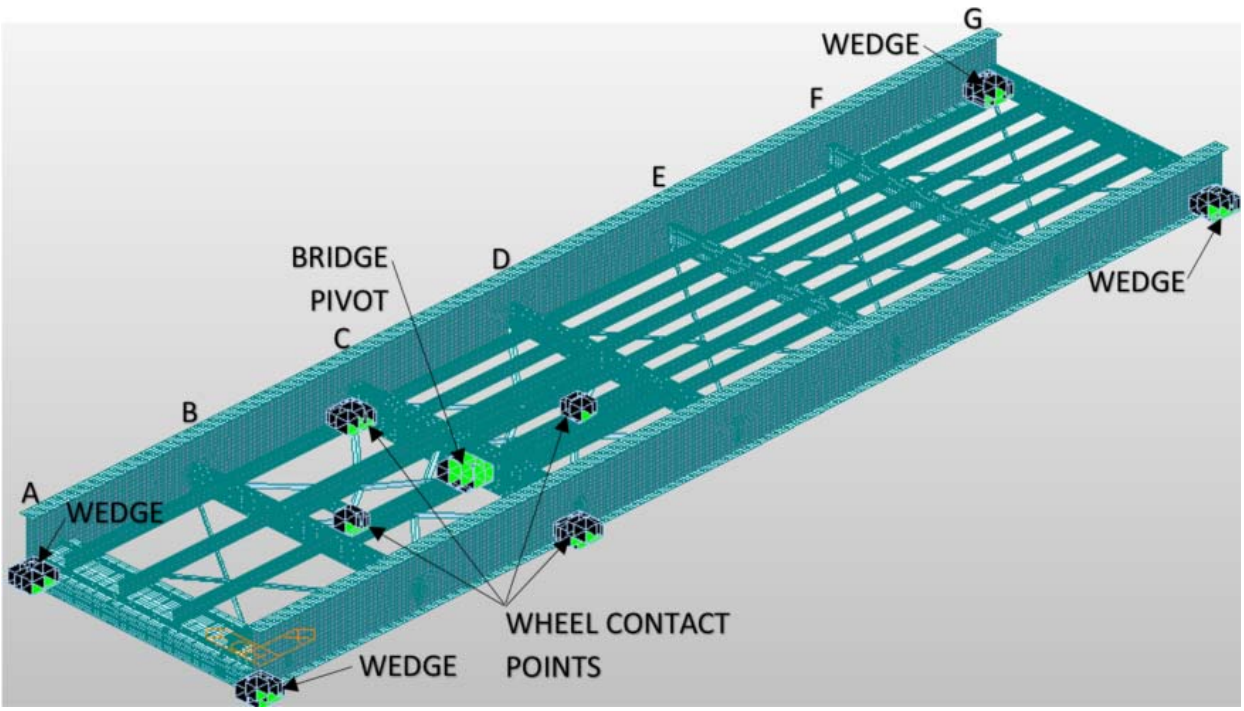

Figure 50. Calibrated FE Model Supports (Deck Not Shown for Clarity)

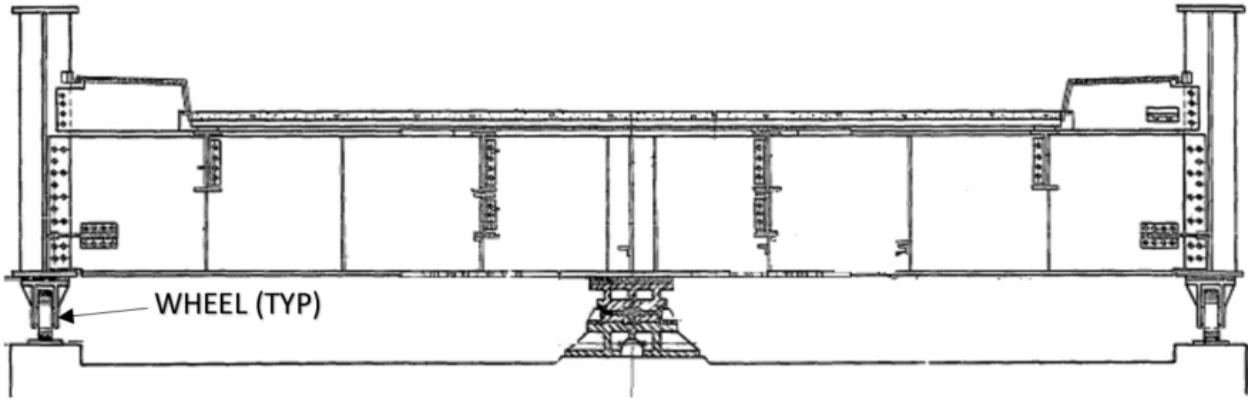

Figure 51. Section Thru Roadway at Pivot Point C

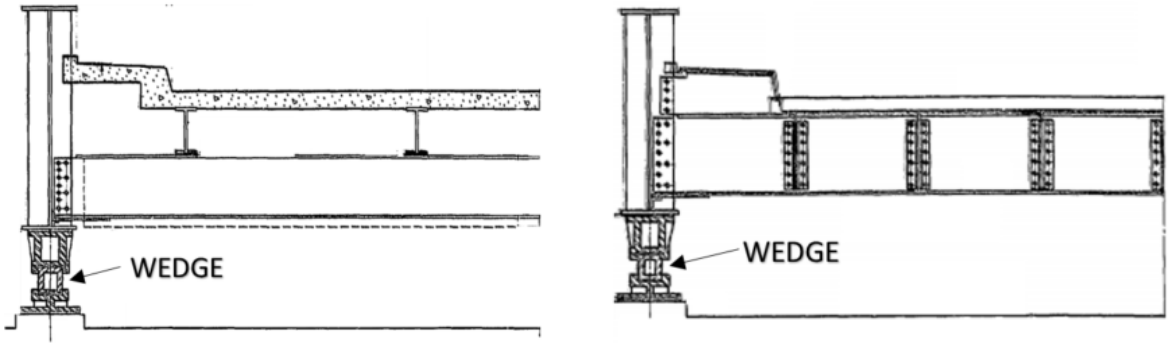

Floorbeam A Floorbeam G

Figure 52. Half Section Thru Roadway at Bridge Ends

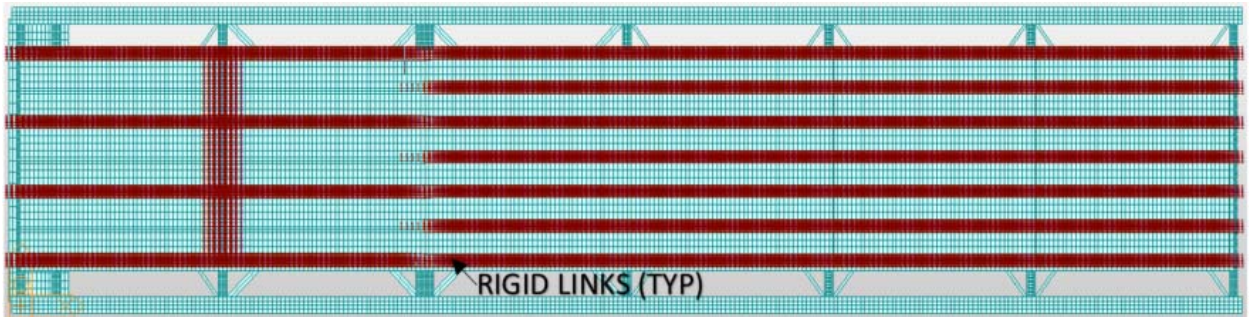

Figure 53. Calibrated FE Model Rigid Links

4.4. Calibrated Finite Element Results

The calibrated finite element results were extracted for Floorbeam B for Position 4 of Two-Lanes Loaded (Load Case 3), for Floorbeam E for Position 4 of Two-Lanes Loaded (Load Case 6), and for Unit 2 Interior Stringer for Position 4 of Longitudinal Loading (Load Case 7). Position 4 produces the maximum mid-span moment of all tested load case positions in each element. The calibrated FE model strain results in both the Composite and Non-Composite models are compared to those obtained from the diagnostic load test in Figure 54, Figure 56, and Figure 58. The corresponding deformed shape and displacement contour (DZ) for each tested element is also provided in Figure 55, Figure 57, and Figure 59.

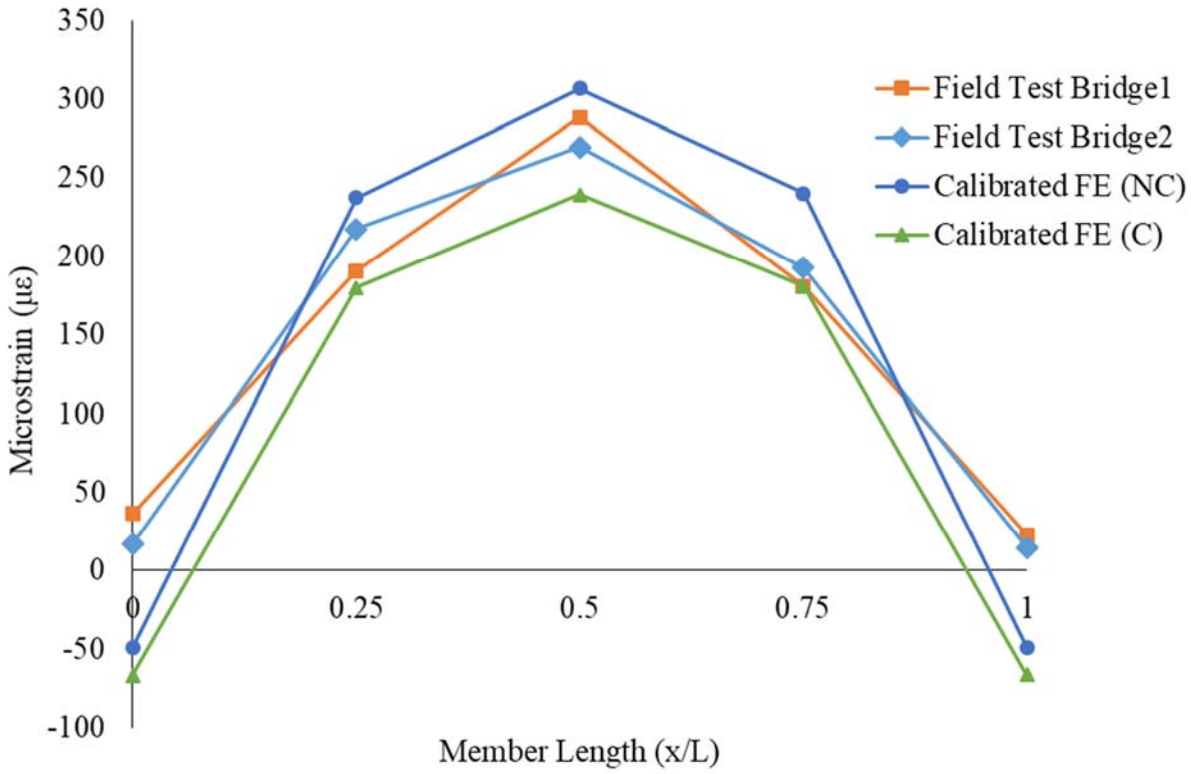

Figure 54. Measured and Computed Strain Comparison for Floorbeam B for Position 4 of Two-Lanes Loaded (Load Case 3)

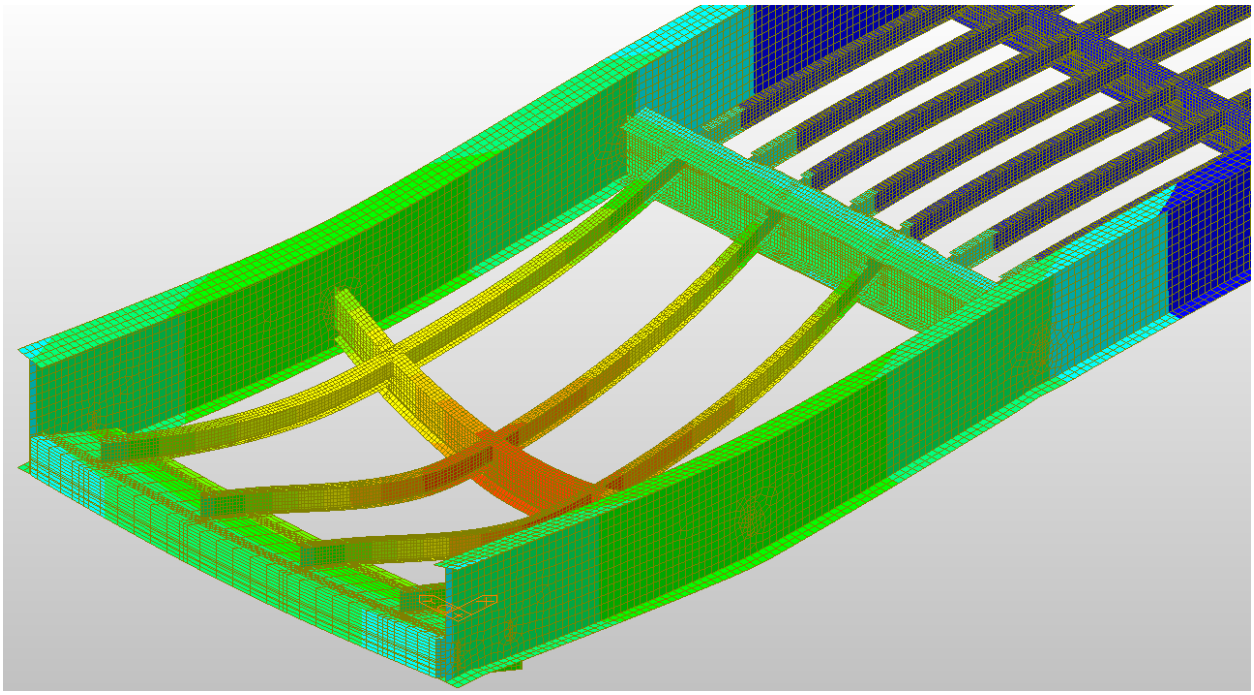

Figure 55. Deformed Shape and Displacement Contour (DZ) for Position 4 of Two-Lanes Loaded (Load Case 3) (Deck, Lateral Bracing, and Pivot Beams Not Shown for Clarity)

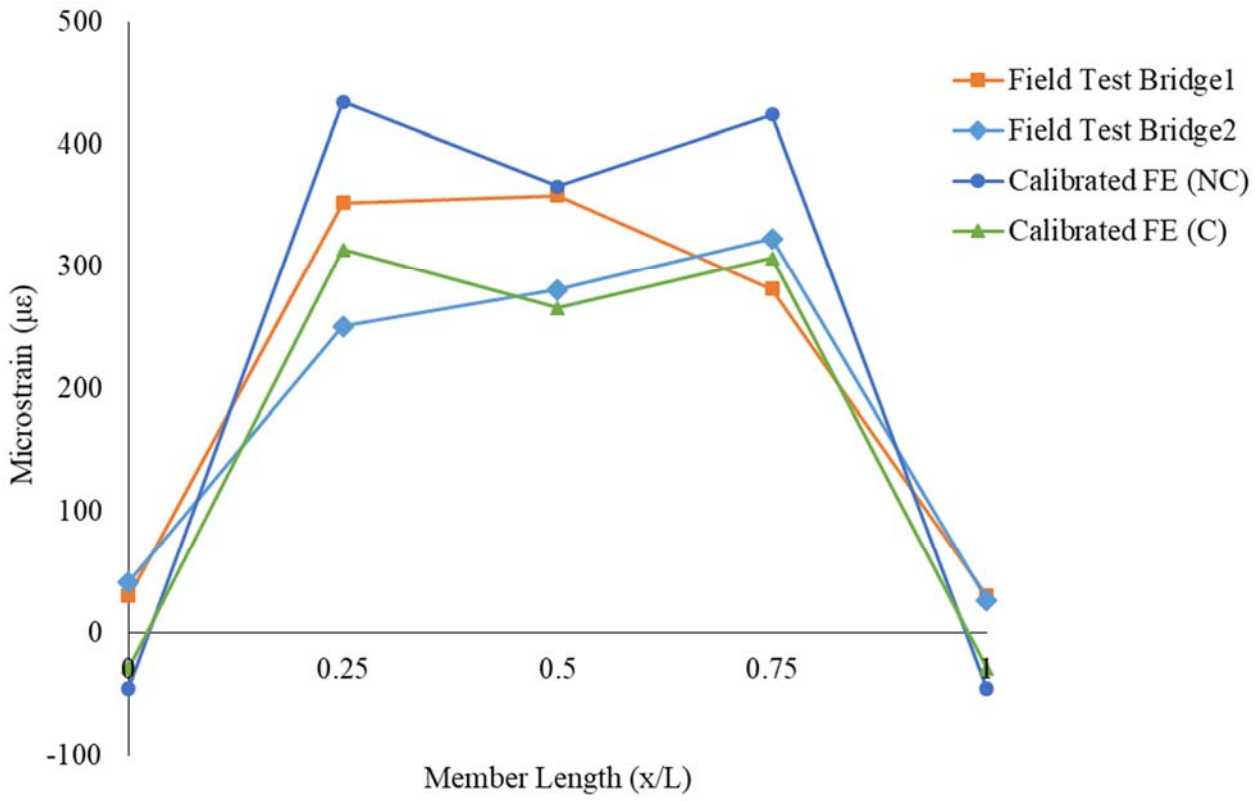

Figure 56. Measured and Computed Strain Comparison for Floorbeam E for Position 4 of Two-Lanes Loaded (Load Case 6)

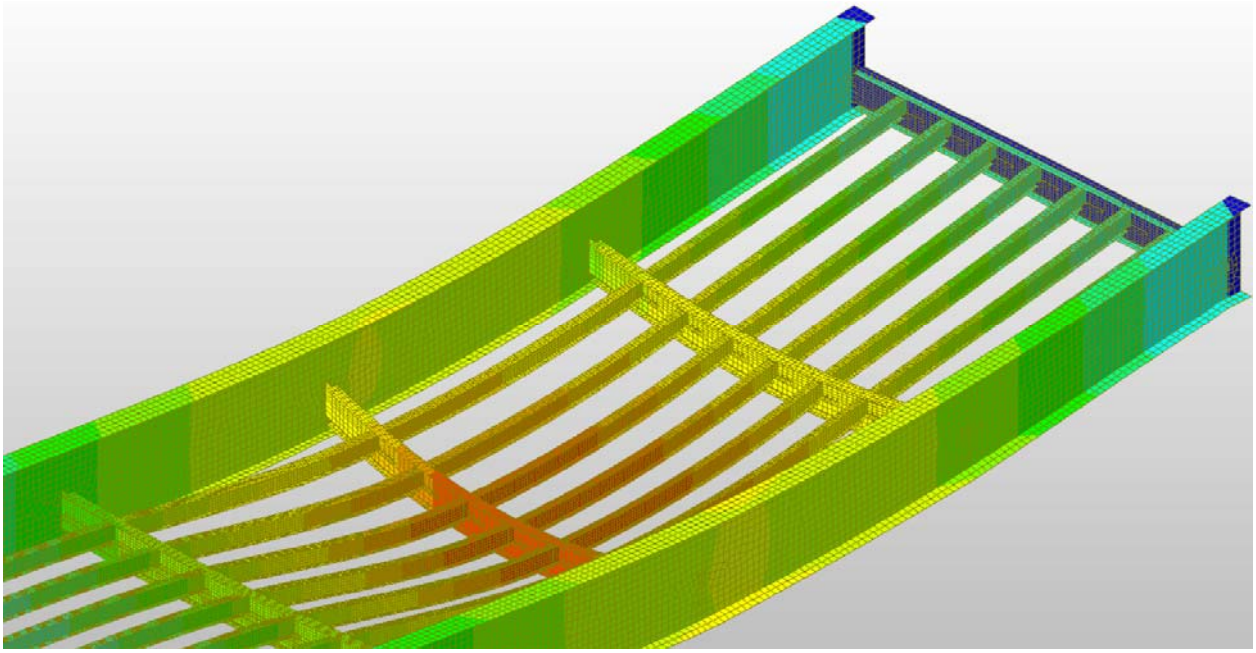

Figure 57. Deformed Shape and Displacement Contour (DZ) for Position 4 of Two-Lanes Loaded (Load Case 6) (Deck and Lateral Bracing Not Shown for Clarity)

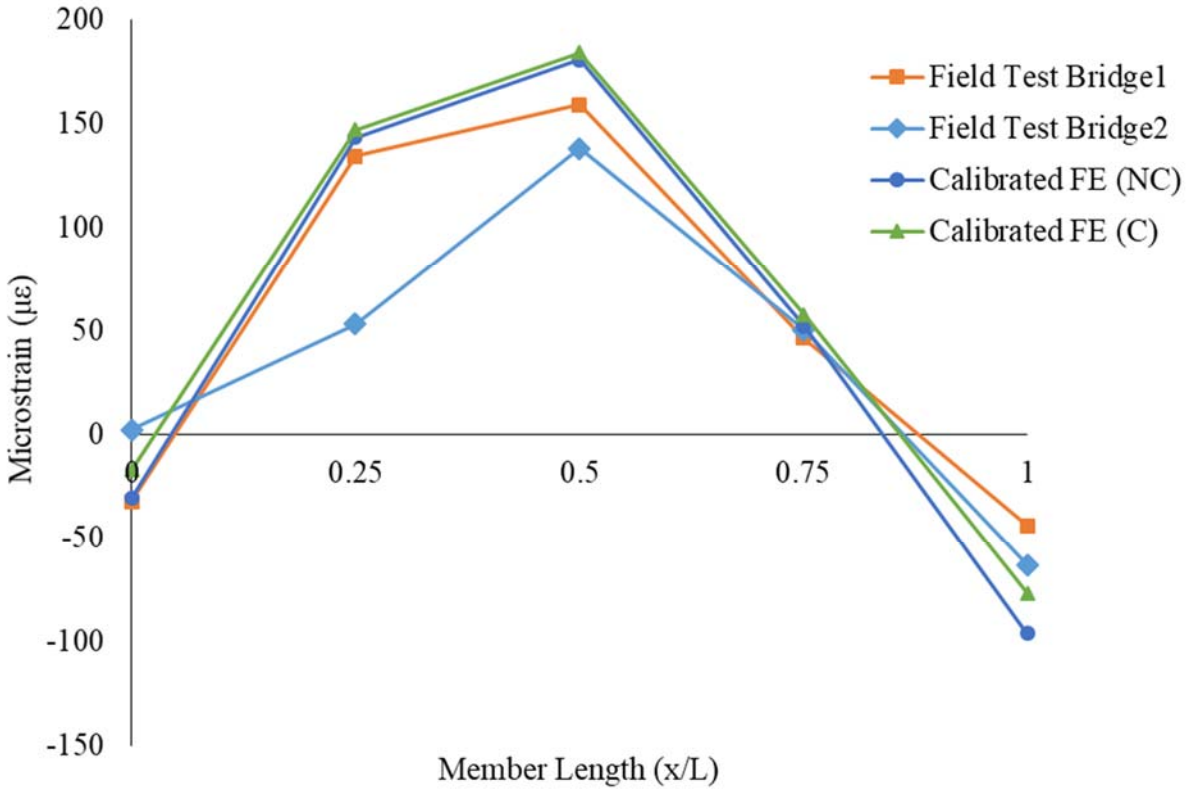

Figure 58. Measured and Computed Strain Comparison for Unit 2 Interior Stringer for Position 4 of Longitudinal Loading (Load Case 7)

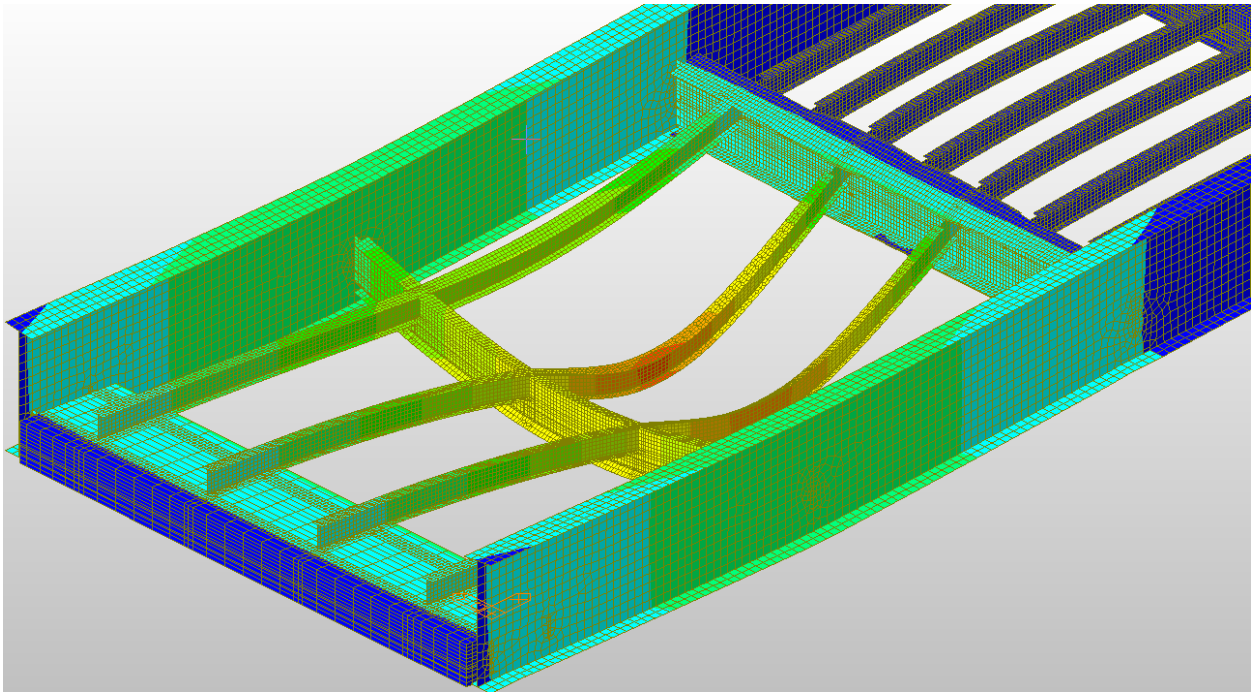

Figure 59. Deformed Shape and Displacement Contour (DZ) for Position 4 of Longitudinal Loading (Load Case 7) (Deck, Lateral Bracing, and Pivot Beams Not Shown for Clarity)

In the provided data comparisons for Floorbeam B and E, the diagnostic testing curves from field testing Bridge1 and Bridge2 generally lie between the Non-Composite and Composite Calibrated Finite Element Models, as can be seen in Figure 54 and Figure 56. As expected, the non-composite curves for both floorbeams result in higher strain values than the composite curves. These trends do not remain true for the Interior Stringer. Here the difference in non-composite and composite results is minimal and both follow a similar trend to the diagnostic test results and can be seen in Figure 58. It should be noted that after the inclusion of the steel plate of thickness ½-inch and a length of approximately 7'-8" centered at the midpoint of Floorbeam E two peaks are then created in the strain curve at locations 0.25L and 0.75L, as can be seen in Figure 56. This is a result of the increased capacity at 0.5L from the bridge rehabilitation that is not present at the other quarter point locations.

There is a noticeable difference in the diagnostic load test data and the strain observed from the calibrated FE models for the end connections of all three tested elements. For Floorbeams B and E the results from the FE models show negative strains at both 0.0L and 1.0L locations while the diagnostic load test results show positive strain values at these locations, as can be seen in Figure 54 and Figure 56. For the tested Interior Stringer, the resulting values at location 1.0L for the diagnostic load tests and the FE models yield negative strain value results of -44, -63, -77, and -96 microstrain for the diagnostic load test of Bridge1, the diagnostic load test of Bridge2, the calibrated composite FE model, and the calibrated non-composite FE model, respectively. The two FE model strain values recorded for this gage were more negative than the results recorded from either field test at this location, as can be seen in Figure 58.

The connections used in the tested bridges are designed as shear connections where the web of the floorbeams and stringers extends beyond the flanges in order to rivet the floorbeam to

the plate girder and the stringer to the floorbeam. These assumed to be simply supported beam connections can transmit up to 40% of the theoretical fixed-end moment. The abrupt change in section causes a large stress concentration and higher bending stresses in the web near the end of the flange; often leading to fatigue cracks in the web. (Chen & Duan, 2014). In rolled sections with coped flanges and built-up sections with flanges terminating short of their end connection, the bending stress in the web can increase by 200 to 300 percent because the web plate has a low section modulus compared to the entire member section (Fisher & Menzemer, 1990). Consequently, strains in the flanges at the beam ends are expected to be negligible in field measurements. However, flange strains predicted by the FE model, especially in the immediate vicinity of the web, may not accurately reflect the actual behavior of this disturbed (D-) region. D-regions exhibit complex variations in strain and include segments near abrupt changes in geometry. It should be noted that after a distance equal to the member depth, this disturbance in recorded and estimated strains becomes negligible according to St. Venant's Principle (FHWA, 2015). As a result, the error estimation of the final FE model does not include strain gage readings from element locations 0.0L and 1.0L.

Utilizing the Error Estimator from Equation (10), the error values from the calibrated FE model compared to the diagnostic load test results are presented in Table 14. The error estimation in Table 14 includes strain gages at 0.25L, 0.5L, and 0.75L on each tested member. The largest error for Floorbeam B, Floorbeam E, and Unit 2 Interior Stringer is 21%, 45%, and 75% respectively. After further review of testing results, the data obtained from Field Test Bridge2 for Interior Stringer of Unit 2 appears to be unreliable. The data could not be replicated and is believed to be a result of a damaged strain gage wire. By disregarding this data, the largest error for Unit 2 Interior Stringer drops to 17%. This also means that the composite FE model

when compared to both tested bridges results in a model with a maximum error of 17%, lower than the goal set in Section 3.4 of 20%.

Table 14. Error Estimation Calibrated FE Model vs Field Tests (End Strain Gages Removed)

Error				
	Field Test Bridge1		Field Test Bridge2	
Element	Calibrated FE Model (NC)	Calibrated FE Model (C)	Calibrated FE Model (NC)	Calibrated FE Model (C)
Floorbeam B	21%	8%	16%	12%
Floorbeam E	25%	15%	45%	12%
Unit 2 Int. Stringer	11%	17%	68%*	75%*

*Eliminated as unreliable data

4.5. Finite Element Load Rating

Load rating analysis was performed using the calibrated finite element models created in this study. Table 15 through Table 18 contains the results for both tested bridges, Bridge1 and Bridge2, and in both model options of Non-Composite and Composite. HL-93 loading was created using point loads at each wheel location. Vehicular loading can be modeled as twin axles with wheel patch loads to more accurately model vehicle loads in reality, but this has little effect for many analysis models (FHWA, 2019). The wheel loads were assumed to be equal within each axle unit per LRFD 3.6.1.3.3 (AASHTO, 2017). The lane loads were applied as pressure loads and were analyzed as a separate load case from the vehicle loads. Keeping these loads separate allowed for the dynamic load allowance factor to be applied to the vehicle load force affects after analysis (FHWA, 2019). An impact factor of 0.33, or 33%, was applied to the vehicle load force affect for all three tested bridge elements. The 0.66 impact factor described in the AASHTO LRFD Movable Bridge Design Specifications (2007) shall be applied to end floorbeams and is therefore not applicable to Floorbeam B, Floorbeam E, or Interior Stringer of Unit 2 (AASHTO, 2007).

Load rating results for Floorbeam E and the Interior Stringer of both the non-composite and composite FE models were initially controlled by the stress concentration occurring at the connection of the web to the flange at the flange end, as described in Section 4.4. To resolve this issue, an average rating factor was taken for the nodes of all flange elements that comprise the flange at the end location. This results in a rating factor more indicative of the bridge behavior in the bottom flange at this location than a rating factor derived solely from the node connecting the web to the bottom flange at the termination of the coped flange.

The controlling load effect for the three tested bridge elements was Strength I – Flexure. The resulting rating factor from the Non-Composite FE Model for Floorbeam E of Bridge1 was the lowest rating factor for any element in any scenario, 0.85 for HL-93 inventory loading under the Strength I – Flexure load effect. The critical location along Floorbeam E was located at 0.25L. It is important to note that the previous bridge rehabilitation project, the addition of a ½-inch steel plate to the top and bottom flange of Floorbeam E at midspan, has transferred the maximum beam moment location from 0.5L to 0.25L and 0.75L, as seen in Figure 56, for both Non-Composite and Composite FE Model scenarios. In Figure 56, it can also be seen that the diagnostic testing curve from Bridge1 lies generally between the Non-Composite and Composite FE Model curves. For strain gage locations 0.25L and 0.75L specifically, the diagnostic testing data is closer to the Composite FE Model results than the Non-Composite FE Model results. This trend remains true when comparing the error of the two models to the testing data from the diagnostic field test. As seen in Table 14, when comparing an error estimation of the diagnostic field test to the Calibrated FE Model in both Non-Composite and Composite scenarios to strain gage locations 0.25L, 0.5L, and 0.75L the Composite FE Model performs more closely to the testing data for Floorbeam E when compared to the Non-Composite FE Model; an error

comparison of 15% to 25% respectively. Therefore, it can be said that the rating factor for this specific bridge element can be expressed as some value between the Non-Composite and Composite rating factors. A conservative assumption can be made that this value is the average between the two FE Model results, while it is shown in Figure 56 and Table 14 that this value is most likely closer to the Composite FE Model result than the Non-Composite FE Model results. The resulting rating factor for Floorbeam E of Bridge1 is therefore 1.11 for HL-93 inventory loading under the Strength I – Flexure load effect at location 0.25L.

For all other elements in all other scenarios, the rating factor for HL-93 inventory is greater than 1.0. As a result, no additional vehicles were analyzed since for all legal loads that fall within the LRFD exclusion limits the bridges will have satisfactory load rating (AASHTO, 2011). The load rating of these three elements using the calibrated composite and non-composite FE models resulted in no load posting recommendation.

Table 15. Load Rating Summary (Bridge1 Non-Composite FE Model)

Element	Vehicle Type	Rating Factor	Controlling Load Effect
Floorbeam B	HL-93 (INV)	1.08	Strength I - Flexure
Floorbeam E	HL-93 (INV)	0.85	Strength I - Flexure
Int. Stringer Unit 2	HL-93 (INV)	1.85	Strength I - Flexure

Table 16. Load Rating Summary (Bridge1 Composite FE Model)

Element	Vehicle Type	Rating Factor	Controlling Load Effect
Floorbeam B	HL-93 (INV)	1.79	Strength I - Flexure
Floorbeam E	HL-93 (INV)	1.37	Strength I - Flexure
Int. Stringer Unit 2	HL-93 (INV)	2.16	Strength I - Flexure

Table 17. Load Rating Summary (Bridge2 Non-Composite FE Model)

Element	Vehicle Type	Rating Factor	Controlling Load Effect
Floorbeam B	HL-93 (INV)	1.33	Strength I - Flexure
Floorbeam E	HL-93 (INV)	1.02	Strength I - Flexure
Int. Stringer Unit 2	HL-93 (INV)	2.20	Strength I - Flexure

Table 18. Load Rating Summary (Bridge2 Composite FE Model)

Element	Vehicle Type	Rating Factor	Controlling Load Effect
Floorbeam B	HL-93 (INV)	2.14	Strength I - Flexure
Floorbeam E	HL-93 (INV)	1.63	Strength I - Flexure
Int. Stringer Unit 2	HL-93 (INV)	2.55	Strength I - Flexure

5. SUMMARY AND CONCLUSIONS

5.1. Summary

Refined analysis can be a useful tool in the analysis of existing structures. In this study, diagnostic load tests were conducted on two nearly identical Steel Plate Girder Swing Span bridges in Louisiana. Both bridges were load posted due to a load rating performed prior to this study using approximate analysis methods. Before testing, an initial Finite Element (FE) model was created using as-built plans for both bridges. After diagnostic load testing was completed the testing results were compared to the initial FE model results, and the model was calibrated accordingly. Two separate models were developed in this study. One model was constructed assuming composite action between the deck and selected structural elements. The other was constructed as non-composite. The results of model calibration show that the bridge performance lies somewhere between the composite and non-composite models. A load rating was then performed on three bridge members that were identified as deficient from the previous analysis which used traditional methods. The load rating of these three elements using the calibrated composite and non-composite FE models resulted in no load posting recommendation.

5.2. Conclusions

The results of this study show that refined analysis is a viable option in the evaluation and determination of load capacity of existing steel plate girder swing span bridges. The resulting load rating using calibrated Finite Element models shows a higher load capacity when compared to approximate analysis. The performance of these models is representative of the bridge performance as confirmed by diagnostic load testing and model calibration. The inclusion of unintended composite action, participation of secondary members, participation of non-structural members, and refinement of bridge boundary conditions all served an important role in the

model calibration process and therefore in determining the load capacity of the structure. The influence of these components on the structural performance of a bridge are best represented using refined analysis. Properly accounting for all contact points of the bridge pivot and including elements such as bridge pivot members, bridge counterweight, and lateral bracing all proved to be important in establishing a more accurate load capacity for a steel plate girder swing span bridge.

Refined analysis is a time-consuming process that requires more engineering skill than typical approximate analysis. However, in many situations, it may be beneficial to bridge owners to choose refined analysis in lieu of approximate analysis to properly assess a structure's performance. This is particularly true for bridges whose load rating factors are less than 1.0 when calculated using such approximate methods. In such scenarios, refined analysis may eliminate the need to apply unnecessary load posting or bridge closure to a bridge that can carry normal traffic conditions.

Unintended composite action is the functioning of a beam as a composite member without the presence of a composite connection between beam and deck elements. This phenomenon is seen under normal live loading. In Burdette (1988), it is stated that "the question of whether or not composite action can be counted on in a bridge not designed for composite action is one which continues to arise but which is almost impossible to answer definitely and confidently without the benefit of some sort of testing" (Burdette & Goodpasture, 1988). This reasoning is applicable as it pertains to this study. However, through the use of refined analysis, composite and non-composite scenarios can be modeled without the necessity of load testing. It is only when the difference in composite or non-composite results becomes significant to the bridge owner, for example load posting or bridge closure, that this scenario then needs to be visited by

diagnostic load testing to confirm composite action assumptions. Furthermore, it is important to note that as loads increase on the structure the horizontal shear force between the member and the deck can exceed the limiting bond strength. Under these circumstances slippage occurs, the composite action is lost, and there is a sudden increase in member stresses. For this reason, non-composite members which are acting compositely cannot have their stress values extrapolated to higher load cases. Therefore, engineers shall use only FE models without the presence of unintended composite action when conducting load ratings for one time permits for overweight vehicles unless the composite action is confirmed by diagnostic load testing up to a level similar to what is used in load testing.

In future research the following recommendations are made when verifying testing results. It is advised that to safely use unintended composite action, it must be verified from load testing that at the desired loading level slippage does not occur. This entails locating the neutral axis of the member of interest. This can be achieved by applying at a minimum two sensors on the beam, one at the beam's soffit, and the other at another location on the same cross section; e.g. the top flange. Additional sensors on the web, e.g. at a vertical location equal to half the height of the member, can improve the quality of the neutral axis position assessment. If this member is acting with full composite action, the strain recorded from the gage located at the midpoint of the web shall not be zero, as can be seen in the Full Composite case of Figure 60. To add redundancy to the instrumentation system, multiple gages located along the vertical axis of the web of the tested element is preferred.

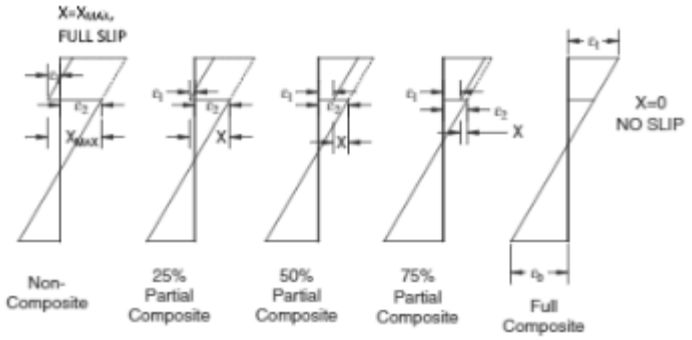

Figure 60. Variations of Composite Action
Source: (Chen & Yossef, 2015)

Also recommended is a more complete instrumentation of beam ends to fully capture the beam end response and the interaction between connected elements. Special attention shall be placed on end connections that consist of disturbed (D-) regions resulting from abrupt changes in section properties as a result of coped flanges. Additional sensors shall be placed along the bottom of the flange at a distance of one and two times the depth of the tested member to properly capture the resultant stress "far away" from the stress concentration created at the end connection. Also, sensors shall be placed along the web in these same locations to obtain a better understanding of the connection as well as possibly assess composite action at these locations. Without fully understanding this connection, engineers can misinterpret the load testing results as a confirmation that the end connection acts as a simple support while such connection can act similar to a fixed end connection.

Refined analysis is another tool that engineers and state departments of transportation can use to properly analyze bridges and possibly extend the service life of existing structures that may have been load posted or closed when evaluated using approximate analysis. This sentiment is magnified by the importance of movable bridges to service both vehicular and marine traffic in their communities. Refined analysis gives engineers the ability to capture a more accurate load

capacity for these structures, giving bridge owners the proper information to manage their aging infrastructure.

APPENDIX. FINAL LOAD RATING.

In this Appendix, the final load ratings are calculated for each tested bridge element, using Equation (1). Each deficient member is rated in both composite and non-composite finite element models. Each member is also rated for Bridge1 and Bridge2, the difference in these two calculations being the ϕ_c factor for both bridges; $\phi_c = 0.85$ for Bridge1 and $\phi_c = 1.0$ for Bridge2. The material used in all three tested members is ASTM A94 with material properties of f_y= 50ksi and f_u= 75ksi. The dynamic allowance for all tested members is IM=0.33. It is important to note that the dynamic allowance of 0.66 for movable bridges is only applicable to end floorbeams. The tested members are two intermediate floorbeams, Floorbeam B and E, and one stringer, Unit 2 Interior Stringer. The controlling load effect for each testing element is Strength – I Steel Flexure Stress as described in the AASHTO LRFD Bridge Design and Specifications Section 6.10.8 Flexural Resistance – Composite Sections in Negative Flexure and Noncomposite Sections (AASHTO, 2017).

Table A. 1. Floorbeam B Rating Factors (Non-Composite)

Flange	Reading Location (L)	Plate	Node	Location on Plate	Loading Case (ksi)				Rating Factor	
					Lane Load	Self Weight	Live Load	Sidewalk	Bridge1	Bridge2
BOT.	0L	116245	Cent	Top	0.01	3.34	0.33	0.13	48.42	57.93
				Bot	-0.22	3.04	-0.51	0.02	28.46	33.05
		116245	217625	Top	-0.12	-0.40	-0.35	-0.03	39.18	46.19
				Bot	0.22	-0.24	0.77	0.13	19.61	23.06
		116245	217629	Top	0.12	-0.06	0.44	0.08	34.17	40.20
				Bot	-0.02	-0.58	-0.02	0.02	421.51	497.21

(table cont'd.)

Flange	Reading Location (L)	Plate	Node	Location on Plate	Loading Case (ksi)				Rating Factor	
					Lane Load	Self Weight	Live Load	Sidewalk	Bridge1	Bridge2
BOT.	0L	116245	210113	Top	-0.41	6.97	-0.82	0.04	18.81	21.54
				Bot	-0.15	6.80	-0.07	0.14	114.13	130.74
		116245	82539	Top	0.41	7.22	1.93	0.40	6.33	7.77
				Bot	-0.97	6.55	-2.83	-0.23	5.88	6.75
	L/4	116505	Cent	Top	1.91	6.72	6.32	0.82	1.83	2.25
				Bot	2.01	6.99	6.63	0.85	1.73	2.12
		116505	218157	Top	1.90	6.66	6.30	0.81	1.84	2.26
				Bot	2.01	6.97	6.64	0.85	1.72	2.12
		116505	218161	Top	1.91	6.70	6.35	0.82	1.83	2.24
				Bot	2.00	6.92	6.59	0.85	1.74	2.14
		116505	206180	Top	1.92	6.77	6.31	0.82	1.83	2.25
				Bot	2.03	7.04	6.65	0.86	1.71	2.11
		116505	41219	Top	1.92	6.76	6.32	0.82	1.83	2.24
				Bot	2.02	7.05	6.64	0.86	1.72	2.11
	L/2	117691	Cent	Top	2.65	7.51	8.69	0.60	1.30	1.60
				Bot	2.78	7.79	9.12	0.62	1.23	1.51
		117691	217430	Top	2.64	7.48	8.60	0.59	1.32	1.62
				Bot	2.76	7.78	9.00	0.61	1.24	1.53
		117691	220580	Top	2.64	7.49	8.60	0.59	1.31	1.62
				Bot	2.76	7.77	9.00	0.61	1.24	1.53
		117691	210886	Top	2.66	7.53	8.79	0.60	1.29	1.59
				Bot	2.79	7.83	9.24	0.62	1.21	1.49
		117691	41208	Top	2.66	7.55	8.79	0.60	1.29	1.59
				Bot	2.79	7.80	9.24	0.62	1.21	1.50
	3L/4	116672	Cent	Top	1.91	6.41	6.32	0.81	1.85	2.27
				Bot	2.01	6.67	6.63	0.85	1.75	2.14

(table cont'd.)

Flange	Reading Location (L)	Plate	Node	Location on Plate	Loading Case (ksi)				Rating Factor	
					Lane Load	Self Weight	Live Load	Sidewalk	Bridge1	Bridge2
BOT.	3L/4	116672	218399	Top	1.90	6.40	6.30	0.81	1.86	2.28
				Bot	2.01	6.70	6.64	0.85	1.74	2.14
		116672	41361	Top	1.92	6.39	6.32	0.81	1.85	2.27
				Bot	2.02	6.66	6.64	0.86	1.74	2.14
		116672	215178	Top	1.92	6.39	6.31	0.82	1.86	2.27
				Bot	2.03	6.66	6.65	0.85	1.74	2.13
		116672	218494	Top	1.91	6.44	6.35	0.82	1.84	2.26
				Bot	2.00	6.66	6.59	0.85	1.76	2.16
	L	117188	Cent	Top	0.01	2.50	0.34	0.13	49.37	58.81
				Bot	-0.22	2.35	-0.51	0.02	27.87	32.45
		117188	219567	Top	-0.13	0.50	-0.36	-0.03	39.60	46.49
				Bot	0.22	0.20	0.77	0.13	19.21	22.63
		117188	82560	Top	0.42	4.07	1.95	0.41	7.00	8.43
				Bot	-0.98	4.94	-2.85	-0.23	5.60	6.46
		117188	205099	Top	-0.42	5.10	-0.84	0.04	17.66	20.35
				Bot	-0.14	3.90	-0.06	0.14	117.41	135.85
		117188	219568	Top	0.12	0.33	0.45	0.08	33.41	39.39
				Bot	-0.02	0.36	-0.03	0.02	380.82	447.24
TOP	0L	118217	Cent	Top	-0.21	-0.71	-0.60	-0.18	22.63	26.74
				Bot	-0.31	-0.92	-0.77	-0.26	16.86	19.94
		118217	221592	Top	-0.18	-0.49	-0.46	-0.15	28.91	34.11
				Bot	0.04	0.20	0.15	0.02	103.45	121.82
		118217	221596	Top	-0.01	0.08	0.04	-0.02	580.44	683.05
				Bot	-0.14	-0.37	-0.35	-0.11	38.30	45.16
		118217	208814	Top	-0.63	-2.24	-1.85	-0.51	6.92	8.25
				Bot	-0.23	-0.88	-0.63	-0.20	21.22	25.09

(table cont'd.)

Flange	Reading Location (L)	Plate	Node	Location on Plate	Loading Case (ksi)				Rating Factor	
					Lane Load	Self Weight	Live Load	Sidewalk	Bridge1	Bridge2
TOP	0L	118217	82536	Top	0.01	-0.34	-0.17	-0.01	109.62	129.17
				Bot	-0.86	-2.78	-2.31	-0.70	5.29	6.34
	L/4	116372	Cent	Top	-2.27	-5.62	-7.28	-0.95	1.56	1.90
				Bot	-2.18	-5.33	-6.93	-0.91	1.65	2.02
		116372	217892	Top	-2.26	-5.69	-7.21	-0.96	1.57	1.91
				Bot	-2.18	-5.40	-6.91	-0.91	1.65	2.02
		116372	217896	Top	-2.28	-5.71	-7.31	-0.96	1.55	1.89
				Bot	-2.17	-5.38	-6.81	-0.92	1.68	2.04
		116372	208052	Top	-2.16	-5.45	-6.79	-0.98	1.67	2.04
				Bot	-2.29	-5.36	-7.51	-0.86	1.54	1.87
		116372	28965	Top	-2.35	-5.63	-7.80	-0.91	1.47	1.79
				Bot	-2.10	-5.18	-6.49	-0.94	1.76	2.15
	L/2	117396	Cent	Top	-2.98	-6.05	-9.77	-0.71	1.16	1.41
				Bot	-2.87	-5.69	-9.29	-0.64	1.23	1.50
		117396	219991	Top	-2.94	-5.80	-9.64	-0.68	1.19	1.45
				Bot	-2.82	-5.42	-9.21	-0.62	1.26	1.53
		117396	219995	Top	-2.96	-5.82	-9.74	-0.67	1.17	1.43
				Bot	-2.80	-5.40	-9.11	-0.62	1.27	1.55
		117396	210047	Top	-2.91	-6.18	-9.36	-0.76	1.20	1.46
				Bot	-3.03	-6.08	-9.90	-0.65	1.14	1.40
		117396	19714	Top	-3.12	-6.40	-10.30	-0.74	1.08	1.33
				Bot	-2.82	-5.85	-8.93	-0.67	1.27	1.55
	3L/4	116280	Cent	Top	-2.27	-4.98	-7.28	-0.95	1.60	1.94
				Bot	-2.18	-4.71	-6.93	-0.91	1.69	2.05
		116280	217634	Top	-2.26	-4.92	-7.21	-0.96	1.61	1.96
				Bot	-2.18	-4.65	-6.91	-0.91	1.70	2.06

(table cont'd.)

Flange	Reading Location (L)	Plate	Node	Location on Plate	Loading Case (ksi)				Rating Factor	
					Lane Load	Self Weight	Live Load	Sidewalk	Bridge1	Bridge2
TOP	3L/4	116280	29054	Top	-2.35	-5.14	-7.81	-0.91	1.49	1.81
				Bot	-2.10	-4.68	-6.49	-0.94	1.80	2.18
		116280	210825	Top	-2.17	-4.92	-6.79	-0.98	1.71	2.07
				Bot	-2.29	-4.89	-7.51	-0.86	1.56	1.90
		116280	217699	Top	-2.28	-4.94	-7.31	-0.96	1.59	1.93
				Bot	-2.17	-4.63	-6.81	-0.92	1.72	2.09
	L	117143	Cent	Top	-0.21	-0.59	-0.66	-0.09	21.13	24.94
				Bot	-0.31	-0.36	-0.35	-0.18	29.97	35.34
		117143	219467	Top	-0.18	-0.88	-1.08	-0.30	13.88	16.42
				Bot	0.04	-0.72	-0.81	-0.29	21.84	25.82
		117143	82557	Top	0.01	-1.25	-1.25	-0.08	13.56	16.05
				Bot	-0.86	-0.35	-0.64	-0.51	13.28	15.69
		117143	212918	Top	-0.63	-0.01	-0.19	-0.05	26.72	31.44
				Bot	-0.23	-0.16	0.11	0.08	290.58	341.99
		117143	219468	Top	-0.01	-0.09	-0.06	0.05	253.23	297.98
				Bot	-0.14	-0.08	-0.01	-0.02	149.36	175.79

Table A. 2. Floorbeam B Rating Factors (Composite)

Flange	Reading Location (L)	Plate	Node	Location on Plate	Loading Case (ksi)				Rating Factor	
					Lane Load	Self Weight	Live Load	Sidewalk	Bridge1	Bridge2
BOT.	0L	116245	Cent	Top	-0.04	-0.69	0.06	0.09	573.00	672.36
				Bot	-0.27	-1.26	-0.77	-0.04	17.43	20.63
		116245	217625	Top	-0.13	-0.49	-0.40	-0.04	34.44	40.62
				Bot	0.23	0.56	0.78	0.14	18.70	22.07
		116245	217629	Top	0.12	0.24	0.42	0.08	35.14	41.40
				Bot	-0.02	-0.16	-0.04	0.01	299.40	352.47
		116245	210113	Top	-0.53	-2.55	-1.44	-0.08	8.76	10.45
				Bot	-0.22	-1.47	-0.49	0.06	25.72	30.46
		116245	82539	Top	0.35	0.00	1.52	0.36	10.12	11.93
				Bot	-1.10	-4.02	-3.45	-0.38	3.55	4.27
	L/4	116505	Cent	Top	1.56	2.44	4.93	0.58	2.73	3.25
				Bot	1.60	2.49	5.04	0.59	2.66	3.18
		116505	218157	Top	1.56	2.39	4.94	0.58	2.73	3.25
				Bot	1.60	2.46	5.04	0.59	2.66	3.18
		116505	218161	Top	1.56	2.40	4.94	0.58	2.73	3.25
				Bot	1.60	2.45	5.04	0.58	2.66	3.18
		116505	206180	Top	1.57	2.49	4.94	0.58	2.71	3.24
				Bot	1.60	2.52	5.03	0.58	2.66	3.18
		116505	41219	Top	1.56	2.47	4.90	0.57	2.74	3.27
				Bot	1.61	2.54	5.07	0.59	2.64	3.15
	L/2	117691	Cent	Top	2.22	3.56	7.03	0.41	1.85	2.22
				Bot	2.27	3.61	7.20	0.41	1.81	2.17
		117691	217430	Top	2.22	3.53	6.96	0.40	1.87	2.24
				Bot	2.26	3.58	7.11	0.40	1.83	2.20

(table cont'd.)

Flange	Reading Location (L)	Plate	Node	Location on Plate	Loading Case (ksi)				Rating Factor	
					Lane Load	Self Weight	Live Load	Sidewalk	Bridge1	Bridge2
BOT.	L/2	117691	220580	Top	2.22	3.53	6.96	0.40	1.87	2.24
				Bot	2.26	3.57	7.11	0.40	1.83	2.20
		117691	210886	Top	2.22	3.58	7.10	0.42	1.84	2.21
				Bot	2.28	3.64	7.29	0.42	1.79	2.14
		117691	41208	Top	2.22	3.58	7.10	0.42	1.84	2.21
				Bot	2.28	3.64	7.29	0.42	1.79	2.14
	3L/4	116672	Cent	Top	1.56	2.44	4.93	0.58	2.73	3.25
				Bot	1.60	2.49	5.04	0.59	2.66	3.18
		116672	218399	Top	1.56	2.39	4.94	0.58	2.73	3.25
				Bot	1.60	2.46	5.04	0.59	2.66	3.18
		116672	41361	Top	1.56	2.47	4.90	0.57	2.74	3.27
				Bot	1.61	2.54	5.07	0.59	2.64	3.15
		116672	215178	Top	1.57	2.49	4.94	0.58	2.71	3.24
				Bot	1.60	2.52	5.03	0.58	2.66	3.18
		116672	218494	Top	1.56	2.40	4.94	0.58	2.73	3.25
				Bot	1.60	2.45	5.04	0.59	2.66	3.18
	L	117188	Cent	Top	-0.04	-0.68	0.06	0.09	540.84	634.64
				Bot	-0.27	-1.26	-0.77	-0.04	17.38	20.57
		117188	219567	Top	-0.13	-0.49	-0.41	-0.04	33.86	39.93
				Bot	0.24	0.57	0.79	0.14	18.54	21.88
		117188	82560	Top	0.36	0.02	1.55	0.36	9.91	11.68
				Bot	-1.11	-4.04	-3.48	-0.38	3.51	4.23
		117188	205099	Top	-0.54	-2.57	-1.46	-0.08	8.65	10.31
				Bot	-0.21	-1.45	-0.47	0.06	26.50	31.38
		117188	219568	Top	0.12	0.24	0.43	0.09	34.81	41.02

(table cont'd.)

Flange	Reading Location (L)	Plate	Node	Location on Plate	Loading Case (ksi)				Rating Factor	
					Lane Load	Self Weight	Live Load	Sidewalk	Bridge1	Bridge2
BOT.	L			Bot	-0.02	-0.17	-0.05	0.01	268.25	315.82
TOP	0L	118217	Cent	Top	-0.21	-0.50	-0.49	-0.16	26.70	31.50
				Bot	-0.28	-0.79	-0.54	-0.20	22.61	26.72
		118217	221592	Top	-0.16	-0.47	-0.27	-0.11	44.92	52.99
				Bot	0.04	-0.01	0.17	0.03	93.40	109.90
		118217	221596	Top	0.00	-0.14	0.14	0.00	133.15	156.55
				Bot	-0.12	-0.34	-0.23	-0.08	53.36	62.90
		118217	208814	Top	-0.61	-1.29	-1.57	-0.45	8.19	9.72
				Bot	-0.25	-0.60	-0.63	-0.19	20.99	24.78
		118217	82536	Top	-0.07	0.11	-0.49	-0.07	32.40	38.11
				Bot	-0.78	-2.00	-1.72	-0.57	7.00	8.34
	L/4	116372	Cent	Top	-0.19	-0.41	-0.55	-0.10	24.99	29.47
				Bot	-0.19	-0.42	-0.53	-0.07	25.85	30.48
		116372	217892	Top	-0.38	-0.77	-1.18	-0.11	11.63	13.74
				Bot	-0.19	-0.43	-0.51	-0.07	26.27	30.98
		116372	217896	Top	-0.29	-0.59	-0.88	-0.09	15.60	18.41
				Bot	-0.29	-0.61	-0.81	-0.08	16.71	19.72
		116372	208052	Top	-0.08	-0.22	-0.04	-0.17	169.61	199.90
				Bot	-0.11	-0.27	-0.41	0.00	35.14	41.39
		116372	28965	Top	-0.02	-0.09	-0.08	-0.03	187.81	221.08
				Bot	-0.18	-0.40	-0.37	-0.14	34.26	40.40
	L/2	117396	Cent	Top	-0.12	-0.26	-0.42	0.00	34.15	40.22
				Bot	-0.10	-0.25	-0.32	0.02	43.95	51.75
		117396	219991	Top	-0.13	-0.27	-0.45	0.00	31.98	37.68
				Bot	-0.09	-0.22	-0.28	0.02	50.31	59.24

(table cont'd.)

Flange	Reading Location (L)	Plate	Node	Location on Plate	Loading Case (ksi)				Rating Factor	
					Lane Load	Self Weight	Live Load	Sidewalk	Bridge1	Bridge2
TOP	L/2	117396	219995	Top	-0.14	-0.29	-0.48	0.00	29.59	34.86
				Bot	-0.08	-0.20	-0.24	0.02	57.71	67.95
		117396	210047	Top	-0.03	-0.11	-0.02	-0.02	415.94	489.62
				Bot	-0.20	-0.41	-0.72	0.04	19.91	23.47
		117396	19714	Top	-0.20	-0.36	-0.71	0.00	20.26	23.88
				Bot	-0.04	-0.16	-0.03	0.02	310.20	365.16
	3L/4	116280	Cent	Top	-0.19	-0.41	-0.54	-0.10	25.13	29.63
				Bot	-0.19	-0.42	-0.52	-0.07	25.96	30.62
		116280	217634	Top	-0.38	-0.77	-1.18	-0.11	11.63	13.74
				Bot	-0.19	-0.43	-0.51	-0.07	26.39	31.12
		116280	29054	Top	-0.02	-0.09	-0.08	-0.03	194.83	229.35
				Bot	-0.18	-0.40	-0.37	-0.14	34.44	40.62
		116280	210825	Top	-0.08	-0.22	-0.04	-0.17	174.12	205.22
				Bot	-0.11	-0.27	-0.41	0.00	35.48	41.79
		116280	217699	Top	-0.29	-0.59	-0.88	-0.09	15.64	18.46
				Bot	-0.29	-0.61	-0.81	-0.09	16.76	19.78
	L	117143	Cent	Top	-0.21	-0.50	-0.49	-0.16	26.70	31.50
				Bot	-0.28	-0.79	-0.54	-0.20	22.64	26.76
		117143	219467	Top	-0.16	-0.47	-0.27	-0.11	45.12	53.23
				Bot	0.04	-0.01	0.17	0.02	93.41	109.90
		117143	82557	Top	-0.07	0.11	-0.49	-0.07	32.31	38.00
				Bot	-0.78	-2.00	-1.71	-0.57	7.03	8.37
		117143	212918	Top	-0.61	-1.29	-1.57	-0.45	8.19	9.72
				Bot	-0.25	-0.60	-0.63	-0.19	20.99	24.78
		117143	219468	Top	0.00	-0.14	0.14	0.00	133.12	156.52
				Bot	-0.12	-0.34	-0.23	-0.08	53.36	62.90

Table A. 3. Floorbeam E Rating Factors (Non-Composite)

Flange	Reading Location (L)	Plate	Node	Location on Plate	Loading Case (ksi)				Rating Factor to be Averaged		Rating Factor	
					Lane Load	Self Weight	Live Load	Sidewalk	Bridge1	Bridge2	Bridge1	Bridge2
BOT.	0L	102902	Cent	Top	0.97	0.75	2.80	0.11	5.04	5.95	13.97	16.46
				Bot	-0.16	-0.12	-0.19	0.01	58.56	68.93		
		102902	188385	Top	-1.19	-0.91	-3.12	-0.10	4.41	5.22		
				Bot	1.30	1.00	3.49	0.12	3.95	4.67		
		102902	188389	Top	0.91	0.70	2.49	0.09	5.63	6.64		
				Bot	-0.62	-0.46	-1.56	-0.04	8.89	10.49		
		102902	95269	Top	-1.99	-1.51	-4.94	-0.14	2.70	3.20		
				Bot	3.34	2.55	9.29	0.34	1.42	1.69		
		102902	82694	Top	5.84	4.49	15.90	0.56	0.77	0.93		
				Bot	-4.50	-3.46	-11.60	-0.35	1.08	1.30		
	0L	102898	Cent	Top	-0.07	-0.05	-0.16	0.00	84.94	99.96		
				Bot	0.12	0.09	0.33	0.01	43.97	51.76		
		102898	82693	Top	0.67	0.52	1.78	0.06	7.85	9.26		
				Bot	-0.66	-0.51	-1.76	-0.06	7.95	9.37		
		102898	188383	Top	-0.38	-0.29	-1.02	-0.03	13.83	16.30		
				Bot	0.39	0.30	1.03	0.03	13.70	16.14		
		102898	188389	Top	0.88	0.67	2.37	0.08	5.89	6.95		
				Bot	-0.82	-0.62	-2.15	-0.07	6.47	7.64		
		102898	188385	Top	-1.40	-1.08	-3.69	-0.12	3.71	4.39		
				Bot	1.51	1.16	4.04	0.14	3.39	4.02		
	0L	102997	Cent	Top	0.98	0.74	2.84	0.11	4.98	5.88		
				Bot	-0.22	-0.17	-0.33	0.01	37.35	43.97		
		102997	95269	Top	-2.03	-1.55	-5.05	-0.14	2.64	3.13		

(table cont'd.)

Flange	Reading Location (L)	Plate	Node	Location on Plate	Loading Case (ksi)				Rating Factor to be Averaged		Rating Factor	
					Lane Load	Self Weight	Live Load	Sidewalk	Bridge1	Bridge2	Bridge1	Bridge2
BOT.	0L			Bot	3.37	2.56	9.40	0.35	1.40	1.67	13.97	16.46
		102997	188545	Top	0.88	0.66	2.44	0.09	5.75	6.79		
				Bot	-0.64	-0.50	-1.61	-0.05	8.59	10.13		
		102997	188538	Top	-1.21	-0.93	-3.21	-0.10	4.30	5.08		
				Bot	1.21	0.92	3.25	0.11	4.26	5.03		
		102997	82694	Top	5.89	4.48	16.10	0.56	0.76	0.91		
				Bot	-4.57	-3.47	-11.80	-0.36	1.06	1.28		
	0L	102994	Cent	Top	-0.06	-0.05	-0.14	0.00	98.57	115.98		
				Bot	0.11	0.08	0.31	0.01	46.37	54.57		
		102994	82695	Top	0.72	0.55	1.93	0.06	7.25	8.55		
				Bot	-0.73	-0.56	-1.95	-0.06	7.17	8.46		
		102994	188538	Top	-1.49	-1.14	-3.95	-0.13	3.47	4.10		
				Bot	1.58	1.20	4.23	0.14	3.24	3.83		
		102994	188545	Top	0.93	0.71	2.49	0.08	5.59	6.60		
				Bot	-0.88	-0.67	-2.34	-0.08	5.94	7.02		
		102994	188540	Top	-0.40	-0.31	-1.06	-0.04	13.28	15.65		
				Bot	0.41	0.32	1.10	0.04	12.82	15.11		
	L/4	104327	Cent	Top	4.03	2.93	12.50	0.32			1.06	1.27
				Bot	4.29	3.11	13.30	0.34			0.99	1.19
		104327	188913	Top	4.05	2.98	12.50	0.33			1.06	1.27
				Bot	4.33	3.17	13.30	0.35			0.99	1.18
		104327	41046	Top	4.00	2.88	12.50	0.31			1.07	1.27
				Bot	4.27	3.06	13.30	0.33			1.00	1.19
		104327	92024	Top	4.00	2.89	12.50	0.31			1.07	1.27

(table cont'd.)

Flange	Reading Location (L)	Plate	Node	Location on Plate	Loading Case (ksi)				Rating Factor to be Averaged		Rating Factor	
					Lane Load	Self Weight	Live Load	Sidewalk	Bridge1	Bridge2	Bridge1	Bridge2
BOT.	L/4			Bot	4.25	3.04	13.20	0.33			1.00	1.20
		104327	190691	Top	4.07	2.99	12.60	0.33			1.05	1.26
				Bot	4.32	3.17	13.30	0.35			0.99	1.18
	L/2	102956	Cent	Top	3.49	2.63	10.80	0.18			1.25	1.49
				Bot	3.87	2.90	12.00	0.20			1.11	1.33
		102956	188480	Top	3.50	2.67	10.80	0.19			1.25	1.48
				Bot	3.89	2.95	12.00	0.21			1.11	1.33
		102956	188485	Top	3.51	2.67	10.90	0.19			1.24	1.47
				Bot	3.89	2.95	12.00	0.21			1.11	1.33
		102956	92541	Top	3.49	2.59	10.90	0.18			1.24	1.48
				Bot	3.86	2.85	12.00	0.19			1.12	1.33
		102956	41034	Top	3.48	2.58	10.80	0.18			1.25	1.49
				Bot	3.86	2.85	12.00	0.19			1.12	1.33
	3L/4	104660	Cent	Top	3.24	2.84	10.10	0.33			1.32	1.58
				Bot	3.44	3.00	10.60	0.35			1.25	1.49
		104660	191225	Top	3.23	2.92	9.96	0.34			1.33	1.59
				Bot	3.42	3.08	10.50	0.36			1.26	1.50
		104660	92999	Top	3.26	2.77	10.20	0.32			1.31	1.57
				Bot	3.43	2.90	10.70	0.34			1.24	1.49
		104660	93000	Top	3.25	2.77	10.10	0.32			1.32	1.58
				Bot	3.47	2.94	10.80	0.33			1.23	1.47
		104660	191227	Top	3.23	2.90	9.98	0.34			1.33	1.59
				Bot	3.43	3.10	10.60	0.36			1.24	1.49
	L	103344	Cent	Top	0.89	0.82	2.49	0.11	5.62	6.64	12.57	14.81

(table cont'd.)

Flange	Reading Location (L)	Plate	Node	Location on Plate	Loading Case (ksi)				Rating Factor to be Averaged		Rating Factor	
					Lane Load	Self Weight	Live Load	Sidewalk	Bridge1	Bridge2	Bridge1	Bridge2
BOT.	L			Bot	-0.31	-0.17	-0.65	0.01	20.66	24.32	12.57	14.81
		103344	189104	Top	-1.21	-0.97	-3.17	-0.11	4.33	5.12		
				Bot	1.20	0.99	3.17	0.11	4.34	5.13		
		103344	82670	Top	5.69	4.78	15.30	0.57	0.79	0.95		
				Bot	-4.69	-3.71	-12.10	-0.36	1.03	1.23		
		103344	93474	Top	-2.15	-1.60	-5.44	-0.14	2.46	2.91		
				Bot	3.15	2.65	8.60	0.35	1.52	1.81		
		103344	189106	Top	0.85	0.72	2.28	0.09	6.11	7.22		
				Bot	-0.65	-0.46	-1.66	-0.04	8.38	9.89		
	L	103345	Cent	Top	-0.07	-0.05	-0.17	0.00	84.74	99.71		
				Bot	0.11	0.09	0.29	0.01	49.75	58.55		
		103345	189106	Top	0.90	0.72	2.39	0.08	5.81	6.86		
				Bot	-0.87	-0.69	-2.29	-0.08	6.06	7.15		
		103345	189098	Top	-0.39	-0.30	-1.04	-0.03	13.54	15.96		
				Bot	0.41	0.32	1.07	0.04	13.14	15.49		
		103345	82669	Top	0.72	0.59	1.90	0.06	7.34	8.65		
				Bot	-0.72	-0.59	-1.91	-0.07	7.30	8.62		
		103345	189104	Top	-1.49	-1.21	-3.91	-0.13	3.49	4.13		
				Bot	1.55	1.27	4.11	0.14	3.32	3.93		
	L	103372	Cent	Top	0.85	0.70	2.41	0.11	5.85	6.90		
				Bot	-0.28	-0.15	-0.57	0.01	23.40	27.54		
		103372	189147	Top	-1.20	-0.93	-3.12	-0.10	4.40	5.20		
				Bot	1.25	0.98	3.35	0.12	4.12	4.87		
		103372	189148	Top	0.85	0.67	2.31	0.09	6.05	7.15		

(table cont'd.)

Flange	Reading Location (L)	Plate	Node	Location on Plate	Loading Case (ksi)				Rating Factor to be Averaged		Rating Factor	
					Lane Load	Self Weight	Live Load	Sidewalk	Bridge1	Bridge2	Bridge1	Bridge2
BOT.	L			Bot	-0.67	-0.53	-1.70	-0.05	8.15	9.61	12.57	14.81
		103372	93474	Top	-2.11	-1.59	-5.32	-0.14	2.51	2.98		
				Bot	3.09	2.57	8.45	0.34	1.55	1.85		
		103372	82670	Top	5.58	4.43	15.00	0.55	0.81	0.98		
				Bot	-4.61	-3.47	-11.90	-0.35	1.05	1.26		
	L	103369	Cent	Top	-0.07	-0.05	-0.17	0.00	81.04	95.36		
				Bot	0.10	0.09	0.29	0.01	49.86	58.68		
		103369	189148	Top	0.87	0.70	2.31	0.08	6.02	7.11		
				Bot	-0.83	-0.65	-2.16	-0.07	6.43	7.59		
		103369	189147	Top	-1.40	-1.08	-3.66	-0.12	3.74	4.42		
				Bot	1.47	1.15	3.90	0.14	3.51	4.15		
		103369	82671	Top	0.66	0.51	1.75	0.06	7.99	9.43		
				Bot	-0.66	-0.51	-1.73	-0.06	8.07	9.52		
		103369	189145	Top	-0.37	-0.31	-0.99	-0.03	14.26	16.80		
				Bot	0.37	0.31	0.99	0.03	14.21	16.74		
TOP	0L	104040	Cent	Top	-0.42	-0.31	-1.33	-0.06			10.95	12.91
				Bot	-0.51	-0.37	-1.63	-0.07			8.95	10.54
		104040	190217	Top	-0.26	-0.18	-0.85	-0.03			17.36	20.44
				Bot	0.10	0.07	0.35	0.01			43.44	51.12
		104040	190221	Top	-0.07	-0.04	-0.17	-0.01			80.22	94.39
				Bot	-0.29	-0.20	-0.93	-0.04			15.79	18.60
		104040	94817	Top	-1.28	-0.93	-4.19	-0.18			3.43	4.05
				Bot	-0.23	-0.19	-0.67	-0.04			21.51	25.33
		104040	82697	Top	-0.01	-0.05	0.07	-0.02			327.14	384.76

(table cont'd.)

Flange	Reading Location (L)	Plate	Node	Location on Plate	Loading Case (ksi)				Rating Factor to be Averaged		Rating Factor	
					Lane Load	Self Weight	Live Load	Sidewalk	Bridge1	Bridge2	Bridge1	Bridge2
TOP	0L			Bot	-1.49	-1.06	-4.88	-0.20			2.93	3.47
	L/4	104416	Cent	Top	-4.33	-3.04	-13.80	-0.31			0.97	1.15
				Bot	-3.98	-2.82	-12.70	-0.29			1.06	1.26
		104416	93099	Top	-3.79	-2.81	-12.00	-0.33			1.12	1.33
				Bot	-4.79	-3.35	-14.60	-0.33			0.89	1.07
		104416	190841	Top	-4.05	-2.80	-13.40	-0.27			1.01	1.21
				Bot	-3.95	-2.72	-13.00	-0.27			1.04	1.24
		104416	102341	Top	-4.89	-3.26	-15.60	-0.30			0.85	1.02
				Bot	-3.08	-2.23	-10.60	-0.24			1.31	1.56
		104416	10117	Top	-4.55	-3.27	-14.10	-0.34			0.93	1.12
				Bot	-4.09	-2.95	-12.60	-0.33			1.05	1.26
	L/2	103788	Cent	Top	-3.95	-2.83	-12.50	-0.18			1.08	1.28
				Bot	-3.45	-2.49	-10.90	-0.17			1.25	1.49
		103788	96152	Top	-3.46	-2.63	-10.80	-0.20			1.25	1.49
				Bot	-4.19	-3.01	-12.90	-0.18			1.03	1.23
		103788	8990	Top	-4.16	-3.06	-12.90	-0.20			1.03	1.23
				Bot	-3.48	-2.59	-10.80	-0.18			1.25	1.49
		103788	99333	Top	-4.45	-3.03	-14.20	-0.16			0.94	1.13
				Bot	-2.70	-1.97	-8.98	-0.16			1.55	1.85
		103788	189826	Top	-3.74	-2.61	-12.10	-0.16			1.12	1.34
				Bot	-3.44	-2.40	-11.10	-0.15			1.23	1.47
	3L/4	103471	Cent	Top	-3.39	-2.69	-10.80	-0.32			1.25	1.49
				Bot	-3.36	-2.67	-10.70	-0.30			1.26	1.50
		103471	189315	Top	-3.39	-2.53	-11.10	-0.29			1.23	1.46

(table cont'd.)

Flange	Reading Location (L)	Plate	Node	Location on Plate	Loading Case (ksi)				Rating Factor to be Averaged		Rating Factor	
					Lane Load	Self Weight	Live Load	Sidewalk	Bridge1	Bridge2	Bridge1	Bridge2
TOP	3L/4			Bot	-3.20	-2.36	-10.50	-0.27			1.31	1.56
		103471	95853	Top	-3.38	-2.86	-10.50	-0.35			1.27	1.52
				Bot	-3.49	-2.96	-10.80	-0.33			1.23	1.47
		103471	95852	Top	-3.63	-3.07	-11.30	-0.35			1.17	1.40
				Bot	-3.27	-2.79	-10.20	-0.33			1.31	1.56
		103471	189314	Top	-3.12	-2.29	-10.40	-0.28			1.32	1.58
				Bot	-3.46	-2.56	-11.30	-0.28			1.20	1.44
	L	103426	Cent	Top	-0.31	-0.26	-0.93	-0.06			15.54	18.31
				Bot	-0.40	-0.30	-1.23	-0.07			11.82	13.92
		103426	189238	Top	-0.17	-0.13	-0.55	-0.02			26.73	31.47
				Bot	0.13	0.11	0.43	0.02			34.29	40.37
		103426	82675	Top	0.08	-0.04	0.33	-0.02			46.68	54.91
				Bot	-1.24	-0.99	-3.94	-0.21			3.62	4.28
		103426	94003	Top	-1.04	-0.93	-3.30	-0.18			4.33	5.12
				Bot	-0.12	-0.12	-0.32	-0.04			44.06	51.87
		103426	189240	Top	-0.04	0.04	-0.07	-0.01			189.17	222.52
				Bot	-0.23	-0.16	-0.72	-0.04			20.28	23.87

Table A. 4. Floorbeam E Rating Factors (Composite)

Flange	Reading Location (L)	Plate	Node	Location on Plate	Loading Case (ksi)				Rating Factor to be Averaged		Rating Factor	
					Lane Load	Self Weight	Live Load	Sidewalk	Bridge1	Bridge2	Bridge1	Bridge2
BOT.	0L	102902	Cent	Top	0.81	0.65	2.21	0.10	6.33	7.47	35.03	41.23
				Bot	-0.04	-0.13	0.06	0.01	590.51	694.37		
		102902	188385	Top	-0.90	-0.85	-2.26	-0.09	6.04	7.14		
				Bot	1.01	0.90	2.58	0.11	5.31	6.27		
		102902	188389	Top	0.72	0.62	1.89	0.08	7.35	8.68		
				Bot	-0.46	-0.48	-1.11	-0.04	12.36	14.58		
		102902	95269	Top	-1.43	-1.46	-3.39	-0.13	3.90	4.62		
				Bot	2.74	2.37	7.20	0.32	1.82	2.16		
		102902	82694	Top	4.62	4.07	11.90	0.51	1.03	1.24		
				Bot	-3.32	-3.17	-8.17	-0.32	1.54	1.84		
	0L	102898	Cent	Top	-0.05	-0.05	-0.11	0.00	123.94	145.85		
				Bot	0.10	0.08	0.25	0.01	56.21	66.16		
		102898	82693	Top	0.51	0.47	1.30	0.05	10.66	12.57		
				Bot	-0.51	-0.47	-1.29	-0.05	10.74	12.67		
		102898	188383	Top	-0.30	-0.29	-0.77	-0.03	18.13	21.36		
				Bot	0.30	0.29	0.77	0.03	18.13	21.36		
		102898	188389	Top	0.69	0.63	1.77	0.07	7.81	9.22		
				Bot	-0.63	-0.59	-1.57	-0.06	8.78	10.36		
		102898	188385	Top	-1.07	-0.99	-2.68	-0.11	5.07	6.00		
				Bot	1.17	1.06	2.99	0.13	4.55	5.39		
	0L	102997	Cent	Top	0.86	0.75	2.31	0.11	6.03	7.12		
				Bot	-0.08	-0.17	-0.05	0.01	171.10	201.43		
		102997	95269	Top	-1.46	-1.46	-3.46	-0.13	3.82	4.53		

(table cont'd.)

Flange	Reading Location (L)	Plate	Node	Location on Plate	Loading Case (ksi)				Rating Factor to be Averaged		Rating Factor	
					Lane Load	Self Weight	Live Load	Sidewalk	Bridge1	Bridge2	Bridge1	Bridge2
BOT.	0L			Bot	2.77	2.43	7.31	0.32	1.79	2.13	35.03	41.23
		102997	188545	Top	0.72	0.66	1.89	0.08	7.34	8.66		
				Bot	-0.46	-0.43	-1.10	-0.04	12.48	14.71		
		102997	188538	Top	-0.94	-0.90	-2.38	-0.10	5.74	6.78		
				Bot	0.96	0.91	2.44	0.10	5.61	6.63		
		102997	82694	Top	4.76	4.39	12.30	0.53	0.98	1.19		
				Bot	-3.45	-3.42	-8.48	-0.33	1.47	1.76		
	0L	102994	Cent	Top	-0.04	-0.04	-0.09	0.00	147.68	173.78		
				Bot	0.09	0.08	0.24	+0.01	58.39	68.72		
		102994	82695	Top	0.57	0.55	1.44	0.06	9.60	11.32		
				Bot	-0.58	-0.54	-1.46	-0.06	9.48	11.18		
		102994	188538	Top	-1.16	-1.11	-2.92	-0.12	4.64	5.49		
				Bot	1.25	1.17	3.18	0.13	4.26	5.04		
		102994	188545	Top	0.73	0.67	1.85	0.08	7.45	8.80		
				Bot	-0.68	-0.64	-1.72	-0.07	8.01	9.45		
		102994	188540	Top	-0.31	-0.27	-0.78	-0.03	17.99	21.19		
				Bot	0.32	0.29	0.82	0.03	17.08	20.13		
	L/4	104327	Cent	Top	3.27	2.24	9.27	0.24			1.44	1.72
				Bot	3.43	2.33	9.71	0.25			1.37	1.64
		104327	188913	Top	3.26	2.20	9.25	0.24			1.45	1.72
				Bot	3.43	2.30	9.70	0.25			1.38	1.64
		104327	41046	Top	3.28	2.28	9.30	0.24			1.44	1.71
				Bot	3.43	2.35	9.69	0.25			1.37	1.64
		104327	92024	Top	3.26	2.26	9.24	0.24			1.45	1.72

(table cont'd.)

Flange	Reading Location (L)	Plate	Node	Location on Plate	Loading Case (ksi)				Rating Factor to be Averaged		Rating Factor	
					Lane Load	Self Weight	Live Load	Sidewalk	Bridge1	Bridge2	Bridge1	Bridge2
BOT.	L/4			Bot	3.44	2.36	9.72	0.25			1.37	1.63
		104327	190691	Top	3.28	2.20	9.28	0.24			1.44	1.72
				Bot	3.43	2.31	9.71	0.25			1.37	1.64
	L/2	102956	Cent	Top	2.88	2.07	8.13	0.13			1.66	1.97
				Bot	3.13	2.24	8.84	0.14			1.52	1.81
		102956	188480	Top	2.87	2.05	8.10	0.13			1.67	1.98
				Bot	3.12	2.23	8.82	0.14			1.52	1.81
		102956	188485	Top	2.88	2.05	8.14	0.13			1.66	1.97
				Bot	3.13	2.23	8.84	0.14			1.52	1.81
		102956	92541	Top	2.88	2.08	8.14	0.13			1.66	1.97
				Bot	3.12	2.24	8.83	0.14			1.52	1.81
		102956	41034	Top	2.87	2.08	8.12	0.13			1.66	1.97
				Bot	3.13	2.24	8.85	0.14			1.52	1.80
	3L/4	104660	Cent	Top	2.58	2.14	7.26	0.25			1.85	2.20
				Bot	2.70	2.24	7.60	0.26			1.76	2.09
		104660	191225	Top	2.56	2.08	7.18	0.25			1.87	2.22
				Bot	2.67	2.18	7.51	0.27			1.78	2.12
		104660	92999	Top	2.60	2.19	7.32	0.25			1.83	2.18
				Bot	2.73	2.29	7.68	0.26			1.74	2.07
		104660	93000	Top	2.62	2.21	7.37	0.25			1.81	2.16
				Bot	2.73	2.29	7.69	0.26			1.73	2.06
		104660	191227	Top	2.56	2.08	7.19	0.25			1.87	2.22
				Bot	2.68	2.19	7.53	0.26			1.78	2.11
	L	103344	Cent	Top	0.81	0.66	2.03	0.10	6.77	7.99	14.72	17.34

(table cont'd.)

Flange	Reading Location (L)	Plate	Node	Location on Plate	Loading Case (ksi)				Rating Factor to be Averaged		Rating Factor	
					Lane Load	Self Weight	Live Load	Sidewalk	Bridge1	Bridge2	Bridge1	Bridge2
BOT.	L			Bot	-0.28	-0.16	-0.54	0.01	24.07	28.34	14.72	17.34
		103344	189104	Top	-1.11	-0.87	-2.63	-0.10	5.12	6.05		
				Bot	1.10	0.85	2.61	0.10	5.16	6.10		
		103344	82670	Top	5.22	4.14	12.60	0.52	0.95	1.15		
				Bot	-4.30	-3.23	-10.00	-0.33	1.24	1.48		
		103344	93474	Top	-1.98	-1.49	-4.54	-0.13	2.88	3.42		
				Bot	2.91	2.41	7.13	0.32	1.80	2.15		
		103344	189106	Top	0.77	0.61	1.88	0.08	7.27	8.58		
				Bot	-0.61	-0.48	-1.40	-0.04	9.69	11.43		
	L	103345	Cent	Top	-0.06	-0.05	-0.14	0.00	98.92	116.40		
				Bot	0.10	0.08	0.24	0.01	58.61	68.98		
		103345	189106	Top	0.83	0.66	1.99	0.08	6.83	8.06		
				Bot	-0.80	-0.63	-1.90	-0.07	7.14	8.43		
		103345	189098	Top	-0.37	-0.31	-0.88	-0.03	15.71	18.51		
				Bot	0.38	0.31	0.90	0.04	15.31	18.04		
		103345	82669	Top	0.66	0.51	1.56	0.06	8.74	10.31		
				Bot	-0.66	-0.52	-1.57	-0.06	8.68	10.24		
		103345	189104	Top	-1.37	-1.06	-3.23	-0.12	4.14	4.89		
				Bot	1.42	1.11	3.39	0.13	3.95	4.67		
	L	103372	Cent	Top	0.80	0.73	2.03	0.10	6.76	7.99		
				Bot	-0.25	-0.14	-0.47	0.01	27.36	32.21		
		103372	189147	Top	-1.11	-0.88	-2.61	-0.09	5.15	6.08		
				Bot	1.17	0.96	2.80	0.11	4.81	5.68		
		103372	189148	Top	0.79	0.67	1.94	0.08	7.04	8.31		

(table cont'd.)

Flange	Reading Location (L)	Plate	Node	Location on Plate	Loading Case (ksi)				Rating Factor to be Averaged		Rating Factor	
					Lane Load	Self Weight	Live Load	Sidewalk	Bridge1	Bridge2	Bridge1	Bridge2
BOT.	L			Bot	-0.61	-0.44	-1.39	-0.04	9.75	11.50	14.72	17.34
		103372	93474	Top	-1.94	-1.44	-4.42	-0.12	2.96	3.51		
				Bot	2.86	2.39	7.03	0.32	1.83	2.18		
		103372	82670	Top	5.19	4.32	12.60	0.52	0.95	1.14		
				Bot	-4.27	-3.36	-9.96	-0.33	1.24	1.48		
	L	103369	Cent	Top	-0.06	-0.05	-0.15	0.00	94.44	111.14		
				Bot	0.10	0.08	0.24	0.01	57.96	68.22		
		103369	189148	Top	0.80	0.64	1.92	0.07	7.08	8.36		
				Bot	-0.76	-0.60	-1.80	-0.06	7.55	8.91		
		103369	189147	Top	-1.29	-1.04	-3.06	-0.11	4.38	5.18		
				Bot	1.36	1.11	3.26	0.13	4.11	4.86		
		103369	82671	Top	0.62	0.50	1.46	0.06	9.34	11.02		
				Bot	-0.61	-0.49	-1.45	-0.05	9.42	11.11		
		103369	189145	Top	-0.34	-0.27	-0.81	-0.03	16.91	19.92		
				Bot	0.35	0.27	0.82	0.03	16.73	19.71		
TOP	0L	104040	Cent	Top	-0.42	-0.34	-1.23	-0.06			11.65	13.73
				Bot	-0.52	-0.49	-1.51	-0.07			9.44	11.14
		104040	190217	Top	-0.26	-0.27	-0.75	-0.03			19.18	22.60
				Bot	0.08	0.09	0.26	0.01			55.82	65.70
		104040	190221	Top	-0.11	-0.19	-0.29	-0.01			48.19	56.74
				Bot	-0.29	-0.30	-0.85	-0.04			16.95	19.97
		104040	94817	Top	-1.22	-0.95	-3.59	-0.17			3.92	4.63
				Bot	-0.27	-0.20	-0.76	-0.04			18.85	22.20
		104040	82697	Top	-0.03	0.19	-0.03	-0.01			360.74	424.08

(table cont'd.)

Flange	Reading Location (L)	Plate	Node	Location on Plate	Loading Case (ksi)				Rating Factor to be Averaged		Rating Factor	
					Lane Load	Self Weight	Live Load	Sidewalk	Bridge1	Bridge2	Bridge1	Bridge2
TOP	0L			Bot	-1.46	-1.36	-4.30	-0.20			3.23	3.82
	L/4	104416	Cent	Top	-2.33	-1.58	-6.60	-0.19			2.07	2.46
				Bot	-2.14	-1.45	-6.03	-0.18			2.28	2.70
		104416	93099	Top	-2.19	-1.54	-6.24	-0.21			2.20	2.60
				Bot	-2.61	-1.75	-7.25	-0.17			1.87	2.22
		104416	190841	Top	-2.04	-1.33	-5.73	-0.16			2.40	2.85
				Bot	-2.56	-1.74	-7.27	-0.21			1.87	2.22
		104416	102341	Top	-2.82	-1.89	-7.97	-0.19			1.70	2.02
				Bot	-1.61	-1.10	-4.58	-0.17			3.04	3.59
		104416	10117	Top	-2.40	-1.65	-6.79	-0.18			2.01	2.39
				Bot	-1.92	-1.30	-5.38	-0.17			2.56	3.03
	L/2	103788	Cent	Top	-1.85	-1.32	-5.28	-0.07			2.63	3.11
				Bot	-1.52	-1.08	-4.26	-0.06			3.27	3.86
		103788	96152	Top	-1.53	-1.12	-4.28	-0.07			3.25	3.84
				Bot	-1.89	-1.31	-5.41	-0.06			2.57	3.04
		103788	8990	Top	-1.94	-1.39	-5.61	-0.08			2.47	2.93
				Bot	-1.47	-1.03	-4.04	-0.05			3.44	4.06
		103788	99333	Top	-2.13	-1.49	-6.18	-0.07			2.24	2.65
				Bot	-1.19	-0.87	-3.20	-0.05			4.34	5.13
		103788	189826	Top	-1.80	-1.26	-5.04	-0.06			2.75	3.25
				Bot	-1.54	-1.12	-4.41	-0.06			3.17	3.74
	3L/4	103471	Cent	Top	-2.19	-1.84	-6.09	-0.24			2.22	2.63
				Bot	-2.04	-1.72	-5.69	-0.21			2.38	2.83
		103471	189315	Top	-2.30	-1.91	-6.43	-0.23			2.10	2.49

(table cont'd.)

Flange	Reading Location (L)	Plate	Node	Location on Plate	Loading Case (ksi)				Rating Factor to be Averaged		Rating Factor	
					Lane Load	Self Weight	Live Load	Sidewalk	Bridge1	Bridge2	Bridge1	Bridge2
TOP	3L/4			Bot	-2.09	-1.73	-5.81	-0.21			2.33	2.77
		103471	95853	Top	-1.96	-1.67	-5.40	-0.24			2.51	2.98
				Bot	-1.98	-1.71	-5.56	-0.20			2.44	2.90
		103471	95852	Top	-2.27	-1.92	-6.36	-0.23			2.12	2.52
				Bot	-1.74	-1.52	-4.81	-0.21			2.83	3.36
		103471	189314	Top	-2.30	-1.89	-6.37	-0.25			2.11	2.51
				Bot	-2.42	-2.00	-6.82	-0.22			1.98	2.35
	L	103426	Cent	Top	-0.30	-0.33	-0.83	-0.06			17.10	20.15
				Bot	-0.40	-0.50	-1.11	-0.07			12.75	15.04
		103426	189238	Top	-0.17	-0.21	-0.47	-0.02			30.75	36.21
				Bot	0.12	0.14	0.34	0.02			41.86	49.28
		103426	82675	Top	0.08	0.19	0.23	-0.01			62.79	73.93
				Bot	-1.19	-1.39	-3.35	-0.20			4.10	4.86
		103426	94003	Top	-0.97	-0.95	-2.70	-0.17			5.15	6.09
				Bot	-0.14	-0.20	-0.40	-0.04			35.99	42.38
		103426	189240	Top	-0.07	-0.20	-0.19	-0.01			77.17	90.88
				Bot	-0.23	-0.30	-0.64	-0.04			22.11	26.05

Table A. 5. Unit 2 Interior Stringer Rating Factors (Non-Composite)

Flange	Reading Location (L)	Plate	Node	Location on Plate	Loading Case (ksi)				Rating Factor to be Averaged		Rating Factor	
					Lane Load	Self Weight	Live Load	Sidewalk	Bridge1	Bridge2	Bridge1	Bridge2
BOT.	0L	127791	Cent	Top	0.01	0.30	0.87	0.27			20.56	24.25
				Bot	0.14	0.53	0.74	0.29			20.97	24.76
		127791	43653	Top	-0.50	-0.53	1.24	0.32			21.21	24.93
				Bot	0.71	1.75	1.02	0.49			10.97	13.04
		127791	243949	Top	0.03	0.26	0.62	0.20			28.10	33.12
				Bot	0.08	0.35	0.60	0.22			26.98	31.82
		127791	243948	Top	0.04	0.24	0.55	0.16			30.89	36.40
				Bot	0.04	0.21	0.40	0.15			41.42	48.81
		127791	234009	Top	0.46	1.25	1.04	0.40			12.51	14.83
				Bot	-0.28	-0.21	0.94	0.29			25.00	29.42
	L/4	129749	Cent	Top	0.95	1.62	3.18	0.28			4.42	5.25
				Bot	1.00	1.68	3.37	0.29			4.17	4.95
		129749	247443	Top	0.96	1.67	3.19	0.29			4.40	5.23
				Bot	1.00	1.72	3.37	0.30			4.17	4.95
		129749	247866	Top	0.95	1.65	3.17	0.29			4.43	5.26
				Bot	1.00	1.72	3.36	0.30			4.18	4.96
		129749	236117	Top	0.95	1.59	3.19	0.27			4.42	5.24
				Bot	1.00	1.64	3.38	0.29			4.17	4.95
		129749	43511	Top	0.95	1.58	3.17	0.27			4.45	5.28
				Bot	1.00	1.63	3.35	0.29			4.20	4.99
	L/2	129344	Cent	Top	1.19	2.21	7.52	0.30			2.01	2.39
				Bot	1.25	2.31	8.13	0.31			1.86	2.21

(table cont'd.)

Flange	Reading Location (L)	Plate	Node	Location on Plate	Loading Case (ksi)				Rating Factor to be Averaged		Rating Factor	
					Lane Load	Self Weight	Live Load	Sidewalk	Bridge1	Bridge2	Bridge1	Bridge2
BOT.	L/2	129344	246573	Top	1.19	2.24	7.47	0.30			2.02	2.40
				Bot	1.26	2.34	8.06	0.32			1.87	2.23
		129344	247056	Top	1.20	2.24	7.48	0.30			2.02	2.40
				Bot	1.26	2.35	8.10	0.32			1.86	2.22
		129344	237992	Top	1.18	2.18	7.57	0.29			2.00	2.38
				Bot	1.25	2.28	8.18	0.30			1.85	2.20
		129344	43550	Top	1.18	2.18	7.55	0.29			2.01	2.39
				Bot	1.25	2.27	8.17	0.30			1.85	2.21
	3L/4	127822	Cent	Top	0.32	1.21	3.11	0.14			5.23	6.19
				Bot	0.33	1.24	3.30	0.15			4.94	5.85
		127822	239187	Top	0.33	1.21	3.14	0.14			5.18	6.13
				Bot	0.34	1.24	3.35	0.15			4.86	5.75
		127822	244009	Top	0.31	1.21	3.07	0.15			5.31	6.28
				Bot	0.32	1.24	3.26	0.15			5.00	5.92
		127822	244005	Top	0.32	1.21	3.10	0.15			5.25	6.22
				Bot	0.33	1.25	3.29	0.15			4.95	5.86
		127822	43580	Top	0.32	1.20	3.13	0.14			5.20	6.15
				Bot	0.33	1.22	3.30	0.14			4.95	5.85
	L	130016	Cent	Top	-1.92	-1.65	-2.74	-0.20			4.13	4.90
				Bot	-2.00	-1.70	-2.98	-0.20			3.85	4.56
		130016	240671	Top	-3.00	-2.45	-4.51	-0.27			2.48	2.96
				Bot	-3.56	-3.14	-5.09	-0.38			2.11	2.52
		130016	248409	Top	-0.74	-0.63	-1.02	-0.08			11.32	13.37
				Bot	-0.76	-0.66	-1.16	-0.08			10.31	12.17

(table cont'd.)

Flange	Reading Location (L)	Plate	Node	Location on Plate	Loading Case (ksi)				Rating Factor to be Averaged		Rating Factor	
					Lane Load	Self Weight	Live Load	Sidewalk	Bridge1	Bridge2	Bridge1	Bridge2
BOT.	L	130016	248405	Top	-0.26	-0.20	-0.43	-0.02			28.99	34.14
				Bot	-0.35	-0.33	-0.40	-0.05			27.23	32.09
		130016	43640	Top	-3.30	-2.98	-4.45	-0.38			2.37	2.84
				Bot	-2.95	-2.35	-4.69	-0.25			2.44	2.91
TOP	0L	127929	Cent	Top	0.34	0.51	-1.44	-0.29			15.49	18.21
				Bot	0.56	1.02	-0.71	-0.21			64.54	75.66
		127929	244223	Top	0.37	0.62	-1.52	-0.29			14.84	17.44
				Bot	0.59	1.14	-0.76	-0.20			60.41	70.78
		127929	238294	Top	0.37	0.59	-1.07	-0.24			23.37	27.45
				Bot	0.51	0.80	-0.84	-0.25			40.62	47.67
		127929	238293	Top	0.23	0.19	-1.70	-0.34			11.90	14.01
				Bot	0.65	1.20	-0.21	-0.15			62.04	73.34
		127929	244222	Top	0.42	0.73	-1.34	-0.27			18.05	21.19
				Bot	0.54	1.02	-0.94	-0.22			35.14	41.20
	L/4	129859	Cent	Top	-0.31	-0.04	-2.57	-0.11			6.50	7.65
				Bot	-0.23	0.10	-2.27	-0.09			7.48	8.80
		129859	247663	Top	-0.29	0.05	-2.48	-0.09			6.75	7.95
				Bot	-0.20	0.18	-2.28	-0.08			7.53	8.86
		129859	248086	Top	-0.27	0.06	-2.49	-0.10			6.77	7.97
				Bot	-0.22	0.16	-2.24	-0.08			7.61	8.95
		129859	238363	Top	-0.25	-0.04	-2.73	-0.12			6.22	7.33
				Bot	-0.33	-0.05	-2.21	-0.09			7.41	8.72
		129859	21588	Top	-0.40	-0.21	-2.56	-0.11			6.32	7.45
				Bot	-0.17	0.13	-2.35	-0.11			7.38	8.69

(table cont'd.)

Flange	Reading Location (L)	Plate	Node	Location on Plate	Loading Case (ksi)				Rating Factor to be Averaged		Rating Factor	
					Lane Load	Self Weight	Live Load	Sidewalk	Bridge1	Bridge2	Bridge1	Bridge2
TOP	L/2	129464	Cent	Top	-0.56	-0.65	-7.17	-0.12			2.35	2.78
				Bot	-0.48	-0.49	-6.51	-0.11			2.61	3.08
		129464	246813	Top	-0.56	-0.60	-7.41	-0.13			2.28	2.69
				Bot	-0.45	-0.43	-6.20	-0.11			2.75	3.24
		129464	247296	Top	-0.54	-0.58	-6.73	-0.12			2.50	2.96
				Bot	-0.48	-0.46	-6.88	-0.11			2.48	2.92
		129464	241024	Top	-0.47	-0.58	-6.70	-0.11			2.54	2.99
				Bot	-0.57	-0.65	-7.06	-0.13			2.38	2.81
		129464	21614	Top	-0.66	-0.82	-7.80	-0.13			2.14	2.53
				Bot	-0.40	-0.42	-5.94	-0.11			2.88	3.40
	3L/4	127959	Cent	Top	0.37	0.40	-2.49	0.04			8.37	9.83
				Bot	0.38	0.46	-2.25	0.03			9.44	11.08
		127959	240156	Top	0.49	0.53	-2.50	0.05			8.72	10.23
				Bot	0.23	0.25	-2.34	0.02			8.49	9.97
		127959	244283	Top	0.39	0.45	-2.42	0.04			8.72	10.23
				Bot	0.39	0.48	-2.21	0.04			9.68	11.36
		127959	244279	Top	0.36	0.41	-2.46	0.03			8.44	9.91
				Bot	0.42	0.52	-2.22	0.04			9.74	11.43
		127959	21634	Top	0.25	0.23	-2.56	0.02			7.75	9.10
				Bot	0.50	0.58	-2.21	0.04			10.12	11.87
	L	129912	Cent	Top	1.55	1.86	1.85	0.21	5.69	6.76	28.99	34.17
				Bot	2.30	2.73	2.94	0.32	3.56	4.25		
		129912	238570	Top	6.17	7.52	7.92	0.80	1.10	1.35		
				Bot	0.47	0.38	0.46	0.11	22.13	26.09		

(table cont'd.)

Flange	Reading Location (L)	Plate	Node	Location on Plate	Loading Case (ksi)				Rating Factor to be Averaged		Rating Factor	
					Lane Load	Self Weight	Live Load	Sidewalk	Bridge1	Bridge2	Bridge1	Bridge2
TOP	L	129912	248197	Top	0.11	0.12	0.00	0.02	224.62	264.41	28.99	34.17
				Bot	1.25	1.52	1.62	0.17	6.78	8.04		
		129912	248193	Top	1.07	1.31	1.34	0.14	8.15	9.65		
				Bot	-0.73	-0.89	-1.07	-0.09	10.96	12.96		
		129912	21650	Top	-1.37	-1.78	-2.12	-0.15	5.47	6.49		
				Bot	7.66	9.26	10.00	1.01	0.81	1.01		
	L	129911	Cent	Top	0.24	0.30	0.27	0.03	40.14	47.30		
				Bot	0.07	0.08	0.09	0.01	121.30	142.77		
		129911	248195	Top	0.58	0.73	0.66	0.07	16.24	19.18		
				Bot	-0.32	-0.42	-0.42	-0.03	27.35	32.25		
		129911	21814	Top	-0.55	-0.67	-0.74	-0.07	15.43	18.21		
				Bot	0.56	0.69	0.73	0.07	15.53	18.33		
		129911	248193	Top	1.35	1.65	1.78	0.18	6.18	7.34		
				Bot	-1.02	-1.26	-1.40	-0.13	8.08	9.57		
		129911	248197	Top	-0.49	-0.60	-0.74	-0.06	16.26	19.18		
				Bot	0.93	1.13	1.25	0.13	9.01	10.66		
	L	129964	Cent	Top	1.55	1.83	1.84	0.21	5.71	6.78		
				Bot	2.30	2.73	2.93	0.32	3.57	4.26		
		129964	238570	Top	6.18	7.50	7.92	0.80	1.10	1.35		
				Bot	0.47	0.38	0.46	0.11	22.13	26.10		
		129964	21650	Top	-1.37	-1.81	-2.12	-0.15	5.46	6.49		
				Bot	7.66	9.27	10.00	1.01	0.81	1.01		
		129964	248294	Top	1.06	1.30	1.34	0.14	8.18	9.69		
				Bot	-0.73	-0.90	-1.07	-0.09	10.96	12.96		

(table cont'd.)

Flange	Reading Location (L)	Plate	Node	Location on Plate	Loading Case (ksi)				Rating Factor to be Averaged		Rating Factor	
					Lane Load	Self Weight	Live Load	Sidewalk	Bridge1	Bridge2	Bridge1	Bridge2
TOP	L	129964	248297	Top	0.11	0.08	-0.01	0.02	257.16	302.67	28.99	34.17
				Bot	1.25	1.50	1.62	0.17	6.78	8.04		
	L	129963	Cent	Top	0.25	0.29	0.27	0.03	40.27	47.44		
				Bot	0.07	0.09	0.10	0.02	120.39	141.70		
		129963	248294	Top	1.35	1.66	1.79	0.17	6.16	7.31		
				Bot	-1.02	-1.26	-1.41	-0.13	8.05	9.53		
		129963	21815	Top	-0.56	-0.69	-0.77	-0.07	15.05	17.77		
				Bot	0.56	0.69	0.75	0.07	15.20	17.95		
		129963	248292	Top	0.58	0.70	0.67	0.06	16.05	18.95		
				Bot	-0.33	-0.41	-0.43	-0.03	26.55	31.30		
		129963	248297	Top	-0.49	-0.62	-0.74	-0.06	16.15	19.06		
				Bot	0.93	1.15	1.26	0.13	8.96	10.60		

Table A. 6. Unit 2 Interior Stringer Rating Factors (Composite)

Flange	Reading Location (L)	Plate	Node	Location on Plate	Loading Case (ksi)				Rating Factor to be Averaged		Rating Factor	
					Lane Load	Self Weight	Live Load	Sidewalk	Bridge1	Bridge2	Bridge1	Bridge2
BOT.	0L	127791	Cent	Top	-0.08	-0.29	1.03	0.31			18.79	22.10
				Bot	0.07	0.20	0.82	0.33			20.66	24.37
		127791	43653	Top	-0.52	-1.75	1.91	0.37			12.52	14.64
				Bot	0.52	1.71	0.66	0.55			16.14	19.19
		127791	243949	Top	-0.03	-0.16	0.72	0.22			26.22	30.85
				Bot	0.02	0.04	0.69	0.25			25.68	30.26
		127791	243948	Top	-0.03	-0.14	0.64	0.19			29.81	35.08
				Bot	0.02	0.01	0.48	0.17			36.99	43.55
		127791	234009	Top	0.28	0.90	0.83	0.46			16.87	19.97
				Bot	-0.28	-0.96	1.43	0.34			15.21	17.84
	L/4	129749	Cent	Top	0.76	0.94	3.52	0.26			4.30	5.09
				Bot	0.79	0.98	3.63	0.26			4.16	4.93
		129749	247443	Top	0.76	0.93	3.49	0.26			4.34	5.14
				Bot	0.79	0.97	3.60	0.27			4.20	4.97
		129749	247866	Top	0.76	0.93	3.51	0.26			4.32	5.11
				Bot	0.79	0.97	3.61	0.27			4.19	4.95
		129749	236117	Top	0.77	0.95	3.53	0.26			4.29	5.07
				Bot	0.80	0.99	3.66	0.26			4.13	4.88
		129749	43511	Top	0.77	0.96	3.56	0.25			4.25	5.03
				Bot	0.80	0.99	3.65	0.26			4.14	4.90
	L/2	129344	Cent	Top	0.85	1.24	7.04	0.15			2.28	2.70
				Bot	0.88	1.29	7.38	0.15			2.17	2.58

(table cont'd.)

Flange	Reading Location (L)	Plate	Node	Location on Plate	Loading Case (ksi)				Rating Factor to be Averaged		Rating Factor	
					Lane Load	Self Weight	Live Load	Sidewalk	Bridge1	Bridge2	Bridge1	Bridge2
BOT.	L/2	129344	246573	Top	0.84	1.23	6.98	0.15			2.30	2.72
				Bot	0.88	1.28	7.30	0.16			2.20	2.60
		129344	247056	Top	0.85	1.24	6.99	0.15			2.30	2.72
				Bot	0.88	1.29	7.33	0.16			2.19	2.59
		129344	237992	Top	0.84	1.24	7.10	0.14			2.27	2.68
				Bot	0.89	1.29	7.44	0.15			2.16	2.55
		129344	43550	Top	0.86	1.26	7.09	0.14			2.26	2.68
				Bot	0.88	1.28	7.43	0.15			2.16	2.56
	3L/4	127822	Cent	Top	0.03	0.07	2.84	0.00			6.37	7.49
				Bot	0.04	0.08	2.93	0.00			6.16	7.24
		127822	239187	Top	0.06	0.11	2.95	0.00			6.08	7.16
				Bot	0.04	0.07	2.91	-0.01			6.21	7.30
		127822	244009	Top	0.02	0.04	2.78	0.00			6.53	7.69
				Bot	0.03	0.07	2.90	0.00			6.23	7.33
		127822	244005	Top	0.03	0.06	2.83	0.00			6.39	7.52
				Bot	0.03	0.06	2.90	0.00			6.23	7.34
		127822	43580	Top	0.02	0.05	2.78	-0.01			6.53	7.69
				Bot	0.06	0.10	3.02	0.00			5.94	6.99
	L	130016	Cent	Top	-1.66	-2.21	-2.23	-0.22	4.87	5.80	52.38	61.69
				Bot	-1.80	-2.70	-2.77	-0.27	4.04	4.82		
		130016	240671	Top	-2.98	-4.64	-4.74	-0.44	2.22	2.69		
				Bot	-2.90	-3.76	-3.85	-0.40	2.66	3.19		
		130016	248409	Top	-0.61	-0.73	-0.72	-0.08	15.16	17.90		
				Bot	-0.66	-1.04	-1.07	-0.10	11.24	13.30		

(table cont'd.)

Flange	Reading Location (L)	Plate	Node	Location on Plate	Loading Case (ksi)				Rating Factor to be Averaged		Rating Factor	
					Lane Load	Self Weight	Live Load	Sidewalk	Bridge1	Bridge2	Bridge1	Bridge2
BOT.	L	130016	248405	Top	-0.27	-0.54	-0.53	-0.05	24.38	28.76	52.38	61.69
				Bot	-0.16	0.01	0.05	-0.01	264.12	310.72		
		130016	43640	Top	-2.45	-2.51	-2.52	-0.29	3.84	4.58		
				Bot	-3.13	-5.45	-5.62	-0.51	1.89	2.29		
	L	130015	Cent	Top	-0.15	-0.22	-0.21	-0.02	55.83	65.75		
				Bot	-0.16	-0.21	-0.21	-0.02	54.99	64.76		
		130015	248407	Top	-0.14	-0.24	-0.23	-0.02	54.65	64.37		
				Bot	-0.14	-0.12	-0.12	-0.02	82.58	97.20		
		130015	43641	Top	0.03	0.17	0.18	0.01	90.92	107.05		
				Bot	-0.05	-0.19	-0.20	-0.02	76.80	90.44		
		130015	248405	Top	-0.25	-0.60	-0.62	-0.05	22.31	26.32		
				Bot	-0.07	0.16	0.18	0.01	143.21	168.60		
		130015	248409	Top	-0.17	-0.07	-0.05	-0.01	103.78	122.14		
				Bot	-0.26	-0.52	-0.54	-0.05	24.33	28.70		
	L	130070	Cent	Top	-1.66	-2.21	-2.24	-0.23	4.86	5.78		
				Bot	-1.80	-2.70	-2.76	-0.27	4.05	4.83		
		130070	240671	Top	-2.98	-4.64	-4.75	-0.44	2.22	2.68		
				Bot	-2.90	-3.76	-3.84	-0.40	2.66	3.20		
		130070	43640	Top	-2.47	-2.54	-2.54	-0.29	3.81	4.54		
				Bot	-3.12	-5.43	-5.60	-0.51	1.90	2.30		
		130070	248512	Top	-0.27	-0.54	-0.53	-0.05	24.45	28.84		
				Bot	-0.16	0.01	0.05	-0.01	259.03	304.74		
		130070	248515	Top	-0.61	-0.73	-0.72	-0.08	15.15	17.89		
				Bot	-0.67	-1.05	-1.06	-0.11	11.29	13.35		

(table cont'd.)

Flange	Reading Location (L)	Plate	Node	Location on Plate	Loading Case (ksi)				Rating Factor to be Averaged		Rating Factor	
					Lane Load	Self Weight	Live Load	Sidewalk	Bridge1	Bridge2	Bridge1	Bridge2
BOT.	L	130069	Cent	Top	-0.16	-0.22	-0.21	-0.02	54.73	64.45	52.38	61.69
				Bot	-0.16	-0.21	-0.21	-0.02	55.97	65.91		
		130069	248512	Top	-0.24	-0.59	-0.61	-0.05	22.51	26.56		
				Bot	-0.08	0.16	0.18	0.01	151.44	178.29		
		130069	43642	Top	0.02	0.16	0.18	0.01	93.10	109.62		
				Bot	-0.05	-0.19	-0.19	-0.02	78.36	92.27		
		130069	248510	Top	-0.14	-0.25	-0.24	-0.02	52.27	61.57		
				Bot	-0.14	-0.11	-0.10	-0.02	88.73	104.45		
		130069	248515	Top	-0.17	-0.07	-0.05	-0.01	100.29	118.03		
				Bot	-0.26	-0.52	-0.54	-0.05	24.53	28.93		
TOP	0L	127929	Cent	Top	-0.06	-0.33	0.13	0.06			215.48	253.20
				Bot	0.05	-0.08	0.48	0.09			35.09	41.28
		127929	244223	Top	-0.06	-0.33	0.18	0.07			135.87	159.66
				Bot	0.05	-0.07	0.50	0.10			33.92	39.91
		127929	238294	Top	-0.09	-0.37	0.07	0.06			19646.1	23144.7
				Bot	0.08	-0.04	0.50	0.07			32.55	38.30
		127929	238293	Top	-0.04	-0.31	0.11	0.03			227.65	267.50
				Bot	0.03	-0.09	0.45	0.10			38.18	44.92
		127929	244222	Top	-0.04	-0.28	0.18	0.06			124.06	145.81
				Bot	0.04	-0.11	0.50	0.10			34.78	40.91
	L/4	129859	Cent	Top	0.11	0.11	0.41	0.01			36.61	43.09
				Bot	0.14	0.15	0.50	0.02			30.12	35.46
		129859	247663	Top	0.02	-0.03	0.06	0.04			251.66	296.08

(table cont'd.)

Flange	Reading Location (L)	Plate	Node	Location on Plate	Loading Case (ksi)				Rating Factor to be Averaged		Rating Factor	
					Lane Load	Self Weight	Live Load	Sidewalk	Bridge1	Bridge2	Bridge1	Bridge2
TOP	L/4			Bot	0.14	0.13	0.33	0.03			42.36	49.87
		129859	248086	Top	0.10	0.08	0.27	0.02			53.42	62.88
				Bot	0.09	0.07	0.28	0.04			52.91	62.27
		129859	238363	Top	0.20	0.23	0.37	0.00			34.67	40.83
				Bot	0.12	0.14	0.94	0.01			17.65	20.78
		129859	21588	Top	0.12	0.14	0.87	0.00			18.91	22.26
				Bot	0.20	0.22	0.40	0.02			33.00	38.87
	L/2	129464	Cent	Top	0.02	-0.02	0.79	-0.01			22.58	26.56
				Bot	0.08	0.05	1.08	0.00			16.04	18.87
		129464	246813	Top	0.06	0.03	0.18	0.02			78.87	92.80
				Bot	0.13	0.12	1.30	0.01			13.05	15.36
		129464	247296	Top	0.06	0.02	1.00	0.01			17.52	20.62
				Bot	0.10	0.08	0.52	0.02			30.49	35.89
		129464	241024	Top	0.12	0.11	1.47	-0.01			11.65	13.71
				Bot	-0.09	-0.17	0.74	-0.03			27.24	32.02
		129464	21614	Top	-0.13	-0.23	0.49	-0.03			46.82	55.02
				Bot	0.17	0.18	1.65	0.00			10.21	12.02
	3L/4	127959	Cent	Top	0.04	-0.01	0.31	0.01			54.26	63.83
				Bot	0.02	-0.03	0.31	0.00			56.42	66.37
		127959	240156	Top	0.16	0.14	0.37	0.01			37.23	43.83
				Bot	0.06	0.03	0.97	0.00			18.02	21.20
		127959	244283	Top	0.00	-0.07	0.07	0.00			297.78	350.22
				Bot	-0.07	-0.16	-0.08	0.00			134.89	158.81
		127959	244279	Top	-0.16	-0.29	-0.42	-0.01			33.86	39.89

(table cont'd.)

Flange	Reading Location (L)	Plate	Node	Location on Plate	Loading Case (ksi)				Rating Factor to be Averaged		Rating Factor	
					Lane Load	Self Weight	Live Load	Sidewalk	Bridge1	Bridge2	Bridge1	Bridge2
TOP	3L/4			Bot	0.00	-0.07	0.05	0.00			325.58	382.92
		127959	21634	Top	0.13	0.13	1.08	0.02			15.46	18.20
				Bot	0.07	0.03	0.20	-0.01			72.05	84.77
	L	129912	Cent	Top	0.27	0.22	0.22	0.06			42.79	50.40
				Bot	0.16	0.07	0.07	0.05			96.87	114.02
		129912	238570	Top	0.76	0.74	0.56	0.14			15.71	18.56
				Bot	0.30	0.19	0.75	0.06			18.57	21.87
		129912	248197	Top	0.00	-0.03	-0.12	0.01			150.82	177.45
				Bot	-0.07	-0.16	-0.32	0.01			48.30	56.87
		129912	248193	Top	-0.10	-0.18	-0.53	0.01			30.26	35.63
				Bot	-0.21	-0.28	-0.37	-0.02			34.32	40.43
		129912	21650	Top	0.34	0.31	0.90	0.05			15.65	18.44
				Bot	0.56	0.46	0.15	0.13			31.59	37.27

REFERENCES

AASHTO. (2007). *AASHTO LRFD Movable Highway Bridge Design Specifications 2nd Edition.* Washington D.C.: American Association of State Highway and Transportation Officials.

AASHTO. (2011). *The Manual for Bridge Evaluation (MBE).* Washington, D.C.: American Association of State Highway and Transportation Officials.

AASHTO. (2017). *AASHTO LRFD Bridge Design Specifications, 8th Edition.* Washington, D.C.: American Association of State Highway and Transportation Officials.

ASCE. (2017). *Report Card for Louisiana Infrastructure.* United States: American Society of Civil Engineers.

Burdette, E., & Goodpasture, D. W. (1988). *Correlation of Bridge Load Capacity Estimated with Test Data.* Washington, D.C.: National Cooperative Highway Research Program.

Campbell Scientific, Inc. (2008). *ST350 Strain Transducer Instruction Manual.* Logan, Utah.

Catbas, F., Gul, M., Zaurin, R., Gokce, H., Terrell, T., Dumlupinar, T., & Maier, D. (2010). *Long Term Bridge Maintenance Monitoring Demonstration on a Movable Bridge A Framework for Structural Health Monitoring of Movable Bridges.* Tallahassee, FL: Florida Department of Transportation.

Catbas, F., Zaurin, R., Susoy, M., & Gul, M. (2007). *Integrative Information System Design for Florida Department of Transportation.* Tallahassee: Florida Department of Transportation.

Chen, A., & Yossef, M. (2015). Analytical Model for Deck-On-Girder Composite Beam System with Partial Composite Action. *Journal of Engineering Mechanics*, 1-11.

Chen, W.-F., & Duan, L. (2014). *Bridge Engineering Handbook, Second Edition: Fundamentals.* Boca Raton: CRC Press Taylor & Francis Group.

Eamon, C., & Nowak, A. (2002). Effects of Edge-Stiffening Elements and Diaphragms on Bridge Resistance and Load Distribution. *Journal of Bridge Engineering, ASCE*, 258-266.

FHWA. (2014). *Questions and Answers Load Rating of Specialized Hauling Vehicles.* Office or Bridges and Structures Resource Center Federal Highway Administration.

FHWA. (2015). *Load and Resistance Factor Design (LRFD) for Highway Bridge Superstructures - Reference Manual.* Arlington, VA: Federal Highway Administration National Highway Institute.

FHWA. (2016). U.S. Department of Transportation Federal Highway Administration National Bridge Inventory.

FHWA. (2019). *Manual for Refined Analysis in Bridge Design Evaluation.* Mechanicsburg: Federal Highway Administration.

Fisher, J. W., & Menzemer, C. C. (1990). *Fatigue Cracking in Welded Steel Bridges.* Transportation Research Board.

International Technology Scanning Program. (2010). *Assuring Bridge Safety and Serviceability in Europe.* Office of International Programs Federal Highway Administration U.S.

Department of Transportation American Association of State Highway and Transportation Officials.

Laurendeau, L., Barr, P. J., Higgs, A., Halling, M. W., Maguire, M., & Fausett, R. W. (2014). *Live-Load Response of a 65-Year-Old Pratt Truss Bridge.* American Society of Civil Engineers.

Liu, X., Macdonald, J. H., & Chen, W. (2013). Kinetic analysis and rehabilitation of old bascule bridge in Tianjin, China. *Institute of Civil Engineers: Bridge Engineering*, 36-50.

MACK Dump Trucks. (2020). Retrieved from Truck Paper: https://www.truckpaper.com/listings/trucks/for-sale/list/category/217/heavy-duty-trucks-dump-trucks/manufacturer/mack/model/granite-cv713

NCHRP. (2001). *National Cooperative Highway Research Program Report 454 Calibration of Load Factors for LRFR Bridge Evaluation.* Washington D.C.: Transportation Research Board.

Okeil, A. M., Ulger, T. P., & Elshoura, A. (2018). *Live Load Rating of Cast-in-Place Concrete Box Culverts.* Baton Rouge: Louisiana Department of Transportation and Development.

Pennings, K. R., Frank, K. H., Wood, S. L., Yura, J. A., & Jirsa, J. O. (2000). *Lateral Load Distribution on Transverse Floor Beams in Steel Plate Girder Bridges.* Texas Department of Transportation.

Shahsavari, V., Mashayekhi, M., Mehrkash, M., & Santini-Bell, E. (2019). Diagnostic Testing of a Vertical Lift Truss Bridge for Model Verification and Decision-Making Support. *Frontiers in Built Environment*, Volume 5 Article 92.

Suetoh, S., Burdette, E., Goodpasture, D., & Deatherage, J. H. (1990). *Unintended Composite Action in Highway Bridges.* Transportation Research Board of the National Academy of Sciences.

Susoy, M., Zaurin, R., & Catbas, F. N. (2007). *Reliability of a Movable Bridge by Means of a Field Calibrated Model.* Washington, D.C.: Transportation Research Board.

Yousif, Z., & Hindi, R. (2007). AASHTO-LRFD Live Load Distribution for Beam-and-Slab Bridges: Limitations and Applicability. *Journal of Bridge Engineering*, 765-773.

Zhao, J. J., & Tonias, D. E. (2012). *Bridge Engineering: Design, Rehabilitation, and Maintenance of Modern Highway Bridges Third Edition.* McGraw Hill.

VITA

Patrick Gabriel Duffy first began his time at Louisiana State University as an undergraduate in the Fall of 2012. He graduated Magna Cum Laude from undergraduate studies in the Spring of 2016, obtaining his bachelor's degree in Civil Engineering along with a minor in Business Administration. Pursuing a career in structural engineering, Patrick returned to Baton Rouge in 2017 to practice as a bridge engineer. Simultaneously, he began taking courses as part of the LSU Graduate School program for a Master's in Science in Civil Engineering. Upon completion of his master's degree he intends to continue his career as a professional engineer.